1-1-2014

Tmprss2-Erg Regulation Of Androgen Biosynthetic Enzyme Expression, Dht Synthesis, And Androgen Receptor Activation In Prostate Cancer

Katelyn Ann Powell
Wayne State University,

TMPRSS2-ERG REGULATION OF ANDROGEN BIOSYNTHETIC ENZYME EXPRESSION, DHT SYNTHESIS, AND ANDROGEN RECEPTOR ACTIVATION IN PROSTATE CANCER

by

KATELYN A. POWELL

DISSERTATION

Submitted to the Graduate School

of Wayne State University,

Detroit, Michigan

in partial fulfillment of the requirements

for the degree of

DOCTOR OF PHILOSOPHY

2014

MAJOR: CANCER BIOLOGY

Approved by:

_____

Advisor Date

_____

_____

_____

_____

DEDICATION

For my family.

For my parents: Mom and Dad, thank you for all your encouragement and support over the years. Thank you for always encouraging me to follow my dreams, and pushing me to never give up. You truly have been and continue to be an inspiration to me. Most of all, thank you for being there. You were always there for me with love and support whenever I needed you, and for that I am forever grateful.

To my siblings: Sarah and Joe, thank you for always being positive and supportive during all my years of academics. I am lucky to have two amazing and successful siblings to look up to.

For my husband: Mike, words cannot express how grateful I am to you for all your commitment, encouragement, patience, and love throughout the years. Thank you for reminding me to keep a positive attitude even when things get tough. You truly are an amazing husband.

ACKNOWLEDGEMENTS

I would like to acknowledge my mentor Dr. Sreenivasa Chinni for his guidance and commitment during my time in his lab. Thank you for giving me many opportunities to learn new lab techniques, and participate in writing grants, manuscript publications, and review publications. Dr. Chinni allowed me to learn a plethora of techniques while working in his lab. I know this will allow me to be competitive in my field as I move on to my postdoctoral fellowship. Thank you for always having your door open for discussion and making yourself available to meet with me whenever needed.

I would like to thank my committee members, Dr. Larry Matherly, Dr. Shije Sheng, Dr. Krishna Rao Maddipati, and Dr. Michael Cher. It has been a pleasure working with all of you over the past three years. I am honored to have had the opportunity to discuss my project with such a diverse group of highly successful individuals. I am proud to say that every one of my committee members serves as a head leader for at least one department, program, or facility emphasizing the magnitude of their expertise. Dr. Matherly is director of the Wayne State University (WSU) School of Medicine (SoM) Cancer Biology Graduate Program (CBGP), and Program Leader of the Barbara Ann Karmanos Cancer Institute Molecular Therapeutics Program. Dr. Sheng is Program Leader of the Barbara Ann Karmanos Cancer Institute Tumor Microenvironment Program. Dr. Maddipati is director of the WSU SoM Lipidomics and Mass Spectrometry Core Facility. Dr. Cher is chairman of the WSU SoM Urology Department and Chief of Urology at the Barbara Ann Karmanos Cancer Institute. Thank you to all of you for taking time out of your busy schedules to meet with me for my committee meetings. Each of you contributed your own unique insight into my project over the years, which always helped

strengthen the project at each meeting. You have all been wonderful role models to me, and I feel lucky to have had the opportunity to work with you.

I would like to acknowledge my lab members Dr. Katie Conley-Lacomb and Dr. Rajareddy Singareddy for their assistance and guidance in my training during my graduate degree. I would like to thank my rotation mentors Dr. Julie Boerner and Dr. Izabella Podgorski for their patience and training during my first year in the WSU SoM CBGP. Recognition and thanks to Dr. Aliccia Bollig-Fischer and Mr. Jack Wu at the WSU Applied Genomics Technology Center core facility for their assistance and service with lentiviral particle production, as well as Dr. Adele Kruger and Dr. Bollig-Fischer for their assistance with the Oncomine database. Recognition and thanks to Dr. Krishna Rao Maddipati and Mr. Sen-Lin Zhou at the SoM Lipidomics and Mass Spectrometry Core Facility and Dr. Kenneth Honn's lab for assistance and guidance with the Mass Spectrometry experiments. Additional recognition and thanks to the WSU SoM Microscopy, Imaging and Cytometry Resources Core for their services and assistance with the microscopy imaging and Volocity software (PerkinElmer).

I would like to acknowledge and thank the WSU SoM CBGP for their financial support and funding during my entire graduate degree. Special thanks to Ms. Jill Dejesus and Ms. Nadia Daniels for all their help with the CBGP. I would also like to thank the WSU SoM Department of Pathology and Department of Urology for use of technical equipment as well as lab support funding. Special thanks to Dr. Larry Matherly, Dr. Yubin Ge, and Dr. Julie Boerner for advice and guidance during my graduate degree.

TABLE OF CONTENTS

LIST OF TABLES

LIST OF FIGURES

Chapter 1

Introduction

Cancer is one of the leading causes of death worldwide, accounting for 8.2 million deaths in 2012. According to the World Health Organization, trachea bronchus, lung cancers were the 5th leading cause of death worldwide in 2012. The locations around the world with the highest incidences of cancer each year are Australia/New Zealand, North America, Western Europe, and Northern Europe. According to the American Cancer Society, in the United States there was an estimated 1,660,290 newly diagnosed cancer cases in 2013. In addition, there was an estimated 580,350 cancer related deaths in 2013. Cancers of the lung, prostate, breast, and colon were the most commonly diagnosed and the most common forms of cancer-related death in men and women in the United States in 2013. These statistics emphasize the importance of continual improvement in cancer research and treatment.

Cancer is generally characterized by the development of 8 common hallmarks which allow normal cells to become neoplastic and eventually malignant. The 8 common hallmarks of cancer are sustained proliferative signaling, evasion of growth suppressors, activation of invasion and metastasis, enabled replicative immortality, induction of angiogenesis, resistance to cell death, avoidance of immune destruction, and deregulated cellular energetics. Enabling characteristics that facilitate the development of cancer hallmarks are genomic instability/mutation, and tumor-promoting inflammation. Tumors are complicated because they are comprised of a heterogeneous mix of cancer cells, as well as associated cells from the surrounding tumor microenvironment (Hanahan & Weinberg 2011). This makes eliminating

cancer cells difficult because it requires targeting a repertoire of heterogeneous cells that may respond differently to the same treatment.

Prostate Cancer

According to the American Cancer Society statistics, prostate cancer (PCa) is the most commonly diagnosed non-subcutaneous cancer among men living in the United States. PCa is the second most common cause of cancer related death among American men. There were almost 239,000 newly diagnosed cases of PCa in American men in 2013, accounting for 28% of new cancer cases, which was higher than any other type of non-subcutaneous cancer diagnosed that year. There were almost 30,000 PCa related deaths in American men in 2013, accounting for 10% of non-subcutaneous cancer related deaths, second only to lung and bronchus cancer. These statistics emphasize the importance of discovering novel drugs and therapeutics to treat this disease. According to the Surveillance, Epidemiology, and End Results (SEER) Program Cancer Statistics Review, PCa is generally considered to be a disease of old age with the average age of diagnoses being 66 years, and median age of death at 80 years. It is also a slow disease, with 98.9% of diagnosed patients surviving at least 5 years post-diagnosis (2004-2010). Some PCa patients can live up to 10-15 years post-diagnosis. In fact, localized PCa is rarely the cause of cancer related death. Development of advanced PCa in the form of metastatic and castration-resistant PCa (CRPC) is usually the ultimate cause of death in these patients. Patients with metastatic CRPC only have a median survival of about 9-13 months (Kirby et al. 2011). Therefore, it is important to develop novel drugs and therapeutics that prevent, target, and treat advanced forms of PCa.

PCa is generally thought to develop in a sequential manner through a series of stages. First patients develop prostatic intraepithelial neoplastic (PIN) lesions, which can eventually

become high grade, or HGPIN lesions. This stage is considered a precursor to PCa formation. Primary PCa is the next stage, where the cancer is localized to the prostate gland. Many primary PCa cases eventually develop into advanced PCa, which is considered to be the worst and most aggressive form of PCa. Advanced PCa is characterized by the spread, or metastasis, of PCa cancer to distant tissues, such as bone or brain tissue. In addition, many advanced PCa cases become castration-resistant PCa (CRPC), where the PCa no longer responds to androgen ablation therapies that target androgen receptor (AR) signaling (Schrecengost & Knudsen 2013). Therefore, advanced PCa is usually referred to as metastatic PCa or CRPC, and the two are not mutually exclusive and often occur together.

Normal prostate tissue is an endocrine regulated gland and therefore relies on androgen hormones for development, growth, and regulation (Lonergan & Tindall 2011). In many cases, PCa is also dependent on androgens for growth and regulation. Androgens such as dihydrotestostone (DHT) and testosterone bind to the AR, a nuclear hormone receptor, and activate intracellular signaling. The AR normally resides in the cytoplasm of prostate cells and PCa cells, in complex with heat shock protein. Once bound by ligand DHT or testosterone, the AR can dissociate from heat shock protein, translocate into the cell nucleus, homodimerize, and bind to target genes that activate AR signaling pathways. AR signaling can regulate cell proliferation, differentiation, and a multitude of other cellular processes (Lonergan & Tindall 2011). Circulating androgen levels and AR signaling are pivotal and crucial to prostate tissue development and maintenance.

A first line therapy for treatment of primary PCa is androgen deprivation therapy (ADT). ADT is used to prevent the testicular synthesis of testosterone and DHT (Schrecengost & Knudsen 2013). These therapies usually target endogenous endocrine signaling pathways that act

on the testis and adrenal glands where testosterone and other androgens are synthesized, thus preventing androgens from reaching the AR in the prostate tissue (Figure 1). Some examples of currently used ADT therapies are listed in Figure 1. It is important to mention that surgery is often also a first line treatment of primary PCa, where surgeons try to remove as much of the cancer from the prostate as possible. Radiation is also a treatment option for PCa patients, especially in combination with other treatments. Once the PCa has failed first line treatments and developed into advanced PCa other treatments are used such as androgen biosynthetic enzyme inhibitors and AR antagonist. These drugs bind to and block the action of androgen synthesizing enzymes and the AR. Examples of androgen enzyme inhibitors and AR antagonists are listed in Figure 1. Another treatment used for advanced PCa is docetaxel chemotherapy, but it is usually less tolerable especially in older patients due to toxic side effects. With few options to treat advanced PCa patients, the search continues for novel drug targets and development of more effective treatments for this disease.

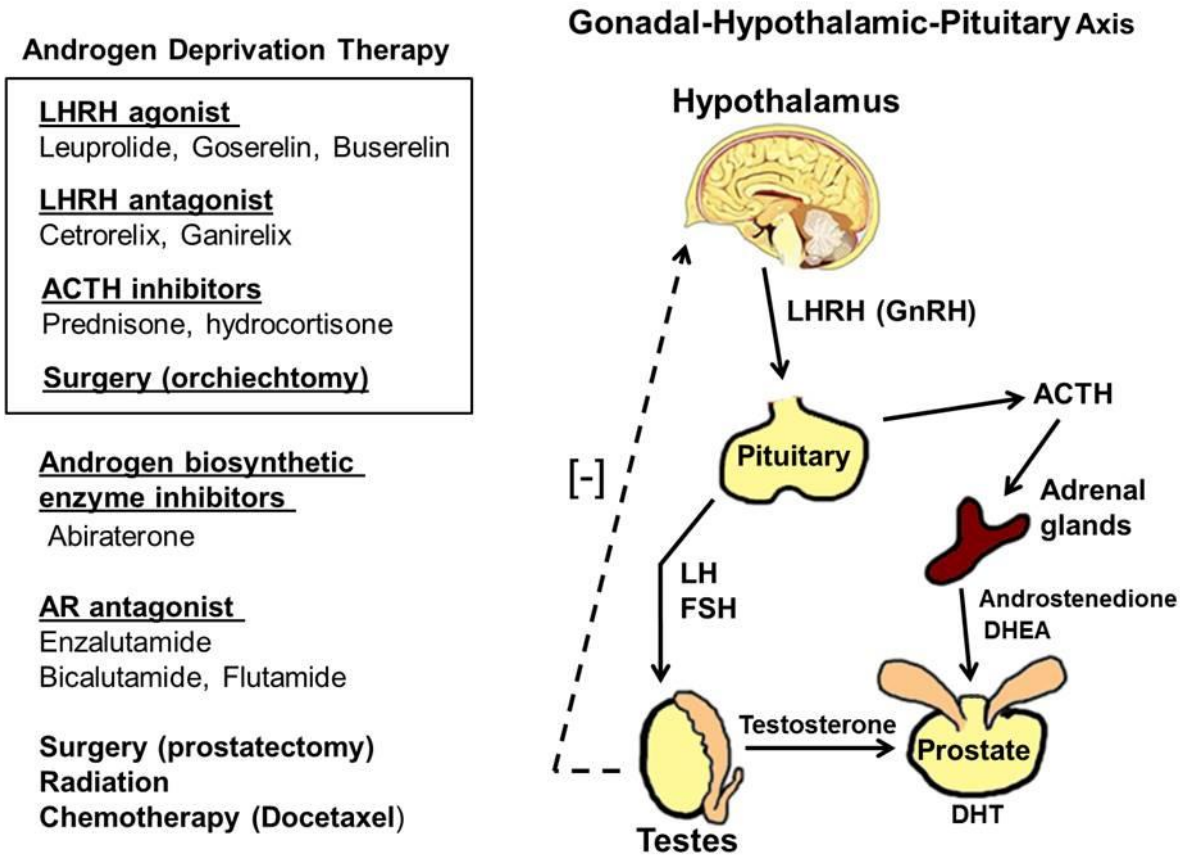

Figure 1. Therapies used in the Treatment of Prostate Cancer. (Left side) List of different therapies used to treat prostate cancer. Orchiechtomy is surgical removal of the testis. Prostatectomy is surgical removal of the prostate gland. (Right side) Diagram illustrating the Gonadal-Hypothalamic-Pituitary signaling axis, which is a part of the endocrine system. The hypothalamus in the brain releases luteinizing hormone-releasing hormone (LHRH), or gonadotropin-releasing hormone (GnRH), which acts on the pituitary gland to release luteinizing hormone (LH), follicle-stimulating hormone (FSH), and adrenocorticotropic hormone (ACTH). These hormones act on the testes to release testosterone and on the adrenal glands to release Dehydroepiandrosterone (DHEA), androstenedione, and other androgens into circulation. These androgens are taken up by the prostate gland and synthesized into DHT. This in turn can activate AR signaling in the prostate gland.

TMPRSS2-ERG Fusion Gene in Prostate Cancer

The TMPRSS2-ERG fusion gene has been shown to be present in approximately 50% of PCa patients, including patients with advanced PCa (Perner et al. 2006). The TMPRSS2 gene encodes for a serine trans-membrane protease and the ERG gene encodes for a transcription factor that belongs to the ETS family of transcription factors. The TMPRSS2 gene and the ERG gene are located on chromosome 21 approximately 3 Mb apart. The TMPRSS2-ERG fusion gene forms through a ~3 Mb deletion on chromosome 21, which fuses the two genes together. The fusion gene occurs through either chromosomal deletion (Edel) or an unbalanced chromosomal translocation (rearrangement) (Figure 2) (Attard et al. 2008). In general, the TMPRSS2 promoter region is fused to the ERG coding region. This places ERG transcription under control of the TMPRSS2 promoter (Tomlins et al. 2005). The coding region of TMPRSS2 gene is lost during the chromosomal deletion resulting in loss or reduction of TMPRSS2 expression. The entire promoter region for ERG is lost in the chromosomal deletion, however only a portion of the ERG coding region on the N-terminus is lost resulting in expression of a truncated but functional protein (Figure 3) (King et al. 2009). It is important to note that the truncated ERG protein does retain its DNA binding domain, and can thus continue to perform its functions as a transcription factor.

At least 18 different splice variants of TMPRSS2-ERG have been identified, with some PCa patients having multiple splice variants (Figure 4) (Clark et al. 2006, Wang et al. 2006, Wang et al. 2008). These splice variants result from either alternative mRNA splicing or different chromosomal fusion break points. The most common ERG splice variant is the T1-E4 variant (TMPRSS2 exon 1 fused to ERG exon 4), accounting for 75-86% of ERG variants in PCa patients (Figure 3 and Figure 4) (Shao et al. 2012, Wang et al. 2006). The high prevalence

of the TMPRSS2-ERG fusion suggests that this region is a hot spot for chromosomal rearrangements and deletions in PCa. It is not exactly known what causes the TMRPSS2-ERG fusion to occur, but AR signaling induced DNA double strand breaks (DSB) have been implicated to play a causal role in the formation of the fusion gene. It is thought that close proximity of high levels of AR signaling to the TMPRSS2 and ERG genes results in a higher amount of DNA DSB. Attempted repair using error-prone non-homologous end joining DNA repair mechanisms can lead to improper DNA repair and chromosome deletions and translocations (Haffner et al. 2010, Lin et al. 2009, Mani et al. 2009).

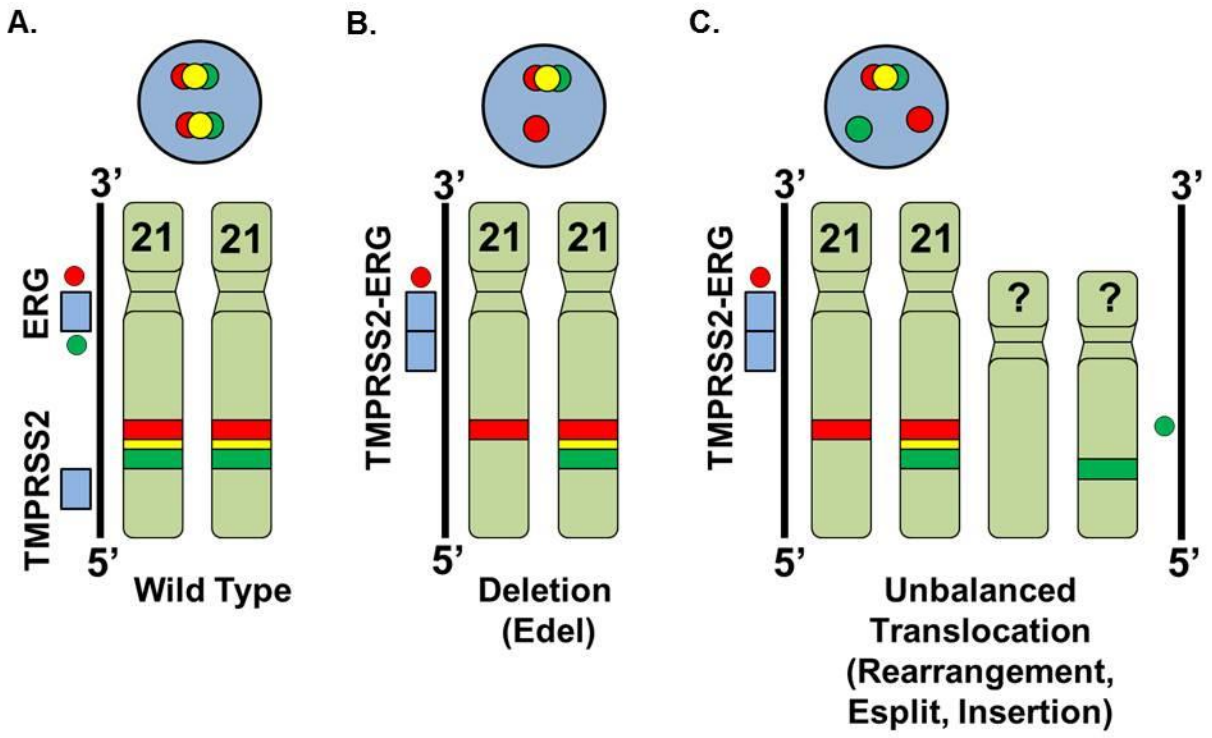

Figure 2. TMPRSS2-ERG Fusion Gene Formation: 3 Mb Deletion on Chromosome 21. A.) Diagram illustrating wild type ERG and TMPRSS2 genes located on chromosome 21. This represents TMPRSS2-ERG fusion-negative chromosomes. B.) Diagram illustrating ~3 Mb deletion of chromosome 21 located between TMPRSS2 and ERG, which fuses the two genes together on TMPRSS2-ERG fusion-positive chromosomes. C.) Diagram illustrating ~3 Mb unbalanced translocation of chromosome 21 located between TMPRSS2 and ERG, which fuses the two genes together on TMPRSS2-ERG fusion-positive chromosomes. The translocated portion of chromosome 21 is inserted into an unknown location in the genome. For A-C, the red and green colors represent ERG specific DNA hybridization probes used in fluorescent *in situ* hybridization (FISH), a technique commonly used for detection of the TMPRSS2-ERG fusion gene. The yellow color appears on TMPRSS2-ERG fusion-negative chromosomes due to overlap of the red and green probes. The blue circles located above chromosome diagrams depict how the FISH results commonly appear. For example in part B, when the green probe labeled 5' end of ERG is lost through deletion, only a single red probe will appear for the affected chromosome.

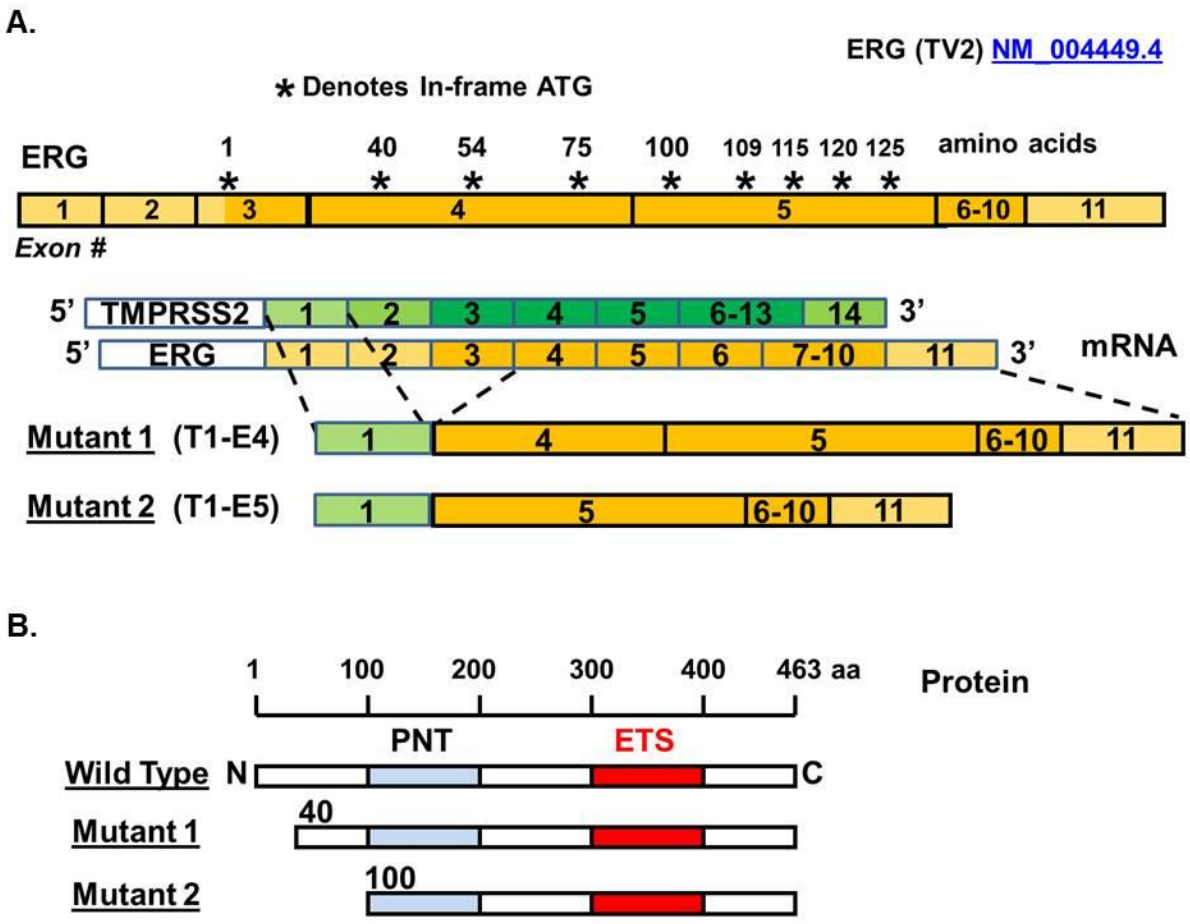

Figure 3. Formation of the TMPRSS2-ERG Fusion Gene in Prostate Cancer: mRNA and Protein Structure. A.) Diagram illustrating the mRNA sequences of TMPRSS2 and ERG. The ERG sequence was modeled using transcript variant 2 (TV2) NM_004449.4, and shows in-frame ATG sites and amino acid numbers. For ERG the light yellow indicates non-coding regions and the dark yellow indicates protein coding regions. For TMPRSS2 the light green indicates non-coding regions and the dark green indicates protein coding regions. The numbers for each mRNA sequence represent exon numbers. Mutant 1 (T1-E4) depicts the fusion of TMPRSS2 exon 1 to ERG exon 4, and mutant 2 (T1-E5) depicts the fusion of TMPRSS2 exon 1 to ERG exon 5. B.) Diagram illustrating the resulting protein sequence of TMPRSS2-ERG mutant 1 (T1-E4) and mutant 2 (T1-E5). The full length (wild type) ERG sequence is shown at the top for a reference. Mutant 1 has an N-terminus truncation of the first 39 amino acids, consistent with the in-frame ATG site (aa 40) shown in exon 4 in part A. Mutant 2 has an N-terminus truncation of the first 99 amino acids, consistent with the in-frame ATG site (aa 100) shown in exon 5 in part A. PNT is the regulatory domain, and ETS is the DNA binding domain.

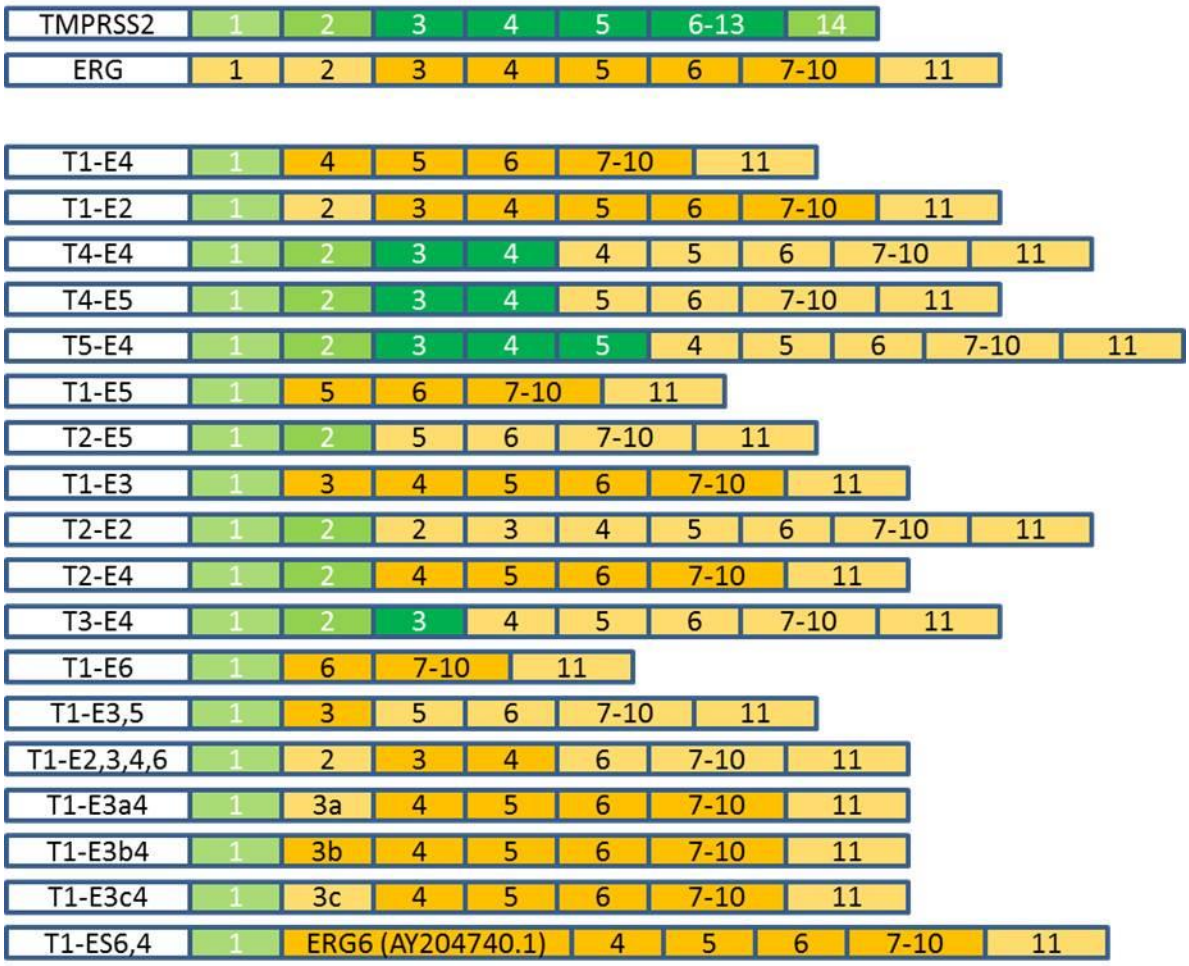

Figure 4. At Least 18 Different mRNA Splice Variants of the TMPRSS2-ERG Fusion Gene Have Been Identified in Prostate Cancer. Diagram illustrating each of the mRNA splice variants identified for the TMPRSS2-ERG fusion gene in PCa. Full length mRNA sequences for TMPRSS2 and ERG are shown at the top for reference. Numbers on mRNA sequences represent exon numbers. For ERG the light yellow indicates non-coding regions and the dark yellow indicates protein coding regions. For TMPRSS2 the light green indicates non-coding regions and the dark green indicates protein coding regions. Each splice variant is named in the white box according to the TMPRSS2-ERG fusion site. For example, T2-E4 indicates TMPRSS2 exon 2 is fused to ERG exon 4.

The TMPRSS2 gene promoter contains AR response elements. In TMPRSS2-ERG fusion-positive PCa, ERG is aberrantly placed under control of AR signaling resulting in overexpression of N-terminal truncated proteins (Tomlins et al. 2005). The ERG protein is an ETS family member transcription factor, and contains a highly conserved, C-terminal DNA binding domain known as the ETS domain. ERG is capable of regulating transcription of target genes via binding to ETS consensus sequences (5'-GGAA/T-3') in the promoter and enhancer regions of target genes (Carrere et al. 1998). ERG protein is not normally expressed in PCa cells, thus in TMPRSS2-ERG fusion-positive cells ERG aberrantly regulates expression of target genes leading to development of PIN lesions and invasive prostatic adenocarcinoma in tumors that have concomitant loss of the tumor suppressor PTEN (Figure 5).

It was shown in prostate-specific transgenic mice overexpressing ERG, that mice developed PIN lesions at 5 months of age (Klezovitch et al. 2008). Prostate-specific ERG/PTEN+/- transgenic mice developed HGPIN lesions at 2 months and invasive prostatic adenocarcinoma at 6 months. PTEN+/- mice did not develop prostatic adenocarcinoma, suggesting ERG cooperated with PTEN loss in the development of adenocarcinoma (Carver et al. 2009). Another study showed that prostate-specific ERG/PTEN-/- transgenic mice developed invasive PCa, whereas PTEN-/- mice did not (Chen et al. 2013). It was shown using tissue recombinant studies that ERG overexpression in combination with PTEN knockdown or expression of constitutively active AKT resulted in development of adenocarcinoma (Zong et al. 2009). These data suggest that ERG fusions and loss of PTEN cooperate to enhance PCa progression and the development of adenocarcinoma. These findings also suggest that PTEN loss may act as a "second hit" in TMPRSS2-ERG fusion-positive tumors resulting in the progression of PIN lesions into highly penetrant invasive prostatic carcinoma (Figure 5).

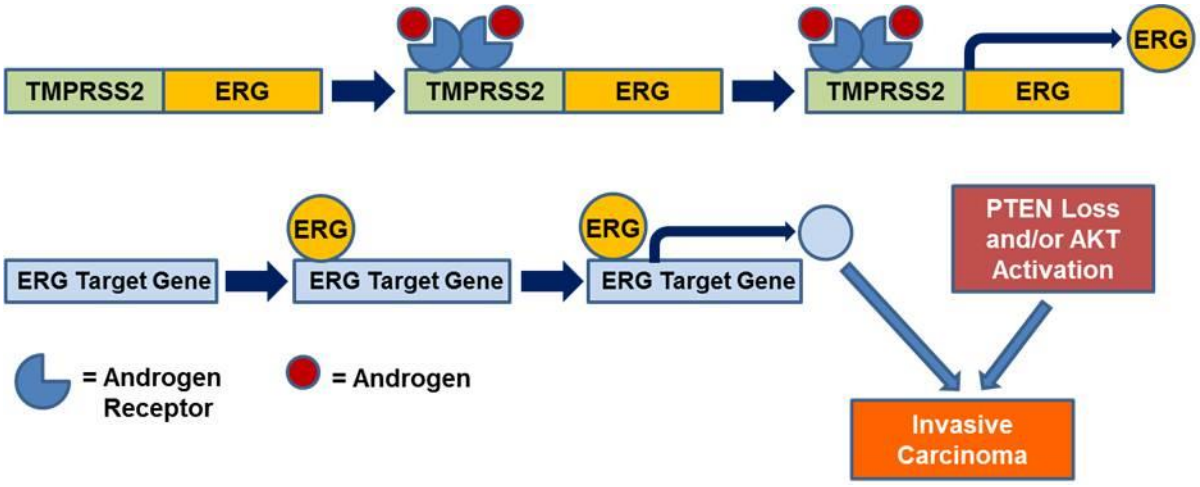

Figure 5. The TMPRSS2-ERG Fusion Gene Results in AR Induced Overexpression of ERG Transcription Factor. Diagram illustrating AR induced overexpression of ERG transcription factor in TMPRSS2-ERG fusion-positive PCa. The TMPRSS2 gene promoter (green) contains androgen response elements which are bound by liganded AR. This induces ERG overexpression resulting in expression of ERG target genes (blue). In combination with PTEN loss in transgenic mice, this can lead to development of invasive prostate carcinoma.

Clinical Findings and Prognosis of the TMPRSS2-ERG Fusion Gene

Frequency and clonal progression of TMPRSS2-ERG fusions in human PCa clinical specimens

As mentioned previously, the TMPRSS2-ERG fusion gene has been shown to be present in almost 50% of PCa patient clinical tumor specimens (Perner et al. 2006). Several studies have been performed using fluorescent *in situ* hybridization (FISH) analysis in PCa tumor specimens in order to positively identify the presence of the fusion gene. The presence of TMPRSS2-ERG fusion gene was not detected in normal prostate tissue or in benign prostate tissue (Han et al. 2009). However, presence of the fusion gene started to appear in HGPIN lesions at low levels of 15-16% (Han et al. 2009, Mosquera et al. 2008). The ERG fusion gene was present at high levels in primary PCa 49-54%, metastatic PCa 35-41%, and CRPC 33-47% (Figure 6A) (Attard et al. 2009, Han et al. 2009, Mehra et al. 2007, Perner et al. 2006, Rickman et al. 2010). These FISH data from clinical PCa specimens suggest that TMPRSS2-ERG may be involved in the progression of PCa, because the presence of the fusion gene becomes more prevalent as the disease progresses from mild to severe stages.

FISH studies can determine the presence of the TMPRSS2-ERG fusion gene, but they cannot detect if the fusion gene is being actively expressed at the mRNA or protein level. However, microarray analysis can detect ERG mRNA expression using primers, and immunohistochemistry (IHC) analysis can detect ERG protein expression using antibodies. Microarray data for ERG mRNA expression in benign, primary, and metastatic PCa patient tumor specimens was extracted from the gene expression omnibus database GDS3289. ERG expression was significantly increased in primary and metastatic PCa compared to benign samples (Figure 6B). In addition, studies using IHC showed that ERG protein expression was significantly increased in advanced and primary PCa compared to HGPIN and benign prostatic

hyperplasia samples (Szasz et al. 2013, Verdu et al. 2013). These microarray and IHC studies for ERG expression indicate that not only does the presence of the TMPRSS2-ERG fusion gene increase from benign to advanced PCa, but the mRNA and protein expression of ERG increases as well. These data further suggest that ERG may play a role in the progression of PCa from benign to more advanced forms.

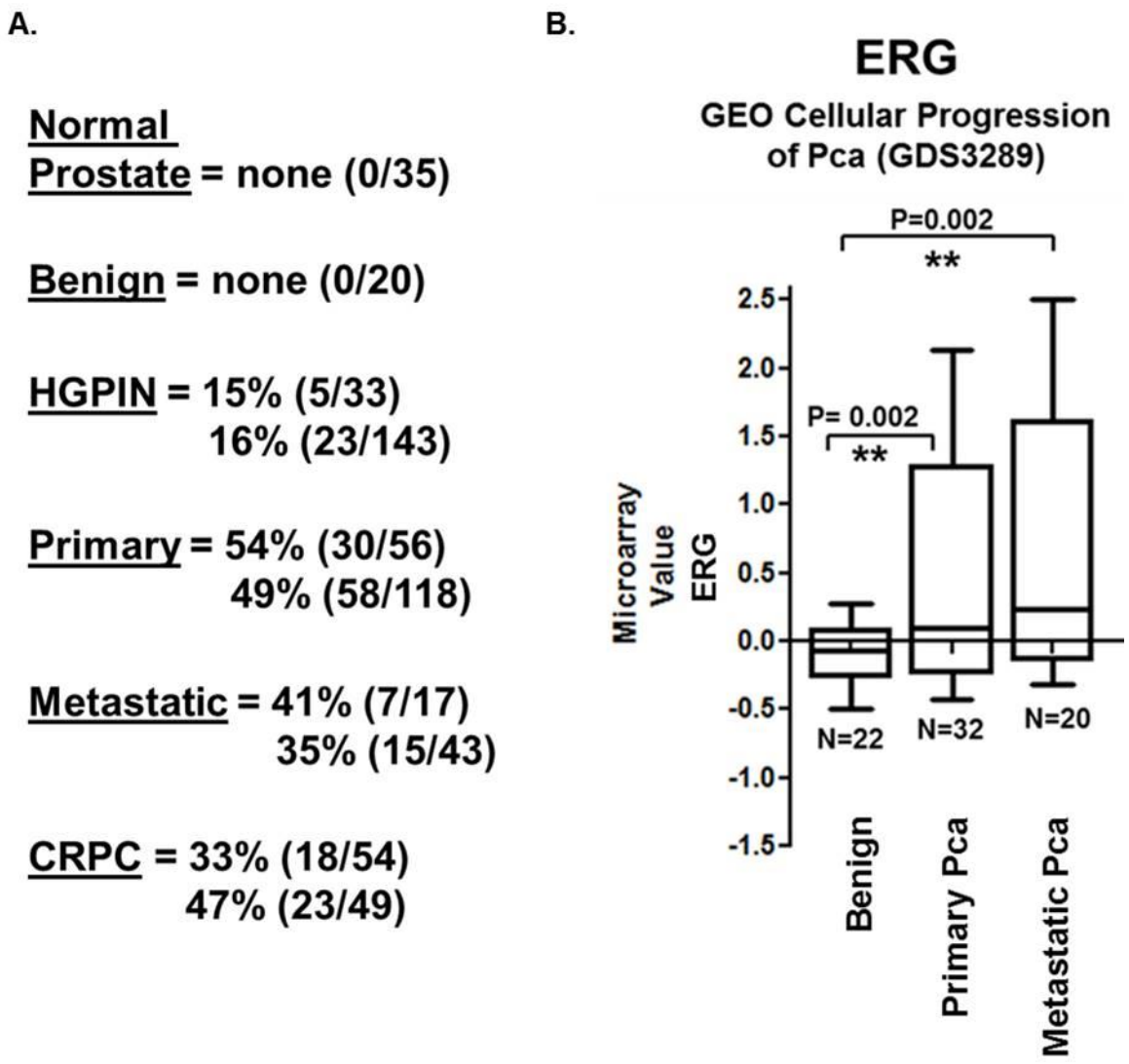

Figure 6. The Presence and Expression of the TMPRSS2-ERG Fusion Gene Increases as Prostate Cancer Progresses from Benign to Primary and Advanced Prostate Cancer. A.) FISH data from human PCa clinical patient tumor specimens. FISH data were extracted from various published literature studies. Clinical specimens are shown from top to bottom in order of PCa progression: normal prostate tissue → benign prostate tissue → high grade prostatic intraepithelial neoplastic lesions (HGPIN) → primary PCa → metastatic PCa and CRPC (advanced PCa). Tumor sample numbers (N values) for each study are shown in parenthesis next to percentages. B.) Microarray data for ERG expression in human clinical specimens of benign, primary PCa, and metastatic PCa. Data were extracted from the gene expression omnibus (GEO) database GDS3289. Statistical analysis was a two-tailed, unpaired, student's t-test N = 22 (benign), N = 32 (primary PCa), N = 20 (metastatic PCa), ** $P<0.01$.

Other studies have also suggested the involvement of ERG in PCa progression. For example, one study showed that PCa patients who had TMPRSS2-ERG fusion-positive HGPIN lesions were significantly more likely to develop PCa compared to patients with fusion-negative HGPIN lesions (Park et al. 2014). IHC analysis in patient specimens showed that 96.5% (82/85) of ERG-positive PCa carcinoma specimens also had PIN lesions with ERG-positive foci, indicating a strong concordance between ERG expression in PIN lesions and in primary PCa. (Furusato et al. 2010). In addition, it was shown in patient specimens that in 73% (11/15) of ERG-positive HGPIN lesions were located directly adjacent to ERG-positive PCa foci. Interestingly, 100% (11/11) of the ERG-positive HGPIN lesions harbored the exact same ERG fusion molecular subtype as the adjacent ERG-positive PCa foci, with both adjacent foci harboring either TMPRSS2-ERG formed through deletion (Edel) or through unbalanced translocation. This same study showed that 100% (41/41) of metastatic sites harbored the same ERG fusion molecular subtype status across multiple sites in the same patient (Han et al. 2009). Similar results were seen where TMPRSS2-ERG mRNA expression was present in 37% (10/27) of metastatic CRPC patient samples. Of these 10 patients, 100% of metastatic sites contained a TMPRSS2-ERG fusion formed through deletion (Edel). All patients that harbored the Edel ERG fusion subtype at their metastatic CRPC site also harbored the Edel ERG fusion subtype at the primary PCa site (Mehra et al. 2008). Taken together, these data suggest a mechanism of clonal selection and clonal expansion of the TMPRSS2-ERG fusions in the progression of HGPIN lesions to PCa to metastatic CRPC.

Clinical prognosis of TMPRSS2-ERG fusions in PCa patients

Since the discovery of the TMPRSS2-ERG gene fusion in 2005, there have been conflicting findings regarding the clinical prognosis of the fusion gene in PCa patients. Some

studies have shown that the presence of TMPRSS2-ERG fusion gene is associated with better clinical prognosis, and some have shown that it has no association with prognosis; however, the majority of studies have shown that TMPRSS2-ERG is associated with a worse clinical prognosis. One study found that the fusion gene was associated with favorable outcome in PCa patients who had radical prostatectomy (Saramäki et al. 2008). Two studies showed that TMPRSS2-ERG was associated with lower Gleason scores, and one study showed it was associated with better survival (Fine et al. 2010, Winnes et al. 2007). Previous studies have found that the fusion gene is not associated with PCa disease grade, biochemical recurrence (PSA), Gleason score, progression, stage, response to endocrine treatment, or prognosis (Albadine et al. 2009, Boormans et al. 2010, Darnel et al. 2009, Esgueva et al. 2010, Furusato et al. 2008, Mosquera et al. 2009, Mwamukonda et al. 2009, Rouzier et al. 2008, Teng et al. 2013, Tu et al. 2007).

Many studies have shown that TMPRSS2-ERG fusion-positive status is associated with factors that promote worse clinical prognosis. It was shown that copy number increases in the TMPRSS2-ERG fusion gene were associated with higher Gleason scores, decreased survival, aggressive disease, and poor prognosis (Fine et al. 2010, FitzGerald et al. 2008, Gopalan et al. 2009, Yoshimoto et al. 2008). Interestingly, one study showed that PCa patients who harbored ERG fusions formed through deletion (Edel) and increased in copy number (2+Edel) had only a 25% survival rate at 8 years (Attard et al. 2008). Other studies have supported the finding that Edel fusions are associated with more aggressive disease compared to translocation fusions, indicating that even the molecular subtype of TMPRSS2-ERG can have an influence on disease outcome. For example, one study showed that 54% of clinically localized (primary) PCa specimens harbored the TMPRSS2-ERG fusion gene, with 39% formed through Edel and 61%

formed through translocation. Interestingly, although the ERG translocation subtype was more prevalent in localized PCa, 100% of metastatic CRPC sites contained ERG Edel subtype (Mehra et al. 2008). Another study showed that Edel fusions were associated with lymph node involvement and higher tumor stage (Perner et al. 2006). These data suggest that ERG copy number increases and Edel ERG subtype are associated with more aggressive PCa.

The presence of TMPRSS2-ERG fusions has been associated with a higher rate of biochemical recurrence (prostate-specific antigen, PSA) compared to fusion-negative PCa patients (Barwick et al. 2010, Bonaccorsi et al. 2009, Nam et al. 2007b). This suggests that ERG may have an effect on AR activation in PCa tumors. For example, it was shown in two independent studies that fusion-positive PCa patients had significantly higher rates of biochemical recurrence at 5 years post-diagnosis compared to fusion-negative patients (58.4% vs. 8.1%, and 79.5% vs. 37.5%) (Nam et al. 2007a, Nam et al. 2007b). Using anti-ERG antibodies and IHC analysis, it was shown that PCa patients with higher ERG staining intensities had significantly higher rates of PSA relapse and metastasis (Spencer et al. 2013). Another study showed that ERG fusions were associated with higher PSA levels and Gleason scores, and more advanced tumor stage compared to fusion-negative PCa (Rostad et al. 2009). Using a Kaplan-Meier survival plot, it was shown that in PCa patients treated with androgen ablation surgery that ERG fusion-positive patients had significantly lower PSA recurrence free-survival compared to fusion-negative patients at 80 months post-surgery (35% vs. 90%) (Baldi et al. 2010). Another Kaplan-Meier survival plot showed similar results where ERG fusion-positive patients had significantly lower PSA recurrence free-survival compared to fusion-negative patients at 80 months post-diagnosis (10% vs. 90%) (Barwick et al. 2010). These data suggest that TMPRSS2-

ERG fusions may be involved in AR activation in PCa, and the Baldi et al. study suggests ERG fusions may regulate androgen synthesis and AR activation in a castrate environment.

Further supporting that ERG fusions may be involved in regulation of androgen synthesis and AR activation, studies have indicated that ERG fusion-positive patients responded better to treatment with the CYP17A1 enzyme inhibitor, abiraterone. It was shown in CRPC patients treated with abiraterone that ERG fusion-positive patients had a significantly higher response rate to abiraterone treatment (>90% PSA decline) compared to fusion-negative CRPC patients (80% vs. 20%) (Attard et al. 2009). Another study in metastatic CPRC patients showed similar results with fusion-positive patients having a higher response rate to abiraterone treatment (>50% PSA decline) compared to fusion-negative patients (46.6% vs. 38.4%). In this study, the median baseline PSA value for ERG fusion-positive patients was 185 ng/ml, and for ERG fusion-negative patients it was 66 ng/ml (Danila et al. 2011). These data suggest ERG may regulate androgen synthesis and AR activation in CPRC. It was shown in bone metastatic CRPC patients treated with enzalutamide, an AR antagonist, that the presence of ERG was associated with the lowest primary resistance (9%) to enzalutamide treatment compared to any other molecular markers such as CYP17A1 (42%), AR mutant receptors (50%), AR overexpression (62%), Ki-67 (75%), phospho-Src (92%), and phospho-Met (91%) (Efstathiou et al. 2014). These data suggest ERG fusion-positive tumors may be less resistant to AR antagonist possibly because these tumors have become highly reliant on ERG regulated androgen synthesis and AR activation for survival and growth.

TMPRSS2-ERG fusion gene has been associated with additional factors that promote worse clinical prognosis. The presence of TMPRSS2-ERG was associated with higher Gleason scores and higher tumor grade (Hagglof et al. 2014, Hofer et al. 2009, Mehra et al. 2007). In

addition, patients with ERG fusions were shown to be more prone to developing metastatic PCa (Hagglof et al. 2014, Perner et al. 2010). ERG was also associated with the presence of prognostic tumor cell markers such as high levels of Ki67, phospho-Akt, and phospho-EGFR (Hagglof et al. 2014). IHC staining of ERG and Kaplan-Meier survival plot revealed that primary and advanced PCa patients with high ERG expressing tumors had significantly worse overall survival compared to patients with low ERG expressing tumors (25% vs. 65%) at 60 months post-diagnosis in patients who underwent radical prostatectomy (Szasz et al. 2013). Similarly, the presence of TMPRSS2-ERG fusion gene was also associated with significantly lower survival probability compared to fusion-negative patients (30% vs. 78%) at 15 years post-diagnosis in patients who underwent transurethral resection of the prostate (Hagglof et al. 2014). Another study showed there was an association between ERG fusion-positive tumors and prostate specific death (Demichelis et al. 2007).

As previously mentioned, the presence of the TMPRSS2-ERG fusion gene has been shown to cooperate with PTEN loss to induce invasive prostate carcinoma in transgenic mice (Carver et al. 2009, Chen et al. 2013). Consistent with these data, the presence of the TMPRSS2-ERG fusion gene was significantly correlated with PTEN loss in prostate patient tumors, and was associated with more aggressive disease (Bismar et al. 2011, Leinonen et al. 2013, Yoshimoto et al. 2008). One study showed significant association between PTEN loss and ERG rearrangement in both localized PCa and metastatic PCa tumor specimens (Han et al. 2009). ERG fusion occurring through deletion (Edel) was significantly correlated with PTEN deletion in CRPC patient specimens (Bismar et al. 2012). It was shown that the presence of TMPRSS2-ERG fusion gene and concomitant PTEN loss was a common event in prostate cancer specimens where 93% (14/15) of ERG fusion-positive tumors had weak/absent PTEN expression, and only 50% (13/26)

of ERG-negative tumors had weak/absent PTEN expression (Carver et al. 2009). Regarding clinical prognosis of ERG fusion-positive and PTEN negative tumors, it was shown that loss of PTEN and ERG-positive expression were significantly associated in prostatectomy and CRPC patient tumors, and these patients had shorter progression-free survival compared to patients with ERG-negative tumors (Leinonen et al. 2013). Concomitant ERG fusion and PTEN loss were also associated with greater risk of capsular penetration in PCa patients who underwent prostatectomy (Nagle et al. 2013). A Kaplan-Meier survival plot showed that PTEN deletion and TMPRSS2-ERG occurring together was a significant predictor of early biochemical recurrence in PCa patients (Yoshimoto et al. 2008). These data suggest that the presence of the TMPRSS2-ERG fusion gene is associated with poor clinical prognosis in PCa patients.

Biological Functions of the TMPRSS2-ERG Fusion Gene

ERG overexpression in prostate cell culture models increases cellular invasion, migration, and proliferation rates.

Cell culture-based studies have been used to elucidate the biological functions of TMPRSS2-ERG. siRNA knockdown of ERG in VCaP cells was shown to significantly inhibit cellular invasion (Sun et al. 2008, Tomlins et al. 2008, Wang et al. 2008). Urokinase plasminogen activator (uPA) and plasminogen activator pathways have been shown to be associated with ERG overexpression. Blocking these pathways in BPH-1, VCaP, and RWPE cells was shown to significantly inhibit cellular invasion (Klezovitch et al. 2008, Tomlins et al. 2008). The chemokine receptor CXCR4 increased cellular invasion in VCaP cells, and gene expression of CXCR4 was directly upregulated via the ERG fusion protein binding to the CXCR4 promoter (Cai et al. 2010). Consistent with the previous results, overexpression of ERG

was shown to significantly increase cellular invasion in BPH-1, RWPE, prostatic epithelial (PrEC), and immortalized prostatic epithelial (PNT1a) cells (Klezovitch et al. 2008, Tomlins et al. 2008, Wang et al. 2008). Overexpression of ERG in BPH-1, PrEC, and PNT1a cells was shown to increase cell proliferation rates, and overexpression of multiple ERG transcript variants increased cell proliferation rates even further in PNT1a cells (Klezovitch et al. 2008, Wang et al. 2008). In addition, knockdown of ERG in VCaP cells reduced cell proliferation rate and tumor growth *in vivo* (Wang et al. 2008). Lastly, overexpression of ERG increased cellular migration rates in BPH-1 and PNT1a cells (Carver et al. 2009, Wang et al. 2008). These cell culture studies suggest that overexpression of ERG can result in increased cellular invasion, proliferation, and migration. These effects are due to the aberrant regulation of downstream target genes of ERG, which in turn are able to alter normal cellular activity.

ERG mediates transcriptional regulation at specific gene loci via direct DNA binding interactions

ERG is associated with the aberrant expression of many genes. Over 30 genes have been identified thus far through chromatin immunoprecipitation (ChIP) assays to be direct binding targets of TMPRSS2-ERG. A list of direct ERG binding targets identified by ChIP studies is shown in Table 1 (Cai et al. 2010, Carver et al. 2009, Flajollet et al. 2011, Leshem et al. 2011, Mani et al. 2011, Mohamed et al. 2011, Rickman et al. 2010, Sreekumar et al. 2009, Sun et al. 2008, Tomlins et al. 2008, Wu et al. 2013, Yin et al. 2011, Yu et al. 2010). These ChIP assays demonstrate that many genes are direct targets of ERG, providing a potential explanation for their aberrant regulation. ERG has been shown to exhibit positive regulation of certain genes, and negative regulation of other genes. Therefore, ERG can act as a transcriptional activator or repressor depending on the specific gene loci. One study even showed that ERG acted as a

positive and negative regulator for the same gene. The study showed that ERG regulated expression of TFF3 via direct binding to the TFF3 gene region in hormone-naïve PCa and in CRPC (Rickman et al. 2010). Interestingly, ERG suppressed TFF3 expression in hormone naïve PCa, and induced TFF3 expression in CRPC. This is an important finding because it suggests that ERG can positively and negatively regulate the expression of the same gene, depending on the context or developmental stage of the PCa.

Table 1. Direct Binding Targets of TMPRSS2-ERG.

Gene Name	ERG Regulation	Cell Line Used for ChIP	Reference Citation
PLAU	Positive	RWPE-ERG, VCaP	Tomlins et al. Neoplasia, 2008
		VCaP	Yu et al. Cancer Cell, 2010
MMP3	Positive	RWPE-ERG, VCaP	Tomlins et al. Neoplasia, 2008
PLAT	Positive	VCaP	Tomlins et al. Neoplasia, 2008
		VCaP	Yu et al. Cancer Cell, 2010
LAMC2	Positive	RWPE-ERG, VCaP	Tomlins et al. Neoplasia, 2008
KCNS3	Positive	RWPE-ERG, VCaP	Tomlins et al. Neoplasia, 2008
PLA1A	Positive	VCaP	Tomlins et al. Neoplasia, 2008
C-MYC	Positive	VCaP	Sun et al. Oncogene, 2008
		VCaP	Mohamed et al. Cancer Biol Ther, 2011
SLC45A3	Negative	VCaP	Sun et al. Oncogene, 2008
		VCaP	Mohamed et al. Cancer Biol Ther, 2011
CXCR4	Positive	PC3-ERG	Carver et al. Nat Genet, 2009
		VCaP	Cai et al. Transl Oncol, 2010
ADAMTS1	Positive	PC3-ERG	Carver et al. Nat Genet, 2009
GNMT	Positive	VCaP	Sreekumar et al. Nature, 2009
SARDH	Positive	VCaP	Sreekumar et al. Nature, 2009
TFF3	Negative/Positive	VCaP	Rickman et al. Neoplasia, 2010
ERG	Positive	VCaP	Mani et al. Cancer Res, 2011
MMP9	Positive	VCaP	Yu et al. Cancer Cell, 2010
NDRG1	Negative	VCaP	Yu et al. Cancer Cell, 2010
AR	Negative	VCaP	Yu et al. Cancer Cell, 2010
KLK2	Negative	VCaP	Yu et al. Cancer Cell, 2010
SLC43A1	Negative	VCaP	Yu et al. Cancer Cell, 2010
CUTL2	Negative	VCaP	Yu et al. Cancer Cell, 2010
KLK3 (PSA)	Negative	VCaP	Yu et al. Cancer Cell, 2010
		VCaP	Mohamed et al. Cancer Biol Ther, 2011
		VCaP	Sun et al. Oncogene, 2008
FKBP5	Negative	VCaP	Yu et al. Cancer Cell, 2010
EZH2	Positive	VCaP	Yu et al. Cancer Cell, 2010
ZBTB16	Negative	VCaP	Yu et al. Cancer Cell, 2010
HPGD	Negative	VCaP	Mohamed et al. Cancer Biol Ther, 2011
ZEB1	Positive	EP-AR/ERG	Leshmen et al. PLoS One, 2011
SPINT1	Negative	EP-AR/ERG	Leshmen et al. PLoS One, 2011
IL1R2	Positive	EP-AR/ERG	Leshmen et al. PLoS One, 2011
OPN	Positive	PC3-ERG	Flajollet et al. Mol Cancer Res, 2011
PSMA	Negative	VCaP	Yin et al. PLoS One 2011
LEF1	Positive	VCaP	Wu et al. Cancer Res, 2013
WNT2	Positive	VCaP	Wu et al. Cancer Res, 2013
WNT11	Positive	VCaP	Wu et al. Cancer Res, 2013

The ERG target genes listed in Table 1. display a diverse repertoire of biological functions. This indicates that ERG can regulate a variety of cellular processes that contribute to an oncogenic phenotype in PCa. As mentioned previously, ERG was shown to increase cellular migration and invasion in PCa cells. Several ERG target genes are known to regulate these cellular processes such as MMP3, MMP9, PLAU, PLAT, CXCR4, ADAMTS1, OPN, WNT, and LEF1 (Cai et al. 2010, Deryugina & Quigley 2006, Flajollet et al. 2011, Tomlins et al. 2008, Wu et al. 2013). ERG has been shown to regulate AR signaling through inhibition of AR target genes, KLK3, KLK2, CUTL2, ZBTB16, NDRG1, SLC43A1, SLC45A3, FKBP5, PSMA and TFF3 (Rickman et al. 2010, Yin et al. 2011, Yu et al. 2010). Several of these AR target genes are involved in promoting prostate differentiation including KLK3, KLK2, PSMA, NDRG1, and SLC45A3 (Dong et al. 2005, Pflueger et al. 2009, Sun et al. 2008, Yao et al. 2008). ERG has been shown to inhibit PCa differentiation by inhibiting these AR pro-differentiation target genes (Yu et al. 2010). In addition, ERG upregulates the expression of C-MYC and EZH2, which are genes known to inhibit prostate differentiation (Sun et al. 2008, Yu et al. 2010). In this manner ERG can promote PCa dedifferentiation and help the PCa cells maintain a more stem cell-like state. Consistent with these findings, ERG has been shown to regulate epithelial-mesenchymal-transition, or EMT, through regulation of ZEB1, SPINT1, ILR12, and TWIST (Leshem et al. 2011). Cells that have undergone EMT tend to have more stem-like properties and resemble stem cells (Mani et al. 2008).

ERG was also shown to increase cell proliferation rate in PCa cells. ERG may increase cell proliferation through transcriptional regulation of C-MYC, AR, WNT, and LEF1 all of which are known to regulate cell proliferation (Balk & Knudsen 2008, Reya et al. 2000, Schmidt 1999). Although ERG was shown to negatively regulate AR target genes involved in

differentiation, it has not been shown to negatively regulate AR target genes involved in cell proliferation. In fact, the data published that ERG inhibits AR expression (Yu et al. 2010) was shown to occur through extremely high levels of ERG overexpression in VCaP cells. Indeed, ERG and AR protein expression do normally co-exist in VCaP cells, suggesting ERG may cooperate with AR to regulate genes involved in cell proliferation and other cellular processes that facilitate an oncogenic phenotype. Recent studies suggest that ERG and AR do in fact cooperate to positively regulate gene expression in PCa, and this will be discussed in further detail in an upcoming section of this introduction.

ERG mediates transcriptional regulation at specific gene loci via direct protein-protein interactions

In addition to ERG transcription regulation via direct binding to target genes, ERG has also been shown to regulate gene expression via protein-protein interactions. *In vitro* studies on ERG protein structure and interactions using co-immunoprecipitation (Co-IP) revealed that the ETS domain was involved in DNA binding and protein interactions. Studies showed that wild type ERG proteins physically interacted through their ETS domain via heterodimerization with other ETS transcription factor family members such as Fli-1, ETS-2, Er81, and Pu-1 (Basuyaux et al. 1997, Carrere et al. 1998). Different ERG isoforms were also involved in the formation of a ternary complex with AP1 family members Fos and Jun, forming an ERG/Fos/Jun complex. In this same study, ERG proteins were shown to physically interact via homodimerization and homo-iso-dimerization with the same isoform or with other ERG isoforms (Carrere et al. 1998). Another study verified that these wild type ERG protein-protein interactions influenced the regulation and expression of the MMP1 and MMP3 gene promoter regions. ERG interacted with

Fos and Jun in order to activate MMP1 promoter activity, and in contrast, ERG inhibited ETS-2-induced activation of MMP3 promoter activity (Buttice et al. 1996).

ERG physically interacted with PARP1 and DNA-PKcs in a DNA independent manner and with Ku70 and Ku80 in a DNA dependent manner. This was shown by Co-IP followed by mass spectrometry analysis or western blot analysis in VCaP cells and ERG fusion-positive human PCa tissues. ERG interacted with all four proteins through its C-terminal region, and it interacted with DNA-PKcs specifically through the ERG-ETS domain amino acid Y373. These protein interactions mediate DNA double stranded breaks and transcriptional regulation. In this same study, PARP1, DNA-PKcs, Ku70, and Ku80 were shown via Co-IP assay to bind to ERG target genes, and PARP1 and DNA-PKcs were required for ERG transcriptional activation of the gene PLA1 (Brenner et al. 2011). Another study in VCaP cells showed that ERG physically interacted with the AR, as verified by Co-IP. *In vitro* studies revealed that the ERG-AR protein-protein interaction was mediated through the ERG-ETS domain in a DNA independent manner (Yu et al. 2010).

Interestingly, a recent study showed that ERG was phosphorylated at serine residues 81 and 215 by AKT and IKK kinases in VCaP cells. AKT serine phosphorylation of ERG was shown to affect ERG transcriptional regulation of the CXCR4 gene, a known ERG binding target (Singareddy et al. 2013). This serine post-translation modification may facilitate ERG protein-protein interactions with other CXCR4 binding proteins and enhance CXCR4 transcription. This study further supports the importance of ERG protein-protein interactions in the regulation of target gene expression. Taken together, these results suggest that ERG can regulate gene transcriptional activity in a protein interaction dependent manner, which is coupled with DNA binding transcriptional regulation. In summary, TMPRSS2-ERG has been shown to regulate a

multitude of oncogenic signaling pathways in PCa including cellular invasion, migration, proliferation, dedifferentiation, AR signaling, EMT, and DNA repair.

Crosstalk between ERG and AR Signaling Pathway

It has been well established for some time now that TMPRSS2-ERG is an AR regulated gene, but more recent findings are suggesting that TMPRSS2-ERG gene regulation and AR signaling are tightly coupled in PCa. Data are beginning to emerge that strongly support the hypothesis that ERG cooperates with AR to negatively and positively regulate select AR target genes. It is almost as if ERG hijacks the AR and redirects AR target gene expression and regulation in order to facilitate tumor growth. As previously mentioned, ERG physically interacted with AR, as verified by Co-IP. In addition, ERG transcriptional regulation often occurred concomitantly with AR. ChIP assays demonstrated that ERG and AR co-occupied many androgen regulated genes, such as KLK3 (PSA) and AR. ERG had an inhibitory effect on several AR target genes involved in prostate cell differentiation, thereby inducing prostate tumor dedifferentiation (Yu et al. 2010).

Other studies have indicated that ERG activates AR target genes. One study found that ERG redirected AR to a fairly large set of genes including SOX9, and positively regulated their expression. The AR/ERG regulation of SOX9 was shown to mediate increased proliferation in mice prostates and increased invasion and proliferation in VCaP PCa cells. ChIP studies revealed that ERG and AR were bound to the SOX9 gene at an overlapping site, and AR binding to this site was dependent on ERG (Cai et al. 2013). As previously mentioned, ERG was shown to regulate the AR target gene TFF3. ERG negatively regulated TFF3 in hormone naïve PCa cells and positively regulated TFF3 in CPRC cells, and this regulation was dependent on AR

signaling. Furthermore, ERG regulation of TFF3 in CRPC cells (DU145) was shown to increase cellular invasiveness (Rickman et al. 2010). Using lentiviral infection and dissociated cell prostate regeneration approach, with engraftment in mice prostate tissue, ERG and AR cooperation was investigated. ERG overexpression alone was sufficient to induce PIN lesions in lentiviral prostate grafts, whereas AR overexpression alone did not give rise to any hyperplastic lesions. Interestingly, overexpression of ERG and AR caused development of poorly differentiated, invasive adenocarcinoma in mice lentiviral prostate grafts (Zong et al. 2009). These data strongly suggest cooperation of ERG with the AR to facilitate PCa tumor growth.

Further support that ERG can activate the AR pathway includes a previous study by Chen et al. that showed that ERG increased AR transcriptional output specifically in the context of homozygous PTEN loss. In ERG(+) and PTEN-/- prostate-specific transgenic mice, ERG increased AR binding across the genome. ERG reprogrammed the AR cistrome, meaning that in ERG(+)/PTEN-/- mice the AR had a significant amount of new binding peaks compared to control mice. In addition, 44% of ERG binding peaks overlapped with AR binding peaks. Consistent with other studies, the ERG(+)/PTEN-/- transgenic mice developed invasive prostate carcinoma (Chen et al. 2013). Another study showed that ETV1, an ERG family member, was associated with androgen synthesis and AR signaling activation, and that ERG was not associated with androgen synthesis or activation of AR signaling (Baena et al. 2013). However, this study used PTEN+/- transgenic mice, and not PTEN-/- mice as the Chen et al. study used. The difference in PTEN status of homozygous vs. hemizygous deletion may account for the differences observed between the two studies. It was shown in two independent studies that the TMPRSS2-ERG fusion was present at higher frequencies in PCa patients with PTEN-/- tumors compared to PTEN+/- tumors (71.4% vs. 44.2% and 44% vs. 18.9%, respectively), suggesting

ERG may cooperate more with a PTEN-/- environment rather than a PTEN+/- environment (Bismar et al. 2012, Bismar et al. 2011). In addition, it was shown that PCa patients with PTEN-/- tumors had a much higher risk of biochemical (PSA) failure compared to PTEN+/- tumors (Hazard Ratio 5.93 vs. 1.53; P=0.0009), further suggesting involvement of PTEN-/- status with AR signaling (Yoshimoto et al. 2008).

In contrast to the previously mentioned study that suggested ERG was not involved in androgen synthesis, findings from another study did provide a link between AR, ERG, and androgen biosynthetic enzyme expression in CRPC. VCaP tumor xenografts were injected into mice and allowed to grow to 1 cm, a time point at which mice were castrated. The xenograft tumors in castrated mice initially regressed to almost 1/4th their original size, but after 6 weeks the tumors relapsed and grew back to 1 cm, and these tumors were collected for analysis. The relapsed tumors from castrated mice showed upregulation of AR, PSA, ERG, and several enzymes from the androgen biosynthetic pathway compared to pre-castration tumors. The upregulated androgen biosynthetic enzymes (ABEs) in the relapsed tumors included AKR1C3, HSD17B3, and HSD17B6 (Cai et al. 2009). The fact that AR, ERG, and several ABEs were all present at high levels in the relapsed tumors of castrated mice suggests that these factors may play a role in the development of CRPC through increased intratumoral DHT and testosterone synthesis and AR signaling.

Androgen Biosynthetic Pathway

The androgen biosynthetic pathway begins with cholesterol as a precursor and results in the synthesis of testosterone and DHT. Under normal physiological conditions, this pathway is most prevalent in the testis and adrenal glands. These organs release testosterone and weaker

androgens such as DHEA and androstenedione into the blood stream where they enter circulation. These androgens are taken up by the prostate gland where they are synthesized into DHT (Lonergan & Tindall 2011). This pathway is important in PCa because DHT is the ligand for the AR. AR signaling helps the PCa tumor grow and progress, therefore inhibition of the androgen biosynthetic pathway can reduce AR signaling in PCa tumors (Danila et al. 2011). Several mechanisms of ADT resistance and AR antagonist resistance have been proposed. Some of these include AR overexpression and gene amplification, AR mutations that result in a gain-of-function promiscuous receptor, AR splice variants that result in a constitutively active receptor, and upregulation of ABEs resulting in intratumoral androgen synthesis (Schrecengost & Knudsen 2013).

Upregulation of ABEs and intratumoral androgen synthesis have been shown to facilitate the development of CRPC (Cai et al. 2009, Mitsiades et al. 2012, Pfeiffer et al. 2011, Rasiah et al. 2009). It is thought that upregulation of ABEs results in higher levels of intratumoral DHT and testosterone synthesis. This can be seen with the success of CYP17A1 enzyme inhibitor, abiraterone, to reduce serum and intratumoral DHT and testosterone levels in CRPC patients (de Bono et al. 2011, Efstathiou et al. 2012, Ryan et al. 2013). For example, CRPC bone metastasis patients treated with abiraterone showed reduced levels of DHT and testosterone at their tumor site as well as in their blood plasma. Patients with high AR and high CYP17A1 expression showed significantly longer time to treatment discontinuation compared to patients with lower expression. As expected, patients with higher pretreatment levels of CYP17A1 expression had significantly higher levels of testosterone at their tumor site (Efstathiou et al. 2012). Another CRPC patient study showed that high AR and high CYP17A1 expression were significantly associated with benefit in patients treated with enzalutamide, an AR antagonist (Efstathiou et al.

2014). These results suggest that overexpression of the ABE CYP17A1 results in higher levels of intratumoral testosterone and DHT synthesis, and inhibition of this enzyme can greatly reduce this synthesis. A diagram of the androgen biosynthetic pathway including the androgen metabolites and enzymes that synthesize DHT is shown in Figure 7 (Lubik et al. 2011). Also shown are the sites in the pathway where abiraterone inhibits the CYP17A1 enzyme.

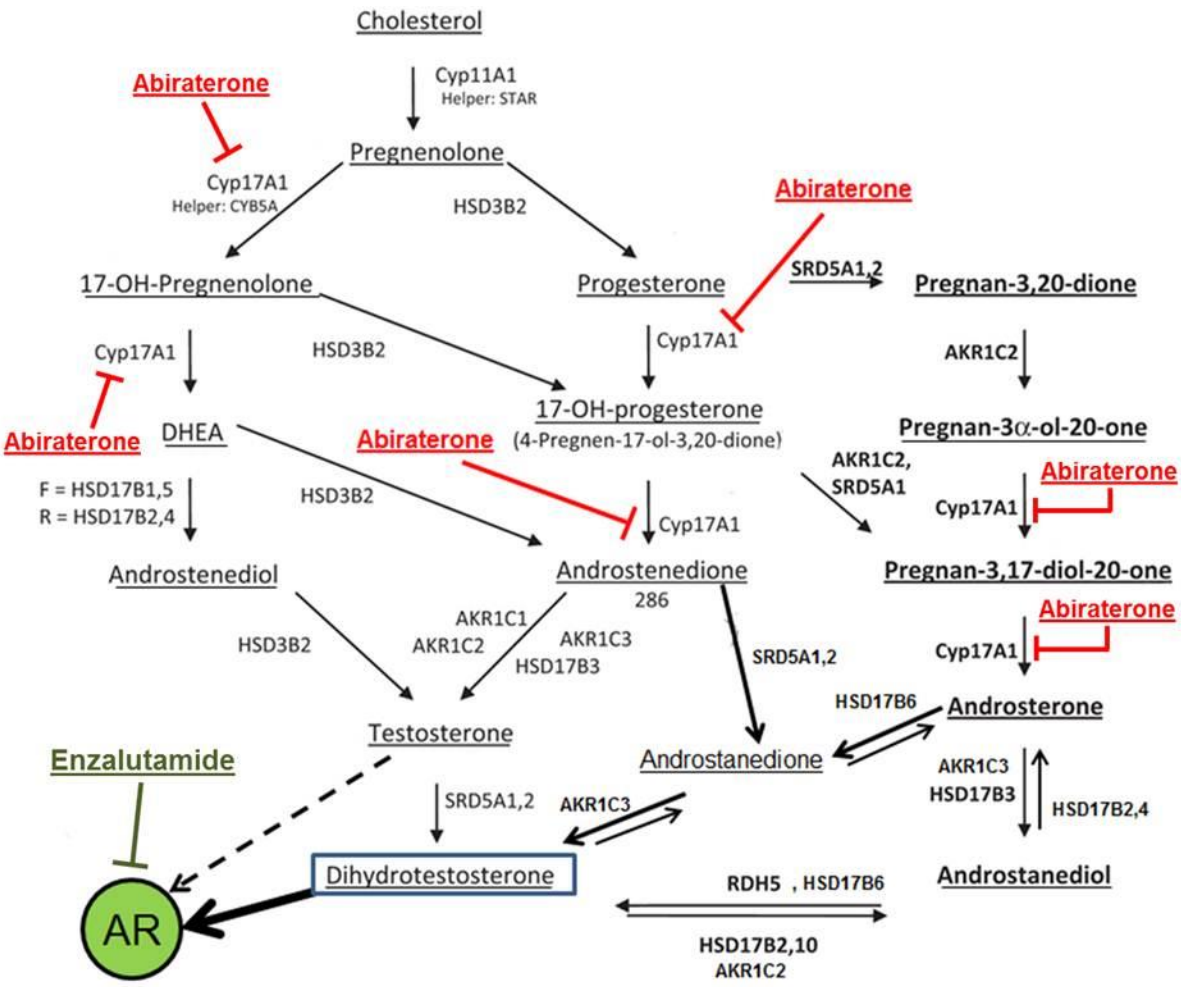

Figure 7. Diagram of the Androgen Biosynthetic Pathway. The androgen biosynthetic pathway begins at cholesterol and results in DHT synthesis. Androgen metabolites are shown as underlined and androgen biosynthetic enzymes are shown next to biochemical reaction arrows. Red text indicates sites in the pathway that are inhibited by the FDA approved drug, abiraterone, which inhibits the CYP17A1 enzyme. Green text indicates the FDA approved drug, enzalutamide, which is an AR antagonist. The backdoor pathway is shown in bold font. The dashed arrow for testosterone binding to the AR versus the bold arrow for DHT binding to the AR signifies that DHT binds to the AR with a much greater affinity compared to testosterone.

Despite the success of abiraterone in the clinic to treat CRPC patients, resistance has been shown to be a problem. In addition, patients who initially respond well to treatment may stop responding and show signs of relapse (Mostaghel et al. 2011, Yuan et al. 2014). This suggests that there may be other factors involved in intratumoral DHT synthesis, in addition to CYP17A1. In fact, it was shown in VCaP cells treated with abiraterone that this drug effectively inhibited AR signaling; however, treatment with androstenedione, a metabolite downstream of CYP17A1 enzyme, was able to restore AR signaling and induce resistance to CYP17A1 treatment. In addition, PSA levels were reduced even further in a castration-resistant VCaP cell line following treatment with a combination of abiraterone and indomethacin, an AKR1C3 enzyme inhibitor (Cai et al. 2011a). Figure 8 shows the androgen biosynthetic pathway downstream of the CYP17A1 enzyme (Bauman et al. 2006, Chang et al. 2013, Chang et al. 2011, Hamid et al. 2012, Ishizaki et al. 2013, Lubik et al. 2011, Mohler et al. 2011, Mostaghel et al. 2011, Penning 2010, Pfeiffer et al. 2011). As shown in Figure 8, there are multiple ABEs downstream of CYP17A1 that may play an important role in DHT and testosterone synthesis in PCa patients.

One ABE that has recently become of particular interest is AKR1C3; this enzyme has been shown to be highly upregulated in CRPC tumors, emphasizing its importance in the progression of this disease (Hamid et al. 2012, Mitsiades et al. 2012). AKR1C3 may play a pivotal role in the bypass pathway of DHT synthesis in CRPC. DHT is synthesized through three sources 1.) the classical pathway where DHT is synthesized from androstenedione to testosterone to DHT 2.) the bypass pathway where testosterone synthesis is bypassed and DHT is synthesized from androstenedione to 5α-androstanedione (5α-Adione) to DHT 3.) the backdoor pathway where testosterone synthesis is bypassed and DHT is synthesized from progesterone or 17-OH-progesterone to androsterone to DHT (Figure 7 and Figure 8) (Chang et al. 2011, Lubik et al.

2011, Mitsiades et al. 2012, Mohler et al. 2011). Interestingly, it was shown that bypass pathway synthesis of DHT (androstenedione → 5α-Adione) as oppose to classical pathway synthesis of DHT (androstenedione → testosterone) was the predominant pathway in 6 different PCa cell lines, as well as in metastatic CRPC tumor specimens (Chang et al. 2011). The synthesis of androstenedione → 5α-Adione → DHT is catalyzed by SRD5A1 and AKR1C3 enzymes, both of which have been shown to be overexpressed in CRPC tumors (Mitsiades et al. 2012). Inhibitors specific for AKR1C3 are currently being developed (Adeniji et al. 2013, Jamieson et al. 2012, Liedtke et al. 2013), and may prove to be beneficial for treatment of CRPC.

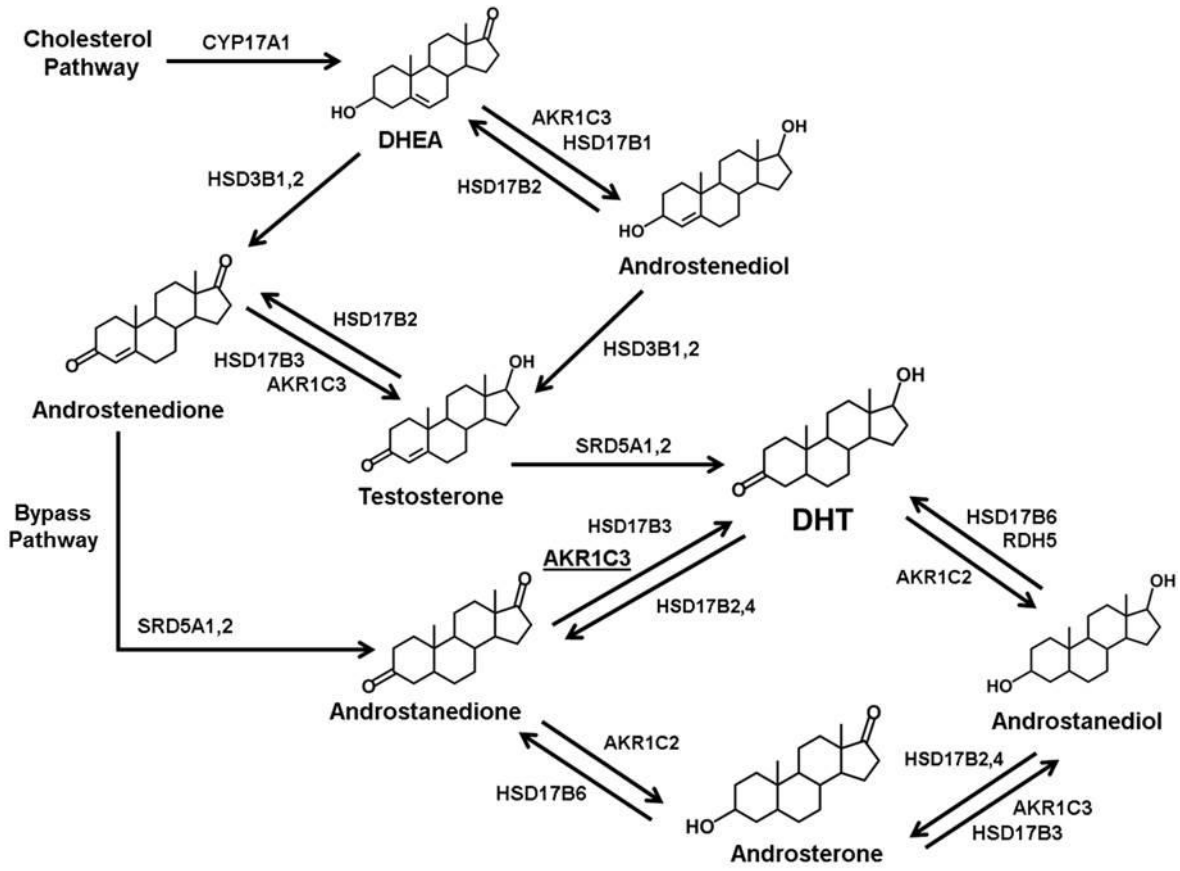

Figure 8. Diagram of the Androgen Biosynthetic Pathway Downstream of the CYP17A1 Enzyme. The androgen biosynthetic pathway downstream of the CYP17A1 enzyme is where the immediate synthesis of testosterone and DHT occur. The bypass pathway is shown where testosterone synthesis is bypassed and DHT is synthesized from androstanedione or androstanediol. Also shown are the chemical structures of the immediate androgen metabolites involved in testosterone and DHT synthesis. The arrows represent forward and backward biochemical reactions, with the enzymes that catalyze the reaction shown next to each arrow.

AKR1C3 Enzyme

AKR1C is family of aldo-keto reductases consisting four isozymes (numbered 1 to 4) with 84% amino acid sequence identity and catalyze similar reduction reactions. AKR1C isozymes are involved in the synthesis of oestrogens, progestins, and androgens, thus having an impact on hormone levels and hormone signaling. Aldo-keto reductases are NADPH dependent reductases that reduce aldehydes and ketones to their corresponding alcohols (Penning & Drury 2007). The AKR1C3 enzyme is part of the aldo-keto reductase family of enzymes. In humans, AKR1C3 has been shown to be expressed in tissues of the prostate and breast and to a lesser extent the lungs and liver. Interestingly, AKR1C3 was expressed at far greater levels in the prostate and breast tissue compared to other AKR isoforms (Penning et al. 2000). It was also shown to be expressed in tissues of the adrenal cortex (Nakamura et al. 2009).

AKR1C3 has been shown to be the predominant AKR isoform to catalyze C17-ketone reduction of several androgen metabolites in the androgen biosynthetic pathway. This results in synthesis of potent androgens testosterone and DHT, as well as weaker androgens androstanediol and androstenediol (Figure 9). Only the AKR1C3 and AKR1C1 isoforms showed measurable rates of C17-ketone reduction, and AKR1C3 catalyzed this reaction at a much higher rate and lower Km compared to AKR1C1 (Penning et al. 2000). AKR1C3 was shown to convert 5α-Adione into DHT at nearly the same rate as androstenedione into testosterone (Rheault et al. 1999). AKR1C3 has also been shown to catalyze the reduction of weak estrogen, estrone to potent estrogen, 17β-estradiol, and reduce progesterone to 20a-hydroxyprogesterone. AKR1C3 has been shown to regulate ligand access of testosterone to the AR and 17β-estradiol to the ER in prostate and breast tissues, respectively (Penning & Drury 2007, Penning et al. 2004). These findings emphasize the pivotal role of AKR1C3 as a regulator of nuclear hormone actions.

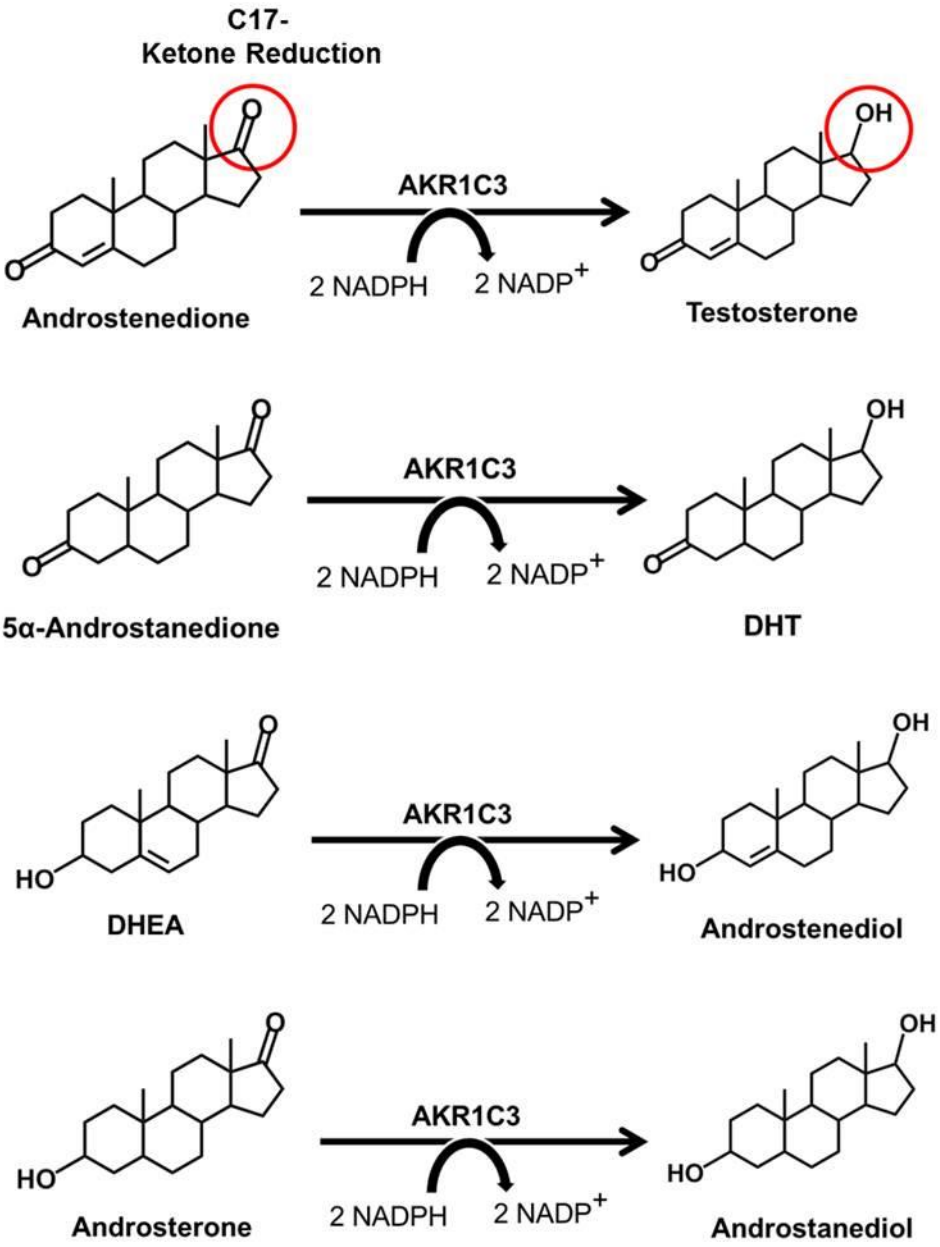

Figure 9. AKR1C3 Catalyzes C17-Ketone Reduction of Several Androgens in the Androgen Biosynthetic Pathway. Diagram illustrating AKR1C3 C17-Ketone Reduction of androstenedione, 5α-androstanedione, DHEA, and androsterone. These biochemical reactions use NADPH as a cofactor, and are therefore NADPH dependent. AKR1C3 is responsible for the synthesis of potent androgens testosterone and DHT, as well as weak androgens androstenediol and androstanediol.

Over the past decade AKR1C3 has become a focus of interest in PCa. Using immunohistochemistry (IHC), it was shown to be expressed at higher levels in human prostate carcinoma specimens compared to normal prostate specimens, and its expression was co-localized with AR expression (Fung et al. 2006). Microarray analysis showed that AKR1C3 was expressed 5.27-fold higher in androgen-independent bone metastasis prostate tumors compared to primary prostate tumors, and this was confirmed by PCR and IHC analysis. In addition, the AR and other androgen biosynthetic enzymes (ABEs), AKR1C1, AKR1C2, SRD5A1, and HSD3B2 were also shown to be overexpressed in androgen-independent bone metastatic prostate tumors, suggesting the presence of intratumoral androgen synthesis (Stanbrough et al. 2006). Similar results were seen in another study where AKR1C3 and SDR5A1 were upregulated in metastatic tumors, and AKR1C3 transcript was detected in circulating-tumor cells from CRPC patients (Mitsiades et al. 2012). AKR1C3 was shown to be associated with increased testosterone production in adrenal gland tissue (Nakamura et al. 2009), a mechanism which could possibly provide continual circulating testosterone in PCa patients being treated with ADT. Overexpression of AKR1C3 in PC3 PCa cells resulted in upregulation of genes involved in androgen signaling, activation of AKT signaling, and promotion of angiogenesis (Dozmorov et al. 2010).

More recent studies have shown that AKR1C3 is upregulated in CRPC tumors, and it has been suggested to use AKR1C3 as a biomarker for CRPC in the clinic (Hamid et al. 2012, Hofland et al. 2010). The biomarker study showed that AKR1C3 protein was more highly expressed in CRPC tumors compared to primary PCa tumors and BPH tissue. However, it was not highly expressed in all the CRPC tumors, suggesting screening CRPC patient tumors for the presence of the enzyme may be more beneficial (Hamid et al. 2012). Another study showed that

overexpression of AKR1C3 promoted growth of CRPC xenografts. This same study tested the ability of an AKR1C3 specific inhibitor, GT-x560, to inhibit AKR1C3 enzyme activity and androgen synthesis. GT-x560 treatment of HEK293 cells overexpressing AKR1C3 was shown to inhibit the synthesis of androstenedione to testosterone. Importantly, GT-x560 treatment was able to inhibit PSA activation in VCaP cells, as well as significantly inhibit xenograft tumor growth in VCaP xenograft mice and LNCaP-AKR1C3 overexpression xenograft mice *in vivo* (Yepuru et al. 2013). The abundance of studies published in the past decade showing overexpression of AKR1C3 in CRPC tumors, and a functional role of AKR1C3 in intratumoral androgen synthesis in PCa and CRPC, have prompted the development of AKR1C3 specific inhibitors for treatment of CRPC.

Implications for ERG and AKR1C3 as Therapeutic Targets in Prostate Cancer

AKR1C3 inhibition is an attractive therapeutic target for multiple reasons. AKR1C3 is an enzyme and therefore contains substrate binding pockets and cofactor binding pockets. This makes targeting the protein with small-molecule inhibitors a much more feasible task. In addition, the protein structure of AKR1C3 has been previously elucidated and can serve as a guide for development of small-molecule inhibitors (Flanagan et al. 2012, Lovering et al. 2004). Moreover, AKR1C3 is commonly overexpressed in PCa patient tumors, making it a relevant target for the clinic. AKR1C3 specific inhibitors are currently being developed for clinical use (Adeniji et al. 2013, Gazvoda et al. 2013, Heinrich et al. 2013, Jamieson et al. 2012, Liedtke et al. 2013, Watanabe et al. 2013, Yin et al. 2014); however there are currently no FDA approved AKR1C3 specific inhibitors used to treat PCa patients in the clinic.

There are some considerations to think about regarding AKR1C3 inhibitor development and treatment. Inhibitors targeting AKR1C3 should be designed to be specific for AKR1C3 and should not target other isoforms such AKR1C2. AKR1C3 synthesizes DHT and testosterone, whereas AKR1C2 breakdowns DHT (Bauman et al. 2006). It would not be wise to inhibit the breakdown of DHT for PCa treatment. In addition, it has been suggested from recent study findings that AKR1C3 specific inhibitors should only be used to treat PCa patients that overexpress this enzyme (Yin et al. 2014). Therefore, PCa patients should have their tumor biopsy validated for AKR1C3 overexpression before being treated with this drug. It has been suggested that multiple enzymes in the androgen biosynthetic pathway play a role in DHT and testosterone synthesis in PCa; therefore it may be beneficial to treat PCa patients with a combination ABE inhibitors. A patient may have greater benefit from a combination treatment of a CYP17A1 inhibitor (Abiraterone), SRD5A inhibitor (Dutasteride), and AKR1C3 specific inhibitor, compared to any of these treatments alone.

TMPRSS2-ERG inhibition is an attractive therapeutic target for multiple reasons. Almost 50% of PCa patients, including primary and advanced PCa patients, have been shown to harbor the TMPRSS2-ERG fusion gene. This provides a large population of PCa patients who may benefit from an ERG inhibitor. Only PCa tumor cells express the TMPRSS2-ERG fusion gene, which reduces the possibilities of adverse side effects in healthy tissue. TMPRSS2-ERG has been shown to have multiple oncogenic biological functions in PCa, so targeting it would impair multiple cancer pathways including cell migration and invasion, DHT biosynthesis, cell dedifferentiation, and cell proliferation. Although TMPRSS2-ERG is an attractive therapeutic target, it is a transcription factor and therefore does not contain any substrate or cofactor binding pockets. This makes targeting ERG protein with small-molecule inhibitors a very difficult task.

Inhibitors for ERG are currently being developed (Rahim et al. 2011, Shao et al. 2012); however, there are currently no FDA approved TMPRSS2-ERG inhibitors used to treat PCa patients in the clinic.

One study published findings with a small-molecule inhibitor for ERG called YK-4-297, but this inhibitor has not moved into clinical trials for ERG inhibition (Rahim et al. 2011). Another used heterocyclic dithiophene diamidines, which disrupted ERG/DNA binding, but this inhibitor has not moved into clinical trials either (Nhili et al. 2013). With small molecule inhibition of ERG being a difficult task, alternative approaches to TMPRSS2-ERG inhibition are currently being investigated. Some of these include liposomal nanovectors, peptide based vaccines, and deubiquitinase inhibition (Kissick et al. 2013, Shao et al. 2012, Wang et al. 2014). Liposomal nanovectors use siRNAs which target and inhibit the TMPRSS2-ERG mRNA sequences, preventing ERG protein synthesis. Peptide based vaccines are ERG-derived immunogenic peptides that ultimately aim to elicit an antigen-specific response in cytotoxic lymphocytes against ERG fusion-positive PCa tumor cells. Deubiquitinase inhibition is a method to inhibit the deubiquitination of ERG which ultimately leads to higher levels of ERG ubiquitination and increased ERG protein degradation. With many different groups of investigators working to discover an effective inhibitor for AKR1C3 and ERG, only time will tell whether these drug targets will be viable options for clinical trial use.

Chapter 2

Materials and Methods

Cell Lines and Treatments

Prostate cancer cell lines VCaP, LNCaP, and HEK293T cells were obtained from American Type Culture Collection (ATCC; Manassas, VA). BPH-1 cells were obtained from Dr. Shije Sheng (Wayne State University). VCaP cells were maintained in ATCC DMEM media supplemented with 10% fetal bovine serum (FBS) and 1% penicillin streptomycin (PS). LNCaP and BPH-1 cells were maintained in Gibco RPMI media (Life Technologies, Gibco, Carlsbad, CA) supplemented with 10% FBS and 1% PS. HEK293T cells were maintained in Gibco DMEM media supplemented with 10% FBS, 1% PS, and 1% sodium pyruvate. HPLC-MS/MS, Immunocytochemistry, and PSA expression experiments were performed using Gibco DMEM phenol red-free media supplemented with 1% charcoal stripped serum (C.S.S.) and 1% PS.

Lentiviral Plasmids and Transduction

The pGIPZ lentivector was used for shRNA ERG knockdown (5'-TGGACAGACTTCCAAGATG-3') and shRNA AKR1C3 knockdown (5'-ACACCAGTGTGTAAAGCTA-3') and the pLOC lentivector was used for ERG overexpression (Open BioSystems, GE Dharmacon, Lafayette, CO). Truncated ERG and full length ERG were cloned into the pLOC lentivector using restriction enzyme digest with SpeI and AscI. Cloning primers are listed in Table 3. Lentiviral particles were generated in HEK293T cells using a Trans-Lentiviral Packaging Kit (Thermo Fisher Scientific, Waltham, MA). VCaP cells were infected with pGIPZ lentiviral particles and selected with (0.3 µg/ml) puromycin for 10 days post-infection. LNCaP and BPH-1 cells were infected with pLOC lentiviral particles and selected

with (2-4 µg/ml) blasticidin for 10 days post-infection. A pooled lentiviral cell population was used for all lentiviral experiments. Transient transfections were performed using Lipofectamine2000 Transfection Reagent (Life Technologies, Invitrogen, Carlsbad, CA) in OptiMEM media obtained from Gibco.

Western Blotting and Antibodies

Western blotting was performed using SDS-PAGE with gel transfer to a nitrocellulose membrane. Membranes were blocked with 5% nonfat milk and probed with primary antibody in 5% milk. Membranes were probed with HRP-linked secondary antibody in 5% milk. Protein bands were detected using enhanced chemiluminescence (ECL) substrate and autoradiography film. Primary and secondary antibodies are listed in Table 2.

RT-PCR and RT-qPCR

RNA was extracted from VCaP, LNCaP and BPH-1 cells using the Trizol method, TRIzol was obtained from Life Technologies (Carlsbad, CA). RNA was synthesized into cDNA using the iScript cDNA synthesis kit obtained from Bio-Rad (Hercules, CA). cDNA was used as a template for primer amplification, PCR primers are listed in Table 3. For RT-PCR experiments cDNA was amplified with primers and DNA Taq polymerase using an Eppendorf Mastercycler PCR machine. PCR was performed for 25 to 40 cycles, and PCR products were loaded onto a 0.8% agarose gel containing ethidium bromide. For RT-qPCR experiments cDNA was amplified with primers and SYBR green from the SensiFAST SYBR No-Rox kit obtained from Bioline (Taunton, MA). An Eppendorf Mastercycler Realplex^2 qPCR machine was used to quantify transcript amplification levels for 40 cycles of PCR. All qPCR samples were normalized to GAPDH.

Chromatin Immunoprecipitation (ChIP) PCR

ChIP-PCR was carried out using the ChIP-IT Express kit obtained from Active Motif (Carlsbad, CA). VCaP cells were plated at a cell density of 10-20 million cells per flask. Cells were fixed with formaldehyde and chromatin was extracted according to the kit instructions. Samples containing 5 million cells per sample were sonicated using the EpiSonic Multi-Functional Bioprocessor 1000 sonicator. For IP pull downs, 15-25 µg of chromatin and 3-5 µg of primary antibody were used per sample. ERG primary antibody ERG1/2/3 (H-95)X (sc-28680X) and IgG antibody (sc-2027) were obtained from Santa Cruz Biotechnology (Dallas, TX). A control IgG pulldown was performed for each ERG pulldown in order to serve as a control for non-specific (background) pulldown. PCR was performed using 750-1000 ng DNA template per sample and run at 30-40 cycles using an Eppendorf Mastercycler PCR machine. ChIP-PCR primers are listed in Table 3. PCR products were loaded onto a 0.8% agarose gel containing ethidium bromide.

Mass Spectrometry (HPLC-MS/MS)

Androgen metabolites obtained from Steraloids and Sigma-Aldrich (St. Louis, MO) (Table 4.) were used as MS standards and *in vitro* steroid treatments. VCaP Scrambled and VCaP shERG cells were plated at a cell density of 500,000 cells per well in a 6-well plate. Cells were serum starved for 24 hours using 1% C.S.S. phenol red-free DMEM media. Cells were treated with androgen metabolites or 0.1% ethanol (vehicle control) for 24 hours in 1% C.S.S. phenol red-free media. Depending on the experiment, cells were treated with either 100 nM androgen metabolites or concentrations of 10 nM, 50 nM, or 100 nM androgen metabolites. At the end of incubation, cells and the incubation media were extracted and analyzed by LC-MS as follows: Deuterated internal standards (1 ng each of DHEA-d2 and DHT-d3) were added to the

wells and mixed thoroughly. The cells and media were collected by scraping and stored at -80 ˚C. The stored samples were thawed on ice, sonicated and the homogenate was applied to conditioned C18 solid phase extraction cartridges (Sep-Pak, Waters, Milford, MA). The cartridges were washed with water and the compounds were eluted with acetonitrile into LC-MS maximum recovery screw top glass vials obtained from MicroSOLV Technology (Eatontown, NJ). The eluates were evaporated to dryness and the residue was reconstituted in 100 µl of HPLC mobile phase (acetonitrile:water:formic acid, 60:40:0.2 v/v). The samples were analyzed for steroids by LC-MS by Wayne State University Lipidomics Core Facility using standard protocols. Data were normalized to the number of cells used in each experiment.

Immunocytochemistry and Immunofluorescence

VCaP cells were plated on cover slips at a cell density of 400,000 cells per cover slip. Cells were serum starved for 24 hours using 1% C.S.S. phenol red-free DMEM media. Cells were treated with (100 nM) 5α-Androstanedione or 0.1% ethanol (vehicle control) for 24 hours in 1% C.S.S. phenol red-free DMEM media. Cell coverslips were washed with 1X PBS, fixed with 4% Formaldehyde, permeabilized with 0.5% Triton X-100, blocked with 2% horse serum, and incubated overnight at 4 °C with either 1.) AR (rabbit) primary antibody (sc-816) obtained from Santa Cruz Biotechnology (Dallas, TX) used at dilution 1:1000 in PBS; or 2.) AR (mouse) primary antibody (sc-7305) obtained from Santa Cruz Biotechnology used at a dilution 1:1000 in PBS. Cover slips were washed with PBS and incubated at room temperature in a dark box for 1 hour with either 1.) fluorophore conjugated antibody Texas Red (rabbit) (TI-1000) obtained from Vector Labs (Burlingame, CA) used at dilution 1:200 in PBS; or 2.) fluorophore conjugated antibody Alexa Fluor 633 (mouse) (A-21050) obtained from Life Technologies, Molecular Probes (Carlsbad, CA) used at dilution 1:200 in PBS. Cover slips were mounted onto slides

using Vectashield mounting medium with DAPI obtained from Vector Labs. Slides were subjected to confocal imaging at the Wayne State University School of Medicine Microscropy, Imaging, and Cytometry Resources Core Facility using the Ziess LSM 780 confocal microscope at a magnification of 40X.

Immunohistochemistry

Formalin-fixed, paraffin-embedded serial tissue sections from human prostate tumor tissue specimens and LuCaP xenograft tumors were deparaffinized with xylene and rehydrated in graded EtOH. Endogenous peroxidase activity was blocked by incubating in 3% H_2O_2 for 20 min. Antigen retrieval was performed with Antigen Retrieval Citra Plus Solution (BioGenex, Freemont, CA) in a steamer. Slides were then blocked with Blocking Serum from ABC Vectastain Kit (Vector Labs, Burlingame, CA). Slides were incubated at 4°C overnight in a humidified chamber with antibodies directed against ERG (1:100; Epitomics, Burlingame, CA) or AKR1C3 (1:5000; Sigma-Aldrich, St. Louis, MO). After washing, sections were incubated with ABC Vectastain Kit, according to the manufacturer's protocol, followed by incubation with 3,3-diaminobenzidine tetrahydrochloride (Vector Labs). Nuclei were counterstained with Mayer's hematoxylin (Sigma-Aldrich). Sections were then dehydrated with graded EtOH, washed with xylene, and mounted with Permount (Sigma-Aldrich).

Cell Proliferation Assay

VCaP shRNA-ERG and VCaP Scrambled cells were seeded in a 96 well plate at a cell density of 17,000 cells per well in 100 µl media (DMEM ATCC + 10% Regular FBS + 1% PS + 10 µM HEPES Buffer). Cells were seeded in triplicate for day 1, day 2, day 5, and day 10 analyses. VCaP shRNA-AKR1C3 and VCaP Scrambled cells were seeded in a 96 well plate at a cell density of 19,000 cells per well in 100 µl media (DMEM ATCC + 10% Regular FBS + 1%

PS + 10 µM HEPES Buffer). Cells were seeded in triplicate for day 1, day 2, and day 5 analyses. The Cyquant NF Cell Proliferation Assay fluorescence kit (Life Technologies, Molecular Probes, Carlsbad, CA) was used to detect fluorescence for each respective day. Relative fluorescence units were quantified using a fluorescent plate reader.

Gene Expression Analysis Using Gene Expression Omnibus Database

Gene expression omnibus (GEO) publicly available microarray data was used to analyze correlation between ERG expression and AKR1C3 expression. The 25 metastatic prostate cancer expression profiles were extracted from database GDS2545 using ERG accession ID 914_g_at and AKR1C3 accession ID 37399_at, and analyzed using "GEO2R." The *in vitro* cell line expression profiles were extracted from databases GSE22010, GSE39353, and GSE39354 using ERG accession ID's 8070297, 211626_x_at, and 211626_x_at respectively, and AKR1C3 accession ID's 7925929, 209160_at, and 209160_at respectively.

Patient Survival Analysis Using Oncomine Database

The Oncomine database was used to extract survival data for 363 prostate tumor specimens from Setlur et al. "prostate cancer" (Setlur et al. 2008). Tumor specimens were from a Swedish watchful waiting cohort of patients who were diagnosed with localized PCa at stages T1-T2. Survival data was given as dead or alive at 1 year, 3 years, 5 years, and endpoint. For survival data past 5 years, the last time to follow up was used as the endpoint. Prostate tumor expression profiles were extracted from the GEO database GSE8402 using AKR1C3 accession ID DAP4_3222. AKR1C3 expression was determined as high or low by taking the median expression value of 363 tumor specimens, and adding or subtracting the standard deviation. This gave a sample size of 46 high tumors and 51 low tumors, with their respective available survival data taken from the Oncomine database. For ERG analysis, the presence or absence of the

TMPRSS2-ERG fusion gene was determined in the Setlur et al. study by FISH or PCR analysis, and this data was available in the Oncomine database as well as the GEO database. Survival data and TMPRSS2-ERG fusion status data were available for analysis from 354 of the prostate tumor specimens.

Table 2. Antibodies Used for Western Blotting Experiments.

Ab Type	Antibody Name	Company Name	Catalogue #	Dilution
1° - Rabbit	ERG-1/2/3 (C-17)X	Santa Cruz	sc-354X	1:5000
1° - Mouse	AKR1C3 Clone NP6.G6.A6	Sigma-Aldrich	A6229	1:5000
1° - Rabbit	HSD17B4	GeneTex	GTX114978	1:3000
1° - Mouse	HSD17B6	Abcam	ab88892	1:300
1° - Rabbit	GAPDH (FL-335)	Santa Cruz	sc-25778	1:5000
1° - Rabbit	AR (N-20)	Santa Cruz	sc-816	1:1000
2° - Rabbit	Rabbit HRP-linked	Cell Signaling	70745	1:5000
2° - Mouse	Mouse HRP-linked	Cell Signaling	7076	1:5000

Table 3. Primers Used for PCR, Cloning, and ChIP-PCR Experiments.

Assay	Gene Name	Forward Primer (5' to 3')	Reverse Primer (5' to 3')	
RT-qPCR/PCR	**AKR1C1**	GTAAAGCTTTAGAGGCCAC	GAGGTCAACATAATCCAATTG	mRNA
RT-qPCR/PCR	**AKR1C2**	ATTCCCATCGACCAGAGTTG	TGCAATCACGGAAGTATGGA	mRNA
RT-qPCR/PCR	**AKR1C3**	CGAGACAAACGATGGGTGG	GGCACAAAGGACTGGGTCCT	mRNA
RT-qPCR/PCR	**HSD17B1**	TATGCGAGAGTCTGGCGGTT	TGCACTGGGCCGCACT	mRNA
RT-qPCR/PCR	**HSD17B2**	GGCCATGCTTTGTGCAAGT	TCATTCAAAACTCCGGCAAAT	mRNA
RT-qPCR/PCR	**HSD17B3**	TGAAATCTTGGCGGGCTTT	GAAGGCACCGCTGTAGAAGG	mRNA
RT-qPCR/PCR	**HSD17B4**	TTGGGCCGAGCCTATGC	CCCCTCCCAAATCATTCA	mRNA
RT-qPCR/PCR	**HSD17B6**	ACTCGGGCTTTGGGAACCT	AGACACGCAGCCAGCACTC	mRNA
RT-qPCR/PCR	**HSD17B10**	TTGCTCGGGATCTGGCTCCCA	TGGCCAAGAAGTTGCACA	mRNA
RT-qPCR/PCR	**CYP17A1**	GCTGACTCTGGCGCACACT	TTGAACAGGGCAAAGGTGG	mRNA
RT-qPCR/PCR	**SRD5A1**	GGCTTGTGGTTAACGGGCAT	CAAATTTCCGGAGGTACCAC	mRNA
RT-qPCR/PCR	**SRD5A2**	CTGGAGAAATCAGCTACAGG	GCTTTCCGAGATTTGGGGTA	mRNA
RT-qPCR/PCR	**HSD3B1**	AGGACGTCTCGGTCATCATC	TTTTGCTGTGTGGGTATGGA	mRNA
RT-qPCR/PCR	**HSD3B2**	GGAAGGAGGCCCATTCCTT	CCAACACTTGACAGGATCCCA	mRNA
RT-qPCR/PCR	**RDH5**	CTGATCTGTGACCCGGACCTAA	GGGGCAGAAATAAATCAAAGTCCTT	mRNA
RT-qPCR/PCR	**PSA**	CAGGAACAAAAGCGTGATCT	CTTTGGGGTCAAGAACTCCT	mRNA
RT-qPCR	**PLAU**	AGGGCAGCACTGTGAAATAGATA	TTCCATCTGCGCAGTCATGCA	mRNA
RT-qPCR	**PLAT**	ACTGCAGAAACCCAGATCGAGACTCA	GGATTCCGGCAGTAATTATGTTTGC	mRNA
RT-qPCR/PCR	**CDC20**	CCTCTGGTCTCCCCATTAC	ATGTGTGACCTTTGAGTTCAG	mRNA
RT-qPCR/PCR	**CDK1**	CCTAGTACTGCAATTCGGGAAATT	CCTGGAATCCTGCATAAGCAC	mRNA
RT-qPCR	**UBE2C**	TGGTCTGCCCTGTATGATGT	AAAAGCTGTGGGGTTTTTCC	mRNA
RT-qPCR/PCR	**ERG**	ACCGAGCGCAGAGTTATCGT	GTGAGCCTCTGGAAGTCGTC	mRNA
RT-qPCR/PCR	**GAPDH**	ATCACCATCTTCCAGGAGCGA	GCCAGTGAGCTTCCCGTTCA	mRNA
ChIP-PCR	**PLAU**	ATTTGCAAGGCAGGAAAATG	GTGATTCTGTCACCCCCATC	Genomic
ChIP-PCR	**AKR1C3 (P1)**	TCCAATGCTGTGTATACTACTTGG	AGAAACAGGAAAACACAGTCCC	Genomic
ChIP-PCR	**AKR1C3 (P2)**	TTGTTCTGTGTCATGACGAT	TCAACATCTTGGAGTTGTCA	Genomic
ChIP-PCR	**AKR1C3 (P3)**	GATCCACCATATTGCTGAA	TCTGAAGAAGATGCAGTCCT	Genomic
ChIP-PCR	**AKR1C3 (P4)**	CTCTTACAACGCAAAGAAAG	CAAACTGACTGATGGTTAACC	Genomic
ChIP-PCR	**AKR1C3 (I1,1)**	CCTATGCACCTCCAGAGG	CTCTAGTCCAGGTCCGGTA	Genomic
ChIP-PCR	**AKR1C3 (I1,2)**	CACCCAGTATTACCGGAC	GTGTGCCAACACTCAAAG	Genomic
ChIP-PCR	**AKR1C3 (I1,3)**	GACTGTTCTCAGGAGATGGC	GTGTCTCAGTTCTTGAGATTTTGAC	Genomic
ChIP-PCR	**AKR1C3 (I1,4)**	CAAGAACTGAGACACCAAAGA	GGAACCTGGAGGAGCAAC	Genomic
ChIP-PCR	**AKR1C3 (-2.5 kb)**	GGGCTTCATACTTCTATATGGTTTC	AGACTATCTTAAAAGCAGCAGGAG	Genomic
ChIP-PCR	**AKR1C3 (-6 kb)**	TCCTTAGAAGTGACTTTAGGTGGT	CAATATCAAGAGGAACTCTCAAAGC	Genomic
Cloning (SpeI/AscI)	**ERG (full length)**	ACGTACTAGTATGGCCAGCACTATTAAGGAAG	ACGTGGCGCGCCTTAGTAGTAAGTGCCCAGATGAGAA	Cloning
Cloning (SpeI/AscI)	**ERG40 (truncated)**	ACGTACTAGTATGACCGCGTCCTCCTCC	ACGTGGCGCGCCTTAGTAGTAAGTGCCCAGATGAGAA	Cloning

Table 4. Androgen Metabolites Used for Mass Spectrometry Experiments.

Common Name	Full Name	MW	Steraloids Cat.#
Androstanedione	5α-androstan-3,17-dione	288.4	A1630-000
Androstanediol	5α-androstan-3α,17β-diol	292.5	A1170-000
Androsterone	5α-androstan-3α-ol-17-one	290.4	A2420-000
Androstenediol	5-androsten-3β,17β-diol	290.4	A7830-000
Androstenedione	4-androsten-3,17-dione	286.4	A6030-100
DHEA	5-androsten-3β-ol-17-one	288.4	A8500-000
Testosterone	4-androsten-17β-ol-3-one	288.4	A6950-000
DHEA-D2	5-androsten-3β-ol-17-one-16,16-d2	290.4	A8500-009
DHT-D3	5α-androstan-17β-ol-3-one-16,16,17-d3	293.5	A2570-020
Common Name	**Full Name**	**MW**	**Sigma-Aldrich Cat.#**
DHT	5α-androstan-17β-ol-3-one	290.4	A8380-1G

Chapter 3

TMPRSS2-ERG Regulation of the Androgen Biosynthetic Pathway in Prostate Cancer

As previously mentioned, TMPRSS2-ERG fusion gene expression persists in patients with CRPC; however, the biological role of ERG in CRPC is still currently unknown. Despite the fact that ERG is an AR regulated gene, ERG expression has been shown to be present in CRPC patients. One study showed that 60% (9/15) of CRPC patient tumor specimens expressed the TMPRSS2-ERG transcript (Attard et al. 2009). Another study showed that 73% (14/19) of CRPC patient tumor specimens expressed the ERG fusion transcript (Rickman et al. 2010). These data suggest that AR signaling does remain active in a CRPC state, even when patients may be treated with ADT that target testosterone and DHT synthesis. The exact sources of testosterone and DHT in CRPC patients still remain to be fully elucidated, but intratumoral androgen synthesis is a contributing factor (Efstathiou et al. 2012, Ryan et al. 2013). This dissertation study is focused on investigating the role of ERG in the development and progression of CRPC through upregulation of androgen biosynthetic enzyme gene expression and intratumoral DHT production.

3.1 Effects of ERG Knockdown on Androgen Biosynthetic Enzyme Expression

RESULTS

TMPRSS2-ERG fusion gene positively regulates the gene expression of androgen biosynthetic enzymes in VCaP prostate cancer cells

VCaP prostate cancer (PCa) cells naturally harbor and express the TMPRSS2-ERG fusion gene, making them a suitable model to study ERG regulation of androgen biosynthetic enzymes (ABEs) (Tomlins et al. 2005). The VCaP cells harbor the truncated form of ERG

protein formed through the T1-E4 gene fusion, with exon 1 of TMPRSS2 gene fused to exon 4 of ERG gene, resulting in truncation of the first 39 amino acids from the N-terminal of the ERG protein (King et al. 2009). T1-E4 ERG does however retain its C-terminal DNA binding domain, making transcriptional regulation of target genes still feasible. The VCaP PCa cell line was extracted from a vertebral bone metastasis tumor in a patient with castration-resistant prostate cancer (CRPC) (Korenchuk et al. 2001), and therefore this cell line represents an advanced form of PCa.

Lentiviral shRNA stable knockdown was used to knockdown endogenous ERG protein levels in VCaP cells. Lentiviral ERG knockdown was validated at the mRNA level (Figure 10A) as well as at the protein level (Figure 10B) in VCaP shERG cells; shScrambled cells were used as a non-targeted control. In addition, VCaP cells were shown to express high levels of the androgen receptor (AR), making them a relevant model to study ERG regulation of ABEs (Figure 10C). In order to test the quality of the VCaP shRNA-ERG knockdown model system, ERG target gene expression was analyzed. ERG has been shown to regulate the gene expression of plasminogen activator urokinase (PLAU), plasminogen activator tissue (PLAT), and chemokine receptor CXCR4 (Carver et al. 2009, Tomlins et al. 2008, Yu et al. 2010). Quantitative PCR (RT-qPCR) analysis revealed a significant decrease in expression of PLAU, PLAT, and CXCR4 target genes in VCaP shERG cells (Figure 11A and 11B), suggesting that the shRNA-ERG knockdown model is reliable for studying ERG gene regulation.

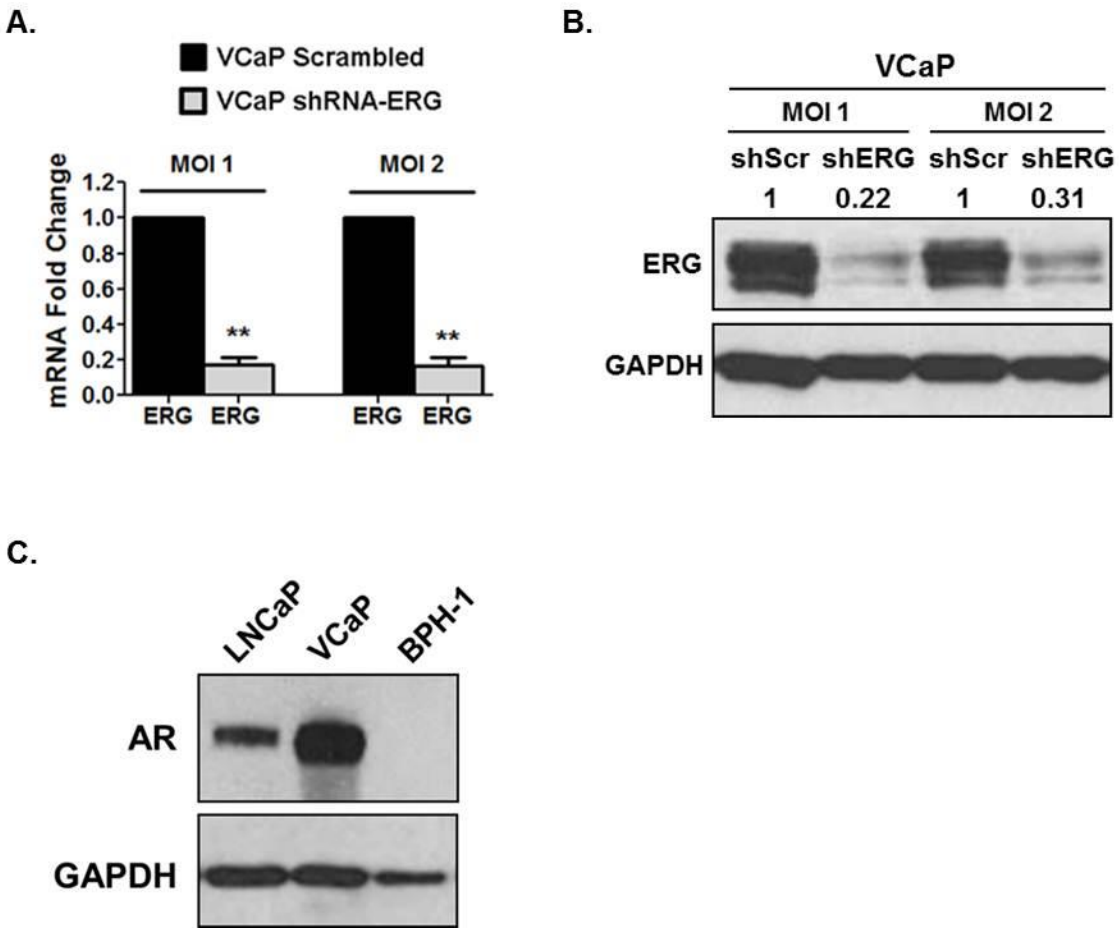

Figure 10. VCaP Prostate Cancer Cells are a Relevant Model to Study ERG Regulation of Androgen Biosynthetic Enzyme Gene Expression. A.) RT-qPCR analysis of ERG expression in VCaP shScrambled (shScr) and VCaP shERG lentiviral cells. Samples were normalized to GAPDH. Statistical analysis was a two-tailed, paired, student's t-test (N = 3) ** $P<0.01$. MOI = multiplicity of infection for lentiviral transduction. B.) Western blot analysis of ERG expression in VCaP shScrambled and shERG cells. Numbers above blot represent fold changes for ERG determined by densitometry. C.) Western blot analysis of AR expression in prostate cancer cell lines LNCaP and VCaP, as well as in benign prostatic hyperplasia cells BPH-1. For western blots GAPDH was used as a loading control.

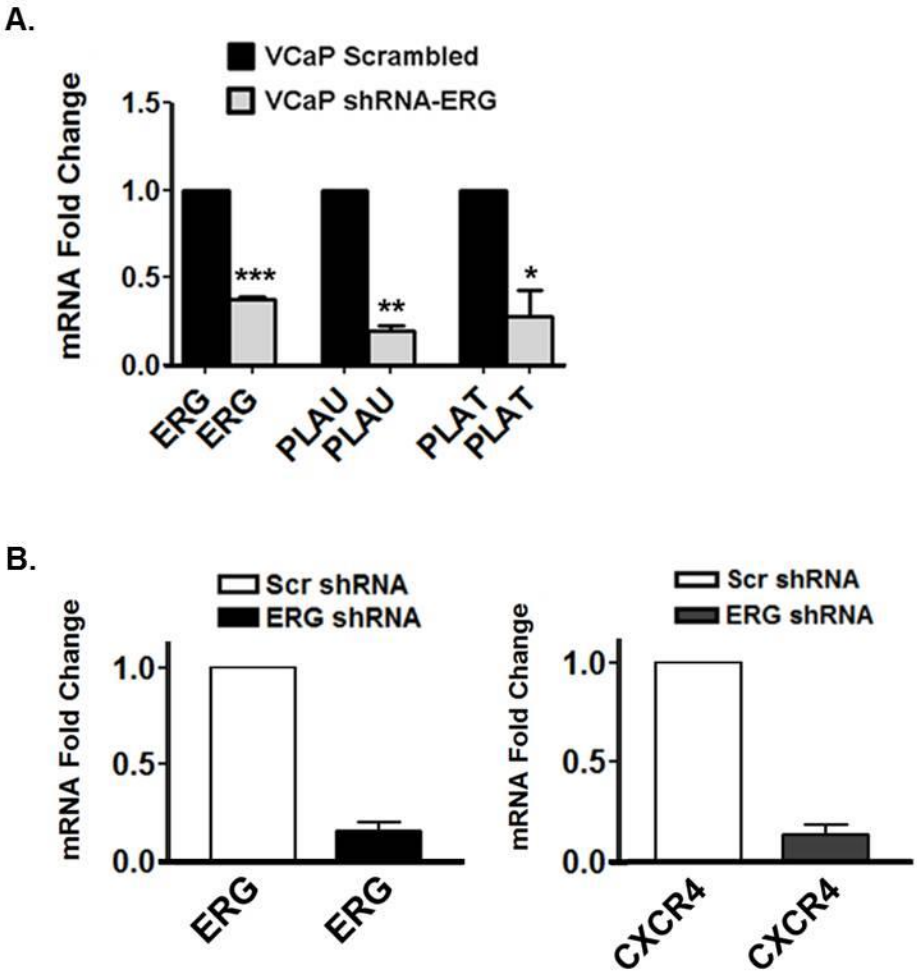

Figure 11. ERG Target Gene Expression is Reduced in ERG Knockdown Cells. A.) RT-qPCR analysis of known ERG target genes PLAU and PLAT in VCaP shScrambled and shERG cells. B.) RT-qPCR analysis of known ERG target gene CXCR4 in VCaP shScrambled and shERG cells. Samples were normalized to GAPDH. Statistical analysis was a two-tailed, paired, student's t-test (N = 3) * $P<0.05$, ** $P<0.01$, *** $P<0.001$.

RT-qPCR primers for 15 ABEs in the DHT biosynthesis pathway were used to perform a non-bias screening of ABE expression in the context of ERG knockdown. RT-qPCR analysis showed a significant decrease in many of the ABEs in VCaP shERG cells compared to shScrambled controls (Figure 12). CT values were shown in order to obtain an idea of which enzymes were most highly expressed in VCaP cells. In order to help validate the qPCR data, RT-PCR analysis of the 15 ABEs was performed in VCaP shERG and shScrambled cells at 3 different PCR cycle numbers. VCaP shERG cells had reduced expression of AKR1C3, HSD17B4, HSD17B6, and HSD3B2 enzymes compared to shScrambled controls (Figure 13A). Consistent with the RT-PCR data, RT-qPCR data indicated a significant decrease in expression of AKR1C3, HSD17B4, HSD17B6, and HSD3B2 in VCaP shERG cells (Figure 13B). Western blot analysis of VCaP shERG cells revealed a decrease in AKR1C3 (Figure 14A) and HSD17B4 (Figure 14B) protein expression compared to VCaP shSrcambled controls and VCaP cells**.** HSD17B6 enzyme was not detectable at the protein level in VCaP cells, as indicated by the human liver lysate positive control, which expressed high levels of HSD17B6 (Figure 14C).

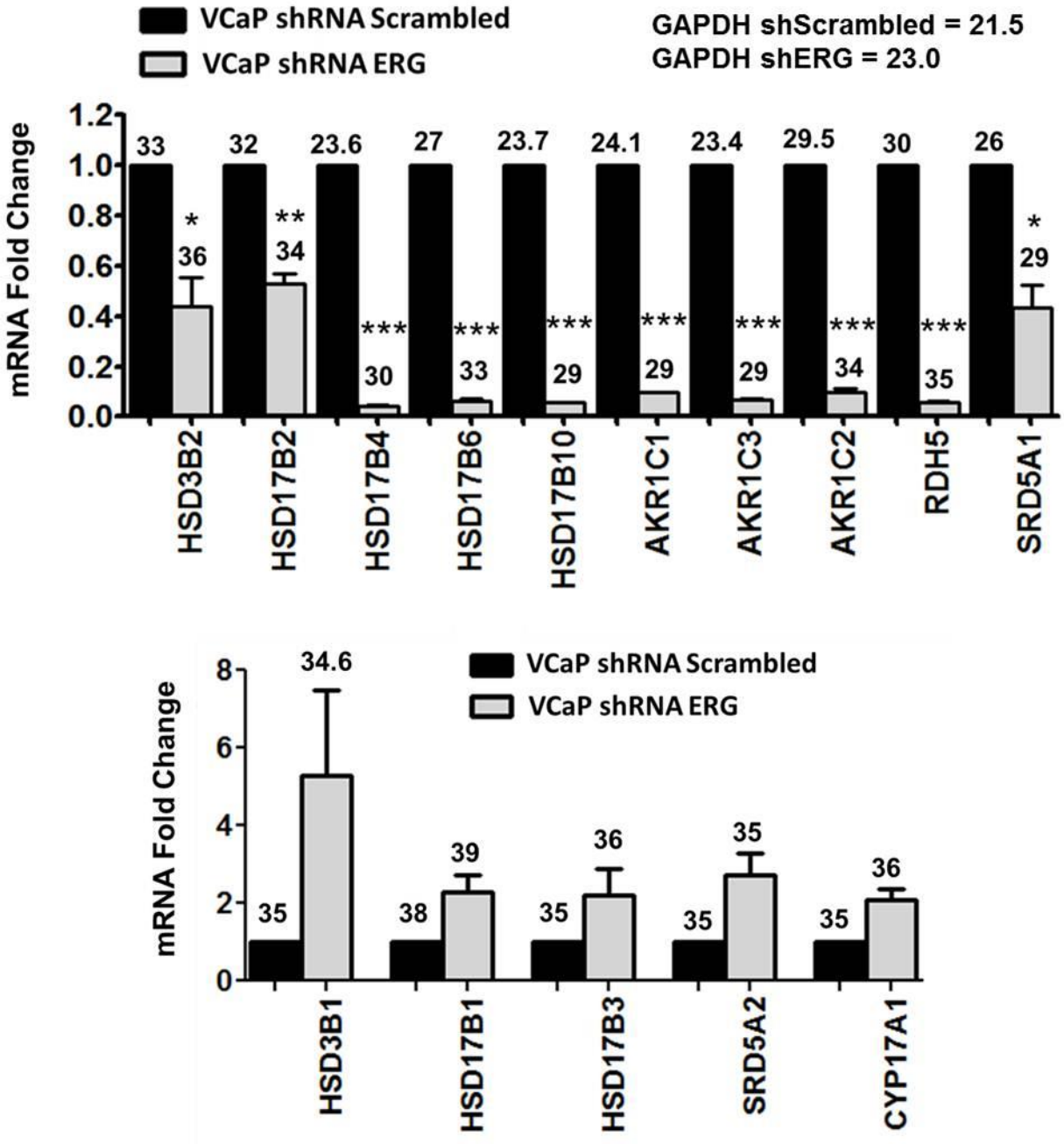

Figure 12. ERG Knockdown Reduces Androgen Biosynthetic Enzyme Gene Expression: CT Values Included. RT-qPCR analysis of ABEs in VCaP shScrambled and shERG cells. Samples were normalized to GAPDH, CT values are listed at the top of graph. CT values for ABEs are listed above each bar graph. Statistical analysis was a two-tailed, paired, student's t-test (N = 3) * P<0.05, ** P<0.01, *** P<0.001.

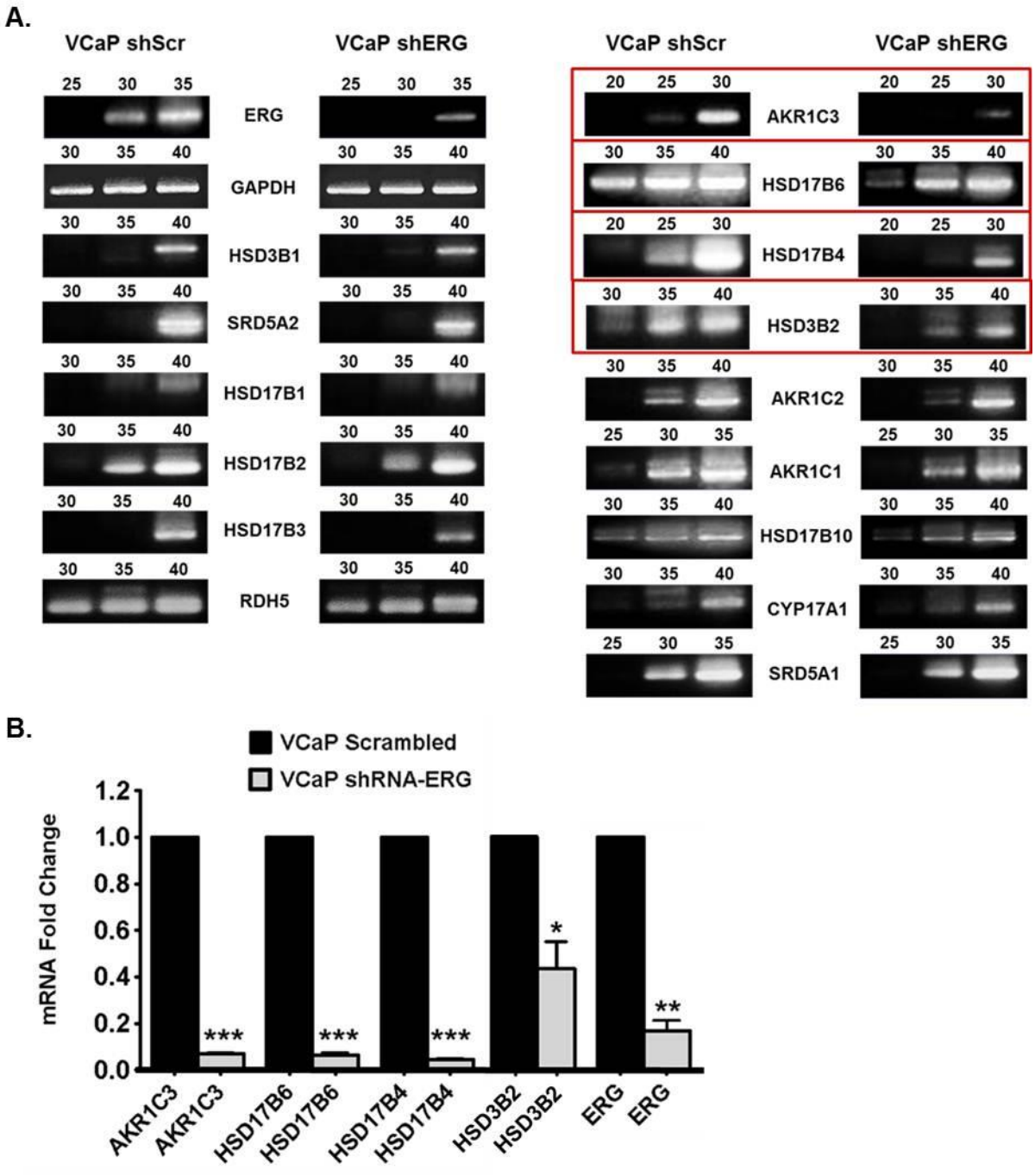

Figure 13. ERG Knockdown Reduces Androgen Biosynthetic Enzyme mRNA Expression. A.) RT-PCR analysis of ABE expression in VCaP shScrambled (shScr) and VCaP shERG cells. PCR cycle numbers are indicated above each DNA gel. B.) RT-qPCR analysis of ABEs in VCaP shScrambled and shERG cells. ABEs that were most consistent between RT-PCR and RT-qPCR data are shown (red boxes in panel A). Samples were normalized to GAPDH. Statistical analysis was a two-tailed, paired, student's t-test (N = 3) * P<0.05, ** P<0.01, *** P<0.001.

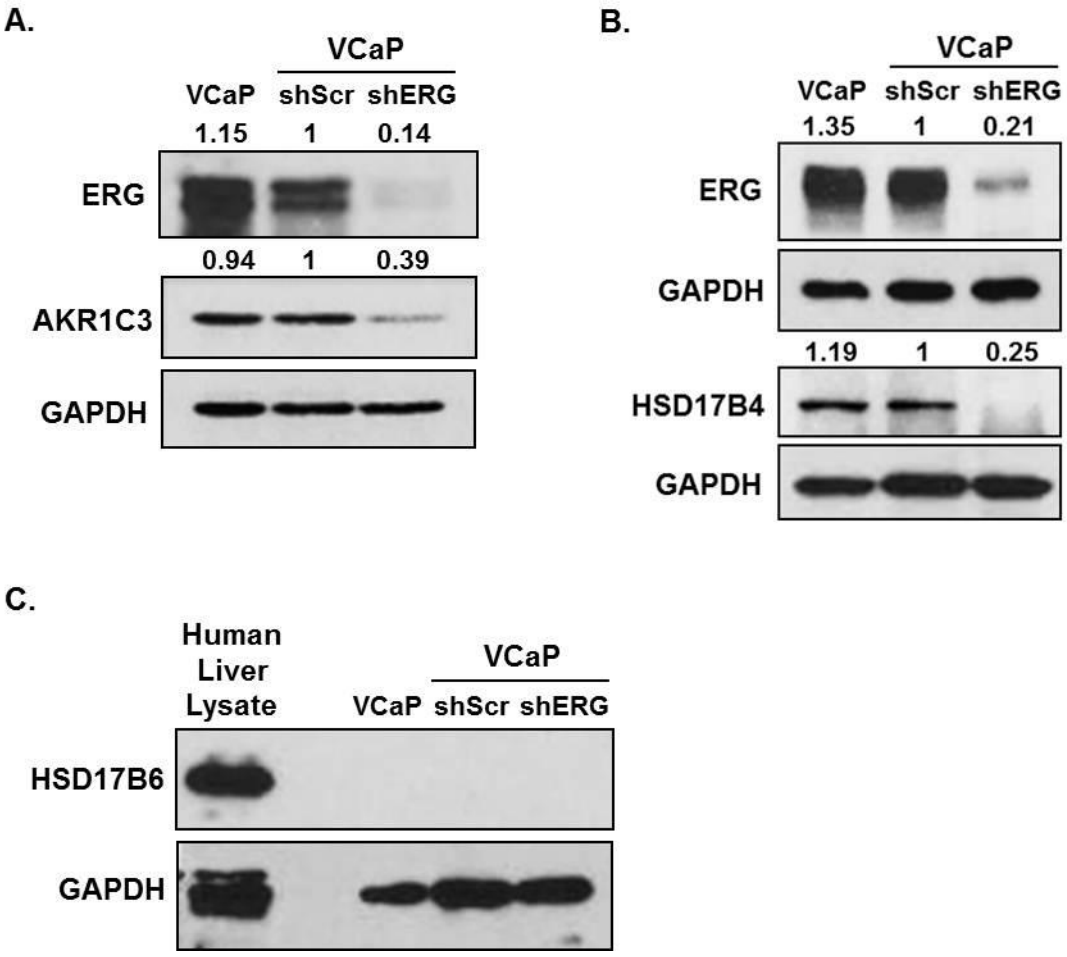

Figure 14. ERG Knockdown Reduces Androgen Biosynthetic Enzyme Protein Expression. A.) Western blot analysis of AKR1C3 expression in VCaP, VCaP shScrambled, and VCaP shERG cells. Numbers above blots represent fold changes for ERG and AKR1C3 determined by densitometry. B.) Western blot analysis of HSD17B4 expression in VCaP, VCaP shScrambled and shERG cells. Numbers above blots represent fold changes for ERG and HSD17B4 determined by densitometry. C.) Western blot analysis of HSD17B6 expression in Human Liver Lysate, VCaP, VCaP shScrambled and shERG cells. For western blots GAPDH was used as a loading control.

DISCUSSION

Results from the VCaP shERG knockdown model suggest that TMPRSS2-ERG positively regulates the expression of several androgen biosynthetic enzymes (ABEs) involved in DHT synthesis, including AKR1C3, HSD17B4, HSD17B6, and HSD3B2. According to the RT-PCR data at cycle 30, and the CT values from the RT-qPCR data, the most highly expressed ABEs in VCaP cells were HSD17B4, AKR1C3, HSD17B6, SRD5A1, and AKR1C1. It is interesting that ERG was shown to regulate 3 of the 5 most highly expressed enzymes in the DHT synthesis pathway. These data suggest that ERG may increase the production of DHT in VCaP cells through upregulation of ABEs. In addition, this would provide a feed-forward activation loop for TMPRSS2-ERG expression by providing continual ligand to the AR.

It was surprising to see that HSD17B6 enzyme was not expressed at detectable amounts at the protein level in VCaP cells, as the RT-PCR data indicated otherwise. However, the RT-qPCR data in VCaP shScrambled cells did indicate that AKR1C3 and HSD17B4 had CT values of 23.5, whereas the CT value for HSD17B6 was only 27; indicating much lower expression. It is unclear at this time as to why ERG was shown to regulate HSD17B6 at the mRNA level when it was not expressed at the protein level. Thus, the significance of ERG's regulation of HSD17B6 gene expression in VCaP cells is currently unknown. The HSD3B2 enzyme has not yet been investigated at the protein level; thus, future experiments will be needed to further investigate ERG's regulation of the HSD3B2 enzyme.

3.2 Effects of ERG Overexpression on AKR1C3 Enzyme Expression

RESULTS

Overexpression of ERG in LNCaP PCa cells and BPH-1 cells leads to upregulation of AKR1C3 enzyme expression

Previous data indicated that knockdown of endogenous TMPRSS2-ERG expression in VCaP cells reduced the expression of AKR1C3 enzyme. As a proof of principle model, truncated ERG (ERG40) was overexpressed in LNCaP PCa cells and BPH-1 benign prostatic hyperplasia cells, and AKR1C3 expression was assessed. LNCaP and BPH-1 cells do not harbor the TMPRSS2-ERG fusion gene and do not express ERG protein, thus making these cell lines a suitable model for ERG40 overexpression. Lentivirus was used to overexpress ERG40 in LNCaP and BPH-1 cells, and ERG40 mRNA expression (Figure 15B and 15D) and protein expression (Figure 15A and 15C) were shown to be increased compared to empty vector controls. The correct truncation size of ERG40 was confirmed in LNCaP ERG40 cells by comparing protein band size to VCaP cells, which were shown to harbor the truncated ERG40 protein (Figure 15E). As expected, the LNCaP ERGwt (wild type) protein band was shifted higher on the gel compared to the ERG40 protein band (Figure 15E). This is due to the fact that ERG40 protein has a truncation of the first 39 amino acids from the N-terminus of the protein (King et al. 2009) (Figure 15F). Truncated ERG40 results from TMPRSS2 exon 1 being fused to ERG exon 4, and this form of TMPRSS2-ERG has been shown to be the most commonly expressed ERG variant in PCa patients (Wang et al. 2006).

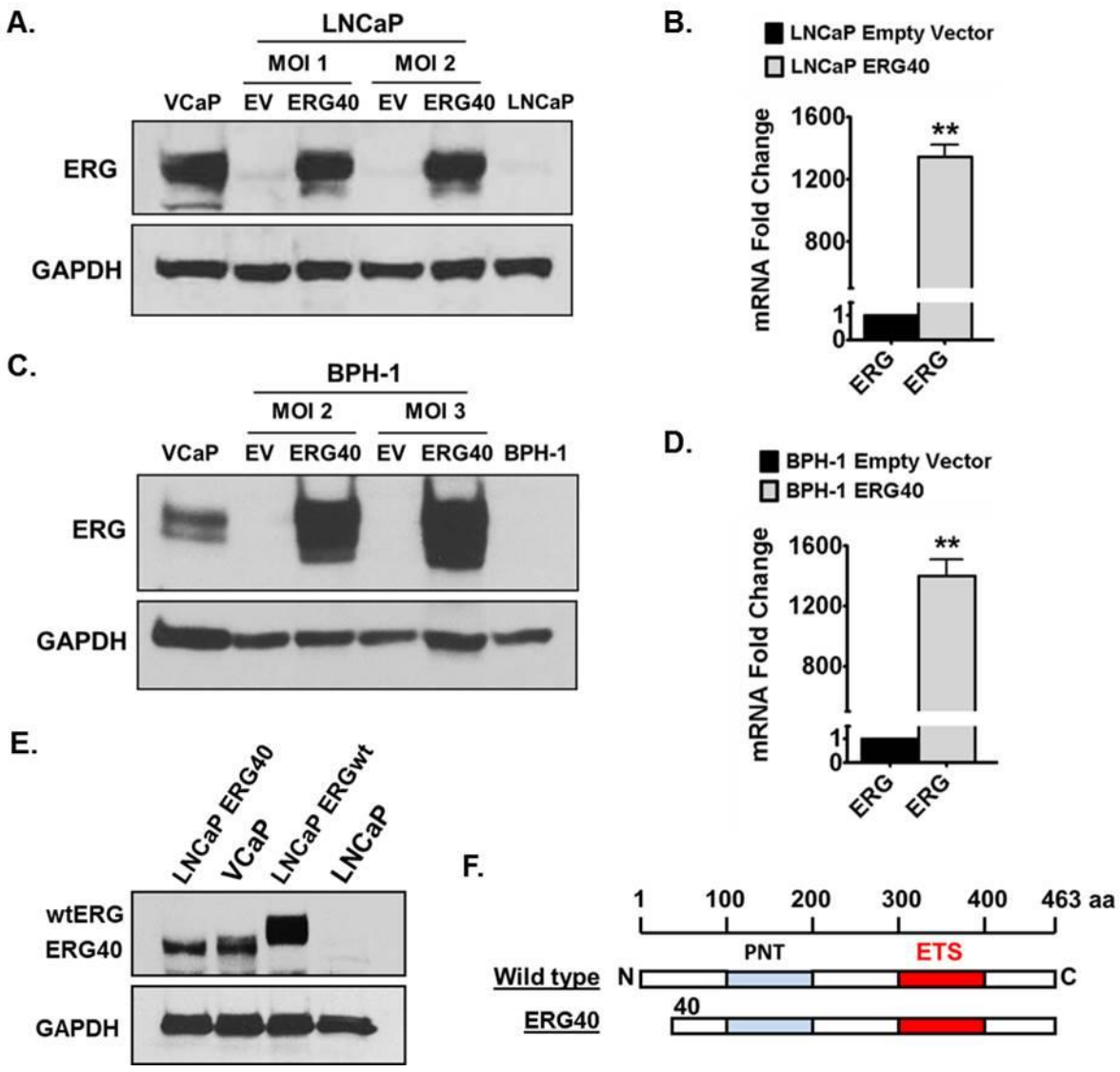

Figure 15. Validation of ERG40 Lentiviral Overexpression. A.) Western blot analysis of ERG expression in LNCaP cells infected with ERG40 lentivirus at multiplicity of infection (MOI) 1 and MOI 2. B.) RT-qPCR analysis of ERG expression in LNCaP ERG40 cells. C.) Western blot analysis of ERG expression in BPH-1 cells infected with ERG40 lentivirus at MOI 2 and MOI 3. D.) RT-qPCR analysis of ERG expression in BPH-1 ERG40 cells. For RT-qPCR samples were normalized to GAPDH. Statistical analysis was a two-tailed, paired, student's t-test (N = 3) ** $P<0.01$. For western blots GAPDH was used as a loading control. EV = empty vector control. E.) Western blot analysis of ERG40 expression in VCaP cells and LNCaP ERG40 cells, and ERG wild type (wt) expression in LNCaP ERGwt cells. F.) Diagram representing the amino acid (aa) protein structure of ERGwt protein and ERG40 protein, showing truncation of the first 39 aa from the N-terminus of ERG40. ETS is the DNA binding domain; PNT is the regulatory domain.

ABE gene expression was screened in LNCaP ERG40 cells and CT values were shown in order to obtain an idea of which enzymes were most highly expressed in LNCaP cells. RT-qPCR analysis revealed a significant increase in AKR1C3 and HSD17B2 expression in LNCaP ERG40 cells compared to empty vector controls; however the CT value for HSD17B2 was so high that conclusions from this would be unreliable (Figure 16). In addition, a small but significant increase in expression of HSD17B4, HSD17B6, HSD17B10, and AKR1C2 was seen in LNCaP ERG40 cells compared to empty vector controls (Figure 16). Data from the LNCaP ERG40 cells revealed that the AKR1C3 enzyme was the most highly regulated by ERG40 overexpression, warranting further investigation at the protein level. Using the ERG40 overexpression models, AKR1C3 mRNA and protein expression levels were assessed in LNCaP and BPH-1 cells. AKR1C3 mRNA and protein expression were significantly increased in LNCaP ERG40 cells compared to empty vector controls (Figure 17A and 17B). In addition, AKR1C3 mRNA and protein expression were increased in BPH-1 ERG40 cells compared to empty vector controls (Figure 17C and 17D). Interestingly, AKR1C3 mRNA and protein expression were also significantly increased in LNCaP ERGwt cells compared to empty vector controls (Figure 17E and 17F). These data are consistent with the ERG knockdown data and suggest that ERG positively regulates the expression of AKR1C3 in PCa cells.

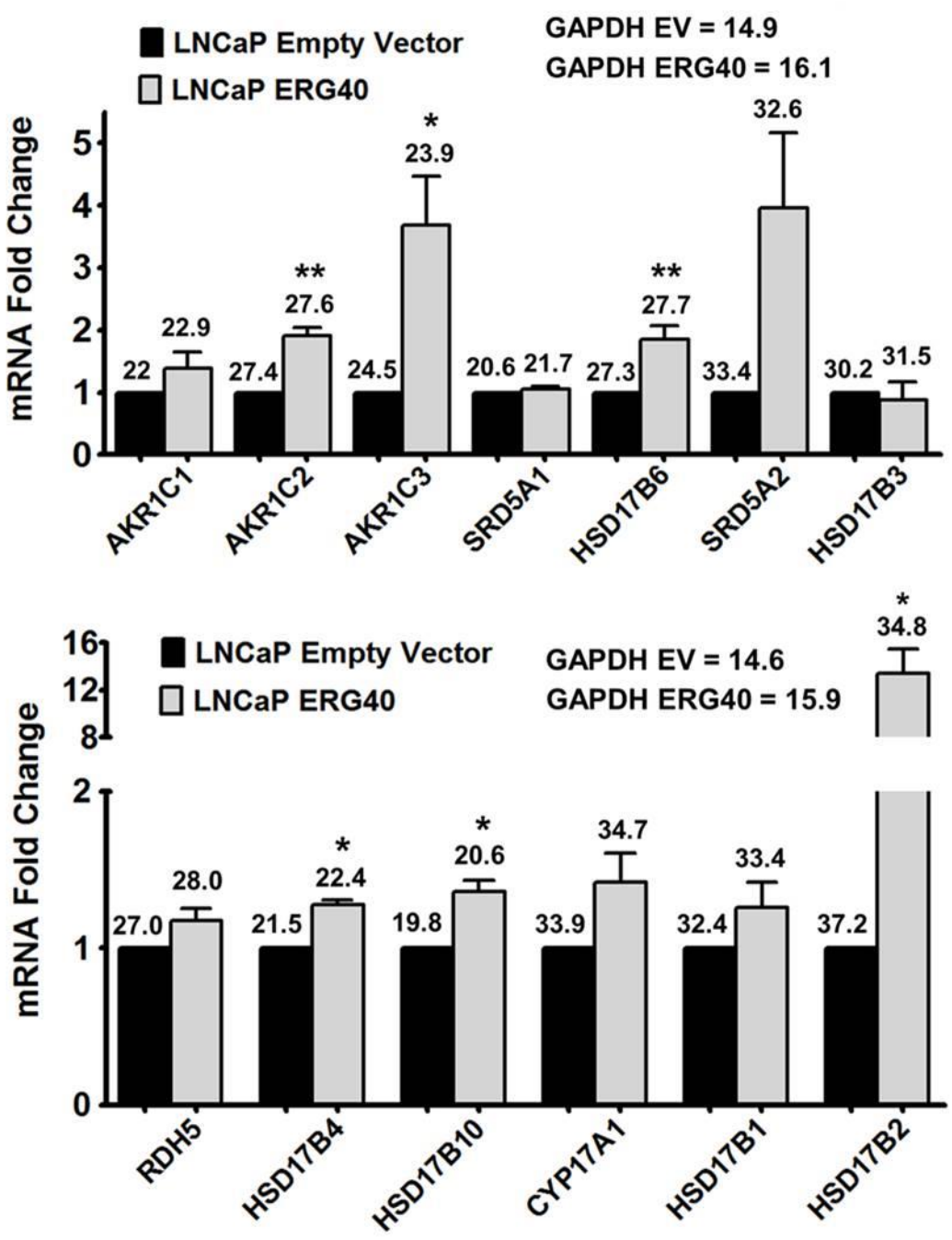

Figure 16. ERG Overexpression Increases Androgen Biosynthetic Enzyme Gene Expression: CT Values Included. RT-qPCR analysis of ABEs in LNCaP ERG40 cells. Cells were grown in 1% C.S.S. phenol-red free for 48 hours prior to RNA collection. Samples were normalized to GAPDH, CT values are listed at the top of graph. CT values for ABE are listed above each bar graph. Statistical analysis was a two-tailed, paired, student's t-test (N = 3) * $P<0.05$, ** $P<0.01$.

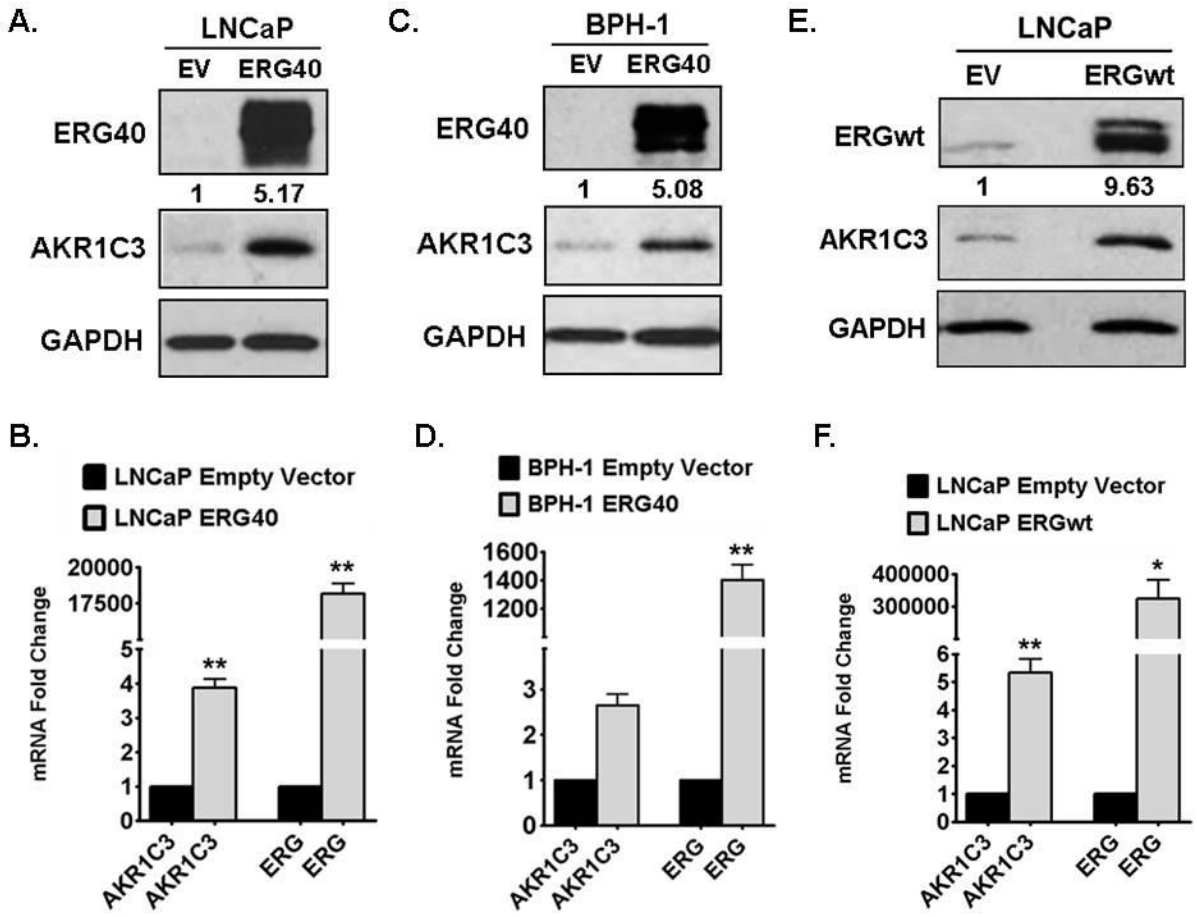

Figure 17. ERG40 and ERGwt Overexpression Increases AKR1C3 mRNA and Protein Expression in LNCaP and BPH-1 Cells. A.) Western blot analysis of AKR1C3 expression in LNCaP ERG40 lentiviral cells. B.) RT-qPCR analysis of AKR1C3 expression in LNCaP ERG40 cells. C.) Western blot analysis of AKR1C3 expression in BPH-1 ERG40 lentiviral cells. D.) RT-qPCR analysis of AKR1C3 expression in BPH-1 ERG40 cells. E.) Western blot analysis of AKR1C3 expression in LNCaP ERGwt cells. F.) RT-qPCR analysis of AKR1C3 expression in LNCaP ERGwt cells. For RT-qPCR samples were normalized to GAPDH. Statistical analysis was a two-tailed, paired, student's t-test (N = 3) * $P<0.05$, ** $P<0.01$. For western blots GAPDH was used as a loading control. EV = empty vector control. Numbers above blot represent fold changes in AKR1C3 determined by densitometry.

AKR1C3 gene expression has been shown to be regulated by androgen levels in the media, with high androgen levels inhibiting AKR1C3 expression and low androgen levels increasing AKR1C3 expression (Cai et al. 2011b, Hamid et al. 2012, Mitsiades et al. 2012). This hypothesis was investigated in VCaP and LNCaP cells in the context of ERG regulation. Consistent with published data, AKR1C3 was shown to be increased in expression when treated with androgen starved media (1% charcoal stripped serum, 1% C.S.S.), and this increase was diminished with the addition of 100 nM 5α-Adione, a DHT precursor androgen (Figure 18A). ERG expression was shown to be reduced when treated with androgen starved media (1% C.S.S.), and this reduction was rescued with the addition of 100 nM 5α-Adione (Figure 18A). VCaP shERG cells were treated with 1% C.S.S. media or 100 nM 5α-Adione supplemented media in order to investigate ERG's regulation of AKR1C3 expression in low and high androgen media conditions; with 1% C.S.S being low androgen conditions and 5α-Adione supplemented media being high androgen conditions. RT-PCR data showed that VCaP shERG cells had reduced AKR1C3 expression in both 1% C.S.S. media and 5α-Adione supplemented media compared to shScrambled controls (Figure 18B). LNCaP ERG40 cells were treated with 1% C.S.S. media or 100 nM 5α-Adione supplemented media in order to further investigate ERG's regulation of AKR1C3 expression in low and high androgen media conditions. RT-qPCR data showed that LNCaP ERG40 cells had significantly increased AKR1C3 expression in both 1% C.S.S. media and 5α-Adione supplemented media compared to empty vector controls (Figure 18C).

Microarray data of AKR1C3 and ERG expression in VCaP siRNA knockdown cells treated with either 1% C.S.S. media or DHT supplemented media were extracted from Gene Expression Omnibus database GSE39354. The microarray data were used to investigate ERG's

regulation of AKR1C3 expression under different androgen media conditions; with 1% C.S.S being low androgen conditions and DHT supplemented media being high androgen conditions. A Pearson's correlation plot was performed for AKR1C3 and ERG expression in 1% C.S.S. media, and data revealed that there was a very strong and significant correlation between AKR1C3 and ERG expression ($r = 0.90$) (Figure 19A). In addition, a correlation plot was performed for AKR1C3 and ERG expression in DHT supplemented media, and data revealed that there was a very strong and significant correlation between AKR1C3 and ERG expression ($r = 0.87$) (Figure 19B).

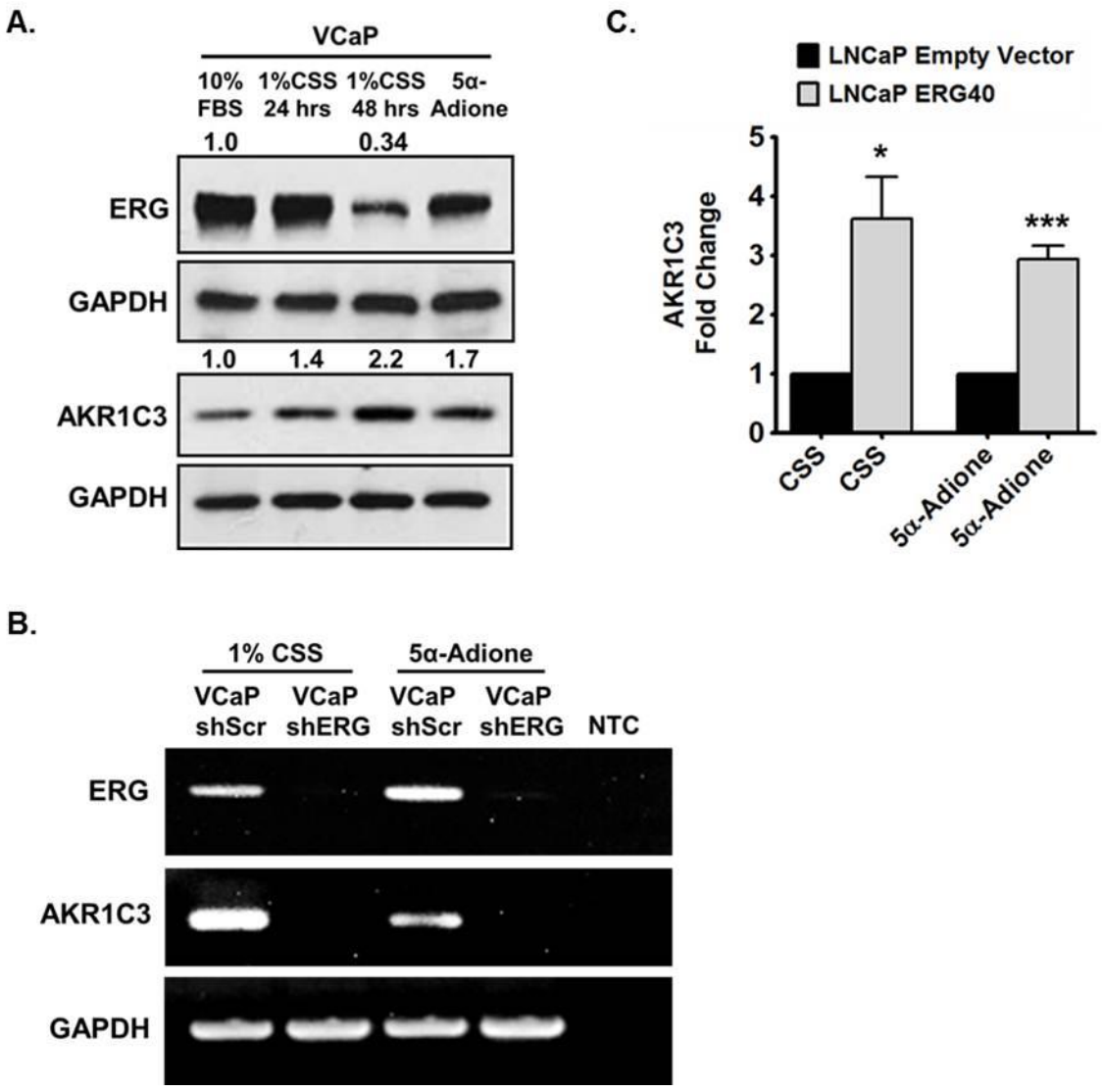

Figure 18. ERG Regulates AKR1C3 Gene Expression During High and Low Androgen Conditions in Prostate Cancer Cells. A.) Western blot analysis of AKR1C3 and ERG expression in VCaP cells treated with four different androgen media conditions 1.) 10% FBS 2.) 1% C.S.S. for 24 hours 3.) 1% C.S.S. for 48 hours 4.) 1% C.S.S. 24 hours + 100 nM 5α-Adione for 24 hours. GAPDH was used as a loading control. Numbers above blots represent fold changes determined by densitormetry. B.) RT-PCR analysis of AKR1C3 and ERG expression in VCaP shERG cells treated with either 1% C.S.S. for 48 hours or 100 nM 5α-Adione for 24 hours. GAPDH was used as a loading control. NTC is non-template control. C.) RT-qPCR analysis of AKR1C3 expression in LNCaP ERG40 cells treated with either 1% C.S.S. for 48 hours or 100 nM 5α-Adione for 24 hours. Samples were normalized to GAPDH. Statistical analysis was a two-tailed, paired, student's t-test (N = 6) * $P<0.05$, *** $P<0.001$.

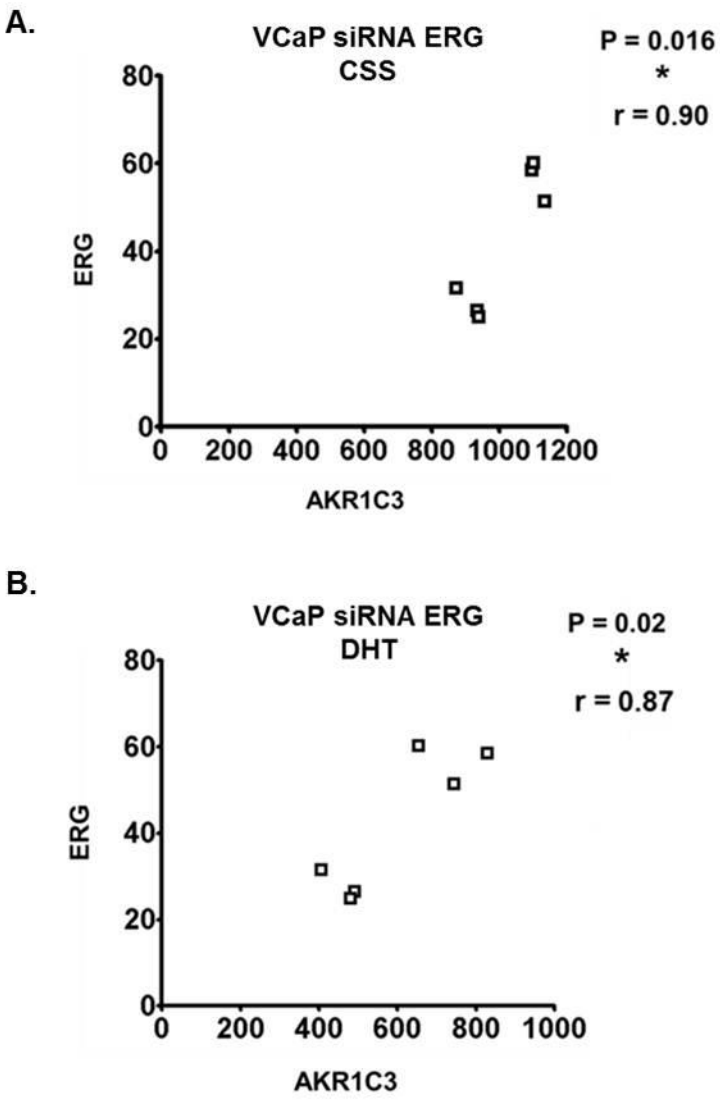

Figure 19. Positive Correlation Between ERG Expression and AKR1C3 Expression During High and Low Androgen Conditions in Prostate Cancer Cells. Correlation plots of ERG and AKR1C3 expression in VCaP siRNA cells treated with A.) 1% C.S.S. media for 48 hours or B.) DHT treated media for 48 hours. Microarray data for ERG and AKR1C3 expression was extracted from Gene Expression Omnibus database GSE39354. Statistical analysis was a Pearson's correlation plot (N =6) with an r value of r = 0.90, * P <0.05.

DISCUSSION

The ERG overexpression data in LNCaP and BPH-1 cells suggests that TMPRSS2-ERG transcription factor positively regulates AKR1C3 enzyme expression. Importantly, ERG was not only shown to regulate AKR1C3 gene transcription at the mRNA transcript level, but also at the protein level. This suggests a functional consequence of ERG's regulation of AKR1C3, wherein this enzyme can enhance DHT production and increase AR activation in PCa cells. It was interesting to see that truncated ERG40 and ERGwt protein overexpression were both shown to increase AKR1C3 expression. This is not surprising considering the ERG40 protein does retain its highly conserved ETS, C-terminal, DNA binding domain. ERG40 can therefore retain its ability to directly bind DNA, in the same manner as its full-length ERGwt counterpart. This finding does not rule out the possibility that truncated ERG40 may have novel biological functions compared to ERGwt in certain contexts. It does however suggest that ERG induced AKR1C3 overexpression is mediated by overexpression of TMPRSS2-ERG, and not by novel biological functions of the ERG40 protein.

The androgen conditioned media studies indicated that ERG and AKR1C3 are inversely regulated by androgen levels and most likely AR signaling. At first appearance this finding seems to contradict the previous results which showed that ERG positively regulated AKR1C3 expression, because in Figure 18A as ERG expression decreased, AKR1C3 expression increased. However, further results suggested that although ERG and AKR1C3 are inversely regulated by the AR, ERG still regulated AKR1C3 expression independent of androgen levels (Figure 18B and 18C; Figure 19A and 19B). It may be that AR regulates AKR1C3, AR regulates ERG, and ERG regulates AKR1C3 expression. These data indicate that ERG regulates AKR1C3 expression independent of AR and DHT regulation. Interestingly, it has been suggested in the

published literature that AKR1C3 regulation by androgens is a feedback mechanism used by the cell in order to maintain a steady balance of intracellular androgen levels (Cai et al. 2011b, Mitsiades et al. 2012). This prevents androgen levels from becoming too high or too low, neither of which are optimal for PCa tumor growth. Indeed, many enzymes in biochemical pathways are subject to feedback loops; when their product becomes too high the gene is turned off, and when their product becomes too low the gene is turned back on. This may very well be the case for the AKR1C3 gene, and this further supports the pivotal role of AKR1C3 as a DHT synthesis enzyme in PCa cells.

3.3 Direct Binding of ERG to the AKR1C3 gene

RESULTS

TMPRSS2-ERG fusion gene binds directly to three regions of the AKR1C3 gene

Chromatin immunoprecipitation (ChIP) PCR was used in order to determine if TMPRSS2-ERG regulation of AKR1C3 enzyme was occurring through a direct DNA binding mechanism. Genomic ChIP-PCR primers were designed that spanned -2 kb and + 2 kb of the AKR1C3 gene region, relative to the transcription start site (TSS). This region includes the promoter and intron 1 region of the AKR1C3 gene; therefore primers were designated as P1-P4 for the promoter region and I1-I4 for the intron 1 region. Primers were specifically designed to amplify regions of the AKR1C3 gene that contained putative ERG consensus binding sites (5'-GGAA/T-3'), and each primer amplified a region of approximately 500 bp (Figure 20A). ChIP-PCR data from VCaP cells indicated that ERG was bound to the intron 1 region directly

downstream of the TSS for AKR1C3, and was not bound to the promoter region upstream of the TSS (Figure 20B).

Plasminogen activator urokinase (PLAU) gene has been shown previously to be a direct binding target gene of TMPRSS2-ERG in VCaP cells (Tomlins et al. 2008, Yu et al. 2010). PLAU gene was used as a positive control for ERG binding in the ChIP-PCR assay, and was indeed shown to be bound by ERG in VCaP cells. In addition, negative control primers were designed that amplified two separate regions of the AKR1C3 gene that do not contain any putative ERG consensus binding sites (-2.5 kb and -6 kb upstream of TSS). Negative control primers revealed that there was no ERG binding to these sites in the AKR1C3 gene in VCaP cells. Positive and negative control primers helped validate that ERG was bound to the AKR1C3 intron 1 region, directly downstream of the TSS (Figure 20C). In order to further interrogate ERG binding to the AKR1C3 gene region in VCaP cells, ChIP-Seq was performed in duplicate. ChIP-Seq data revealed that ERG was bound to the AKR1C3 gene region in three separate locations along the gene. ERG binding could be positively identified by binding enrichment peaks seen along the AKR1C3 gene. A smaller ERG binding peak was identified near the intron 1 region downstream of the TSS, which was consistent with the ChIP-PCR data. In addition, two larger ERG binding peaks were identified far upstream of the TSS near -50 kb and -75 kb (Figure 21).

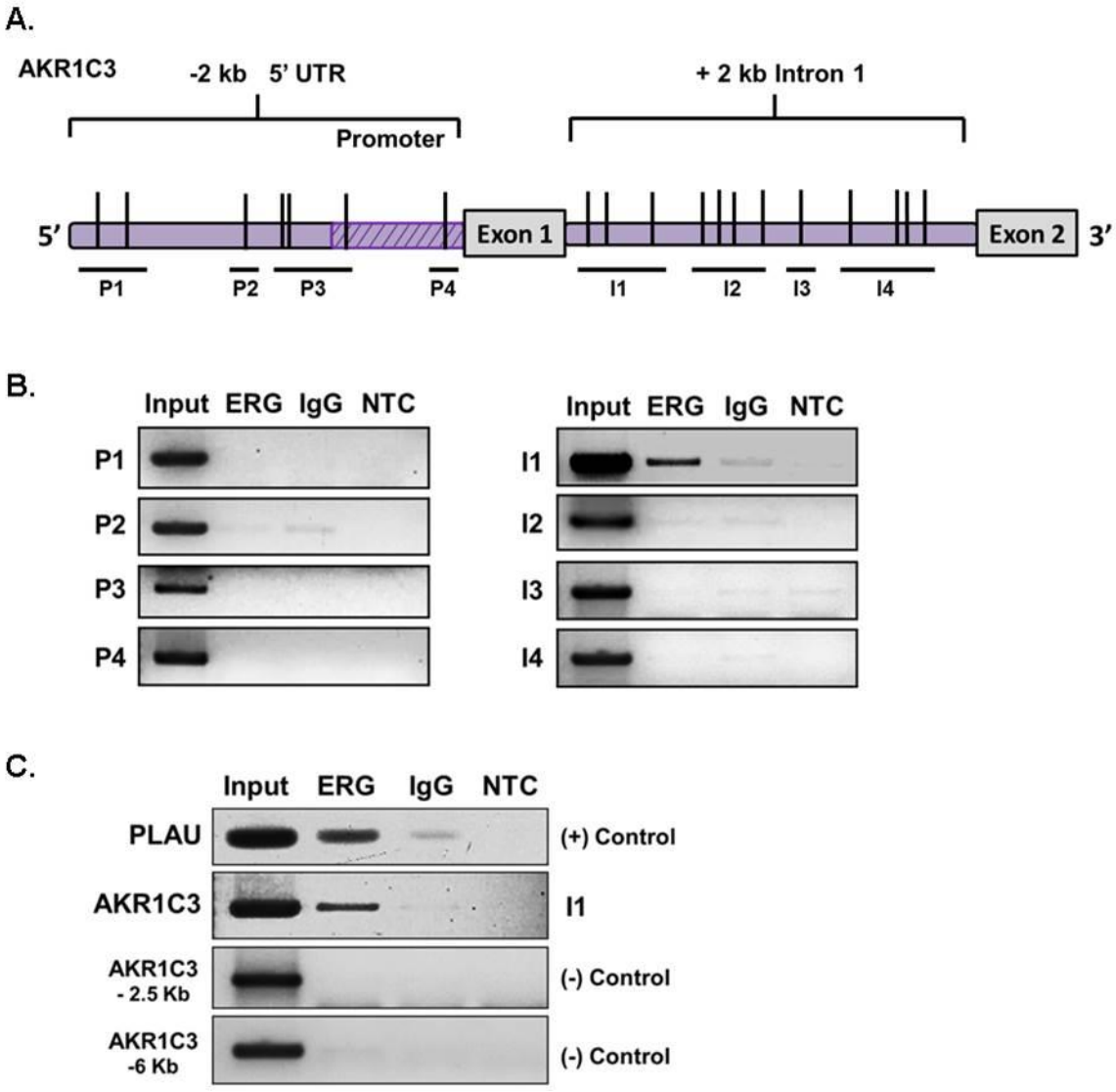

Figure 20. Selective Binding of ERG to the AKR1C3 Intron 1 Gene Region. A.) Diagram illustrating the AKR1C3 gene region located on chromosome 10. Black tick marks indicate ERG binding sites (5'-GGAA/T-3') located in the region of -2 Kb to +2 Kb relative to the transcription start site (TSS). P1-P4 and I1-I4 represent genomic primer amplification sites for the promoter and intron 1 region, respectively. B.) ChIP-PCR analysis of putative ERG binding sites in the AKR1C3 gene. ChIP was performed in VCaP cells using anti-ERG antibody; IgG antibody was used as a control for non-specific binding. NTC = non-template control. ChIP-PCR primer amplification regions in the AKR1C3 gene are indicated to the left of each DNA gel. C.) ChIP-PCR analysis of a known ERG binding site in PLAU promoter region using VCaP cells. ChIP-PCR analysis of ERG binding in AKR1C3 gene in VCaP cells. Negative control primers were used in VCaP cells to demonstrate specificity of the ChIP-PCR technique to detect only ERG binding.

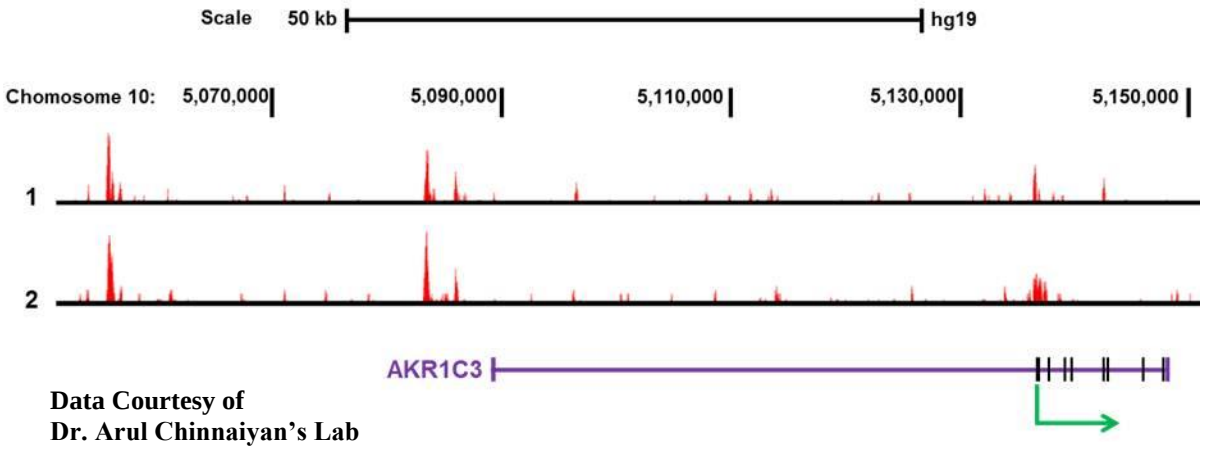

Figure 21. Selective Binding of ERG to Three Sites Along the AKR1C3 Gene. ChIP-Seq analysis was performed in duplicate using anti-ERG antibody in VCaP cells (Data provided by Dr. Chinnaiyan's lab at University of Michigan). The AKR1C3 gene is located on chromosome 10 and is depicted on the scale representing 20 kb intervals shown by black tick marks above the data. ChIP-Seq ERG enrichment binding peaks are shown in red. The AKR1C3 transcription start site is shown by the green arrow below the data, along with exons shown by black tick marks.

DISCUSSION

The ChIP data confirms that TMPRSS2-ERG regulates AKR1C3 enzyme gene expression via direct binding to the AKR1C3 gene. The RT-PCR data and western blot data implies that ERG positively regulates the gene expression of AKR1C3. Thus the ChIP data suggests that TMPRSS2-ERG directly binds to the AKR1C3 gene and enhances its gene transcription. The individual significance of each of the three ERG binding sites is currently unknown at this time. It is possible that each site recruits different cofactors involved in AKR1C3 transcription. It is also possible that the intron 1 binding site is a direct activator of AKR1C3 transcription, while the two distal sites further upstream of the transcription start site serve as enhancer regions.

It was surprising to see that ERG was bound to the intron 1 region as opposed to the promoter region of AKR1C3. However, there is evidence in the published literature that other androgen biosynthetic enzymes are regulated through their intron regions. For example, HSD3B2 enzyme transcription was positively regulated by YY1 transcription factor binding to the intron 1 region (Foti & Reichardt 2004). Sp3 transcription factor was shown to bind HSD3B1 and HSD3B2 intron 1 regions and regulate gene transcription (Foti & Reichardt 2004). Sp family members are known to bind consensus sequences called GC boxes (5’-GGGCGG- 3’) (Kolell & Crawford 2002, Liu et al. 2006). Interestingly, the only GC box in the entire AKR1C3 gene is located in intron 1, near the same site as ERG binding was identified. This suggests that ERG may co-regulate AKR1C3 gene expression with Sp3 in the intron 1 region. Additionally, ERG has been shown to co-regulate gene expression with Fos and Jun transcription factors (Basuyaux et al. 1997, Buttice et al. 1996), which are known to bind as Fos/Jun heterodimers to consensus sequences called AP-1 sites (5’-TGACTCA-3’) (Nakabeppu et al. 1988, Sitlani & Crothers

1996). Interestingly, the only AP-1 site in the entire AKR1C3 gene is located in intron 1, near the same site as ERG binding was identified. This suggests that ERG may co-regulate AKR1C3 gene expression with Fos/Jun in the intron 1 region. The co-regulation of AKR1C3 gene expression by ERG and other transcription factors remains to be further elucidated; indeed it seems unlikely that ERG exerts its regulation of AKR1C3 gene expression in a solo fashion.

Chapter 4

TMPRSS2-ERG and AKR1C3 Regulation of AR Activation and Cell Cycle Progression

4.1 ERG Promotes Bypass Pathway Synthesis of 5α-Androstanedione into DHT via Upregulation of AKR1C3

RESULTS

Bypass pathway metabolite 5α-androstanedione is converted into DHT in TMPRSS-ERG fusion-positive cells, and DHT synthesis is impaired in ERG knockdown cells.

Previous results indicated that ERG positively regulated the gene expression of AKR1C3 enzyme; therefore HPLC tandem mass spectrometry (HPLC-MS/MS) analysis was used in order to quantify androgen synthesis in TMPRSS2-ERG fusion-positive VCaP cells. This would determine 1.) if AKR1C3 has an effect on DHT synthesis in PCa cells and 2.) if ERG regulation of AKR1C3 has an effect on DHT synthesis in PCa cells. In order to deplete the media of androgens, 1% charcoal stripped serum (1% C.S.S.), phenol-red free media was used for all HPLC-MS/MS experiments. VCaP shScrambled cells were serum starved and androgen starved for 24 hours prior to treatment with 10 nM, 50 nM, and 100 nM of bypass pathway androgen metabolites 5α-androstanedione (5α-Adione), androsterone, and androstanediol for 24 hours (Figure 22). These DHT precursor metabolites were used as a substrate feeding experiment in order to determine which enzymes in the DHT pathway were actively synthesizing DHT. Treatment with 5α-Adione caused a significant dose-dependent increase in DHT synthesis in VCaP shScrambled cells (Figure 23). These data suggest the importance of 5α-Adione as a precursor metabolite for DHT synthesis, a reaction that is known to be catalyzed by the AKR1C3 enzyme (Figure 22).

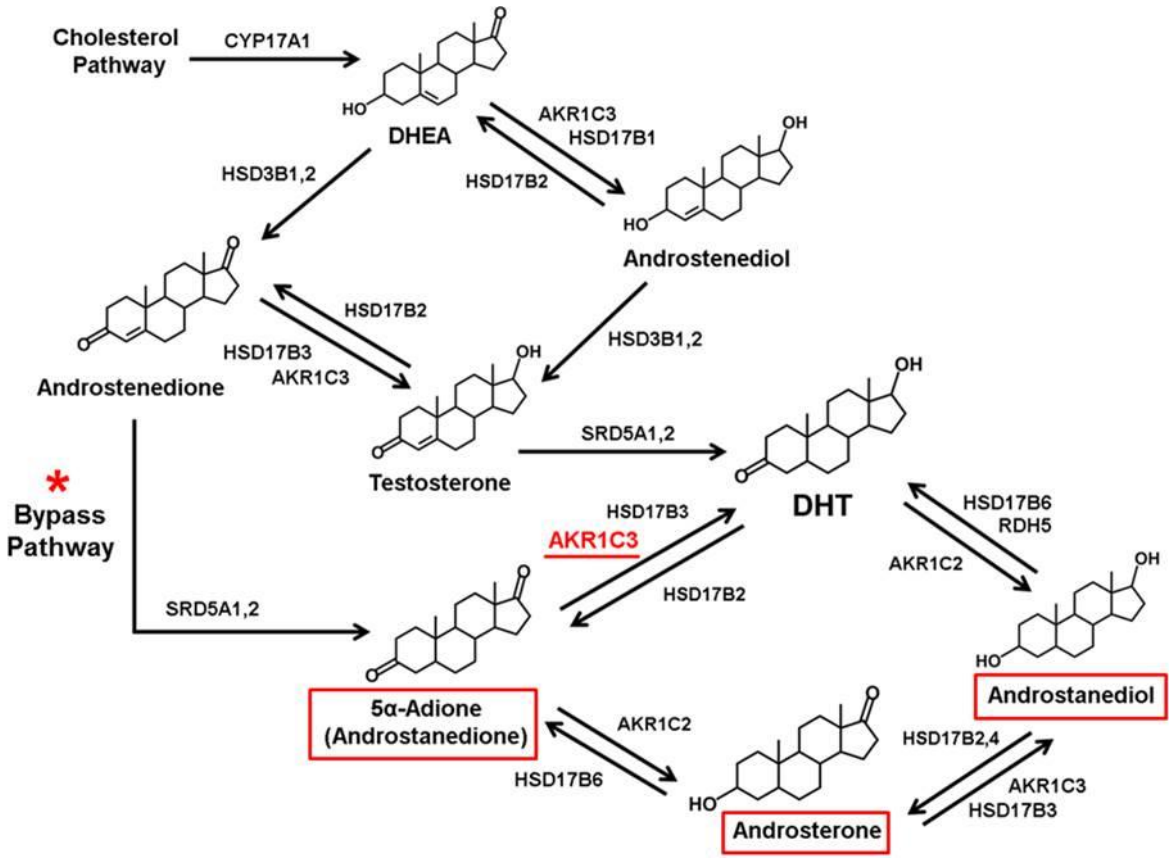

Figure 22. DHT Biosynthetic Pathway: Highlighting the Bypass Pathway and its Androgen Metabolites Used for Mass Spectrometry Analysis. The red asterisk signifies the bypass pathway to DHT synthesis where testosterone synthesis is bypassed and DHT is produced from 5α-Adione. The red boxes indicate substrate feeding androgen metabolites used for HPLC-MS/MS analysis of bypass pathway DHT synthesis. Metabolites in the red boxes were used to treat VCaP shScrambled cells at 10 nM, 50 nM, and 100 nM for 24 hours prior to collection for HPLC-MS/MS analysis. AKR1C3 enzyme is shown in underlined bold red to emphasize its position in the pathway where it catalyzes the biochemical reduction of 5α-Adione to DHT.

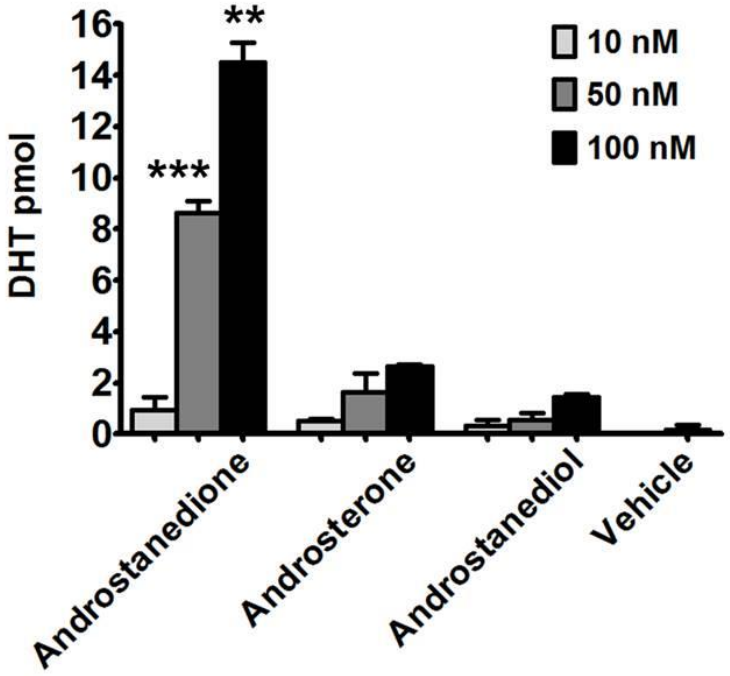

Figure 23. DHT is Produced from Bypass Pathway Androgen 5α-Adione in VCaP Cells. HPLC-MS/MS analysis of DHT levels in VCaP shScrambled cells treated with 10 nM, 50 nM, and 100 nM bypass pathway androgen metabolites for 24 hours. Androgen metabolite treatments are listed on the x-axis. Vehicle controls represent 0.1% EtOH treated samples. Cells and media were collected for HPLC-MS/MS analysis and quantified as pmol/1,000,000 cells. Statistical analysis was a two-tailed, unpaired, student's t-test (N = 3) ** $P<0.01$, *** $P<0.001$.

In order to determine if ERG regulation of AKR1C3 has an effect on DHT synthesis in VCaP cells, a substrate feeding experiment was performed and androgens were quantified with HPLC-MS/MS analysis. VCaP shScrambled and shERG cells were serum starved and androgen starved in 1% C.S.S. phenol-red free media for 24 hours prior to being treated with 100 nM of androgen metabolites androstenedione, androstenediol, 5α-Adione, and androsterone for 24 hours (Figure 24). These DHT and testosterone precursor metabolites were used as a substrate feeding experiment in order to determine which enzymes in the DHT pathway were actively synthesizing DHT and testosterone. Treatment with androstenedione and androstenediol caused a significant increase in testosterone synthesis in both VCaP shRNA cell lines compared to vehicle controls (Figure 25A). There was a significant decrease in testosterone synthesis in VCaP shERG cells treated with androstenediol compared to shScrambled controls; however there was not a significant difference between VCaP shRNA cell lines following treatment with androstenedione (Figure 25A). The largest increase in DHT production was seen in VCaP shScrambled cells following treatment with 5α-Adione (Figure 25B). DHT synthesis was significantly decreased in VCaP shERG cells treated with bypass pathway metabolites 5α-Adione and androsterone compared to VCaP shScrambled controls (Figure 25B). Testosterone precursor metabolites androstenedione and androstenediol did not elicit an increase in DHT synthesis in either VCaP shRNA cell lines compared to the vehicle controls (Figure 25B).

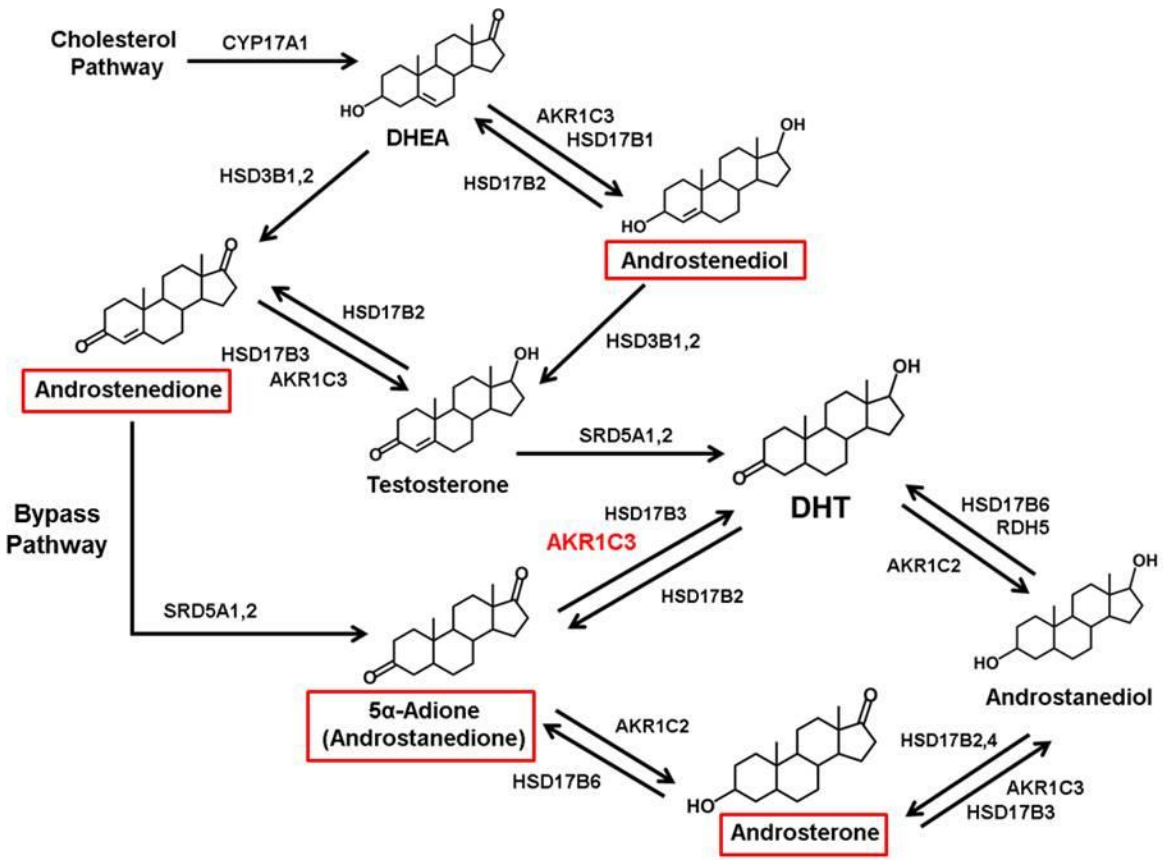

Figure 24. DHT Biosynthetic Pathway: Androgen Metabolites Used for Mass Spectrometry Analysis in ERG Knockdown Cells. The red boxes indicate substrate feeding androgen metabolites used for HPLC-MS/MS analysis of testosterone and DHT synthesis. Metabolites in the red boxes were used to treat VCaP shScrambled and shERG cells at 100 nM for 24 hours prior to collection for HPLC-MS/MS analysis.

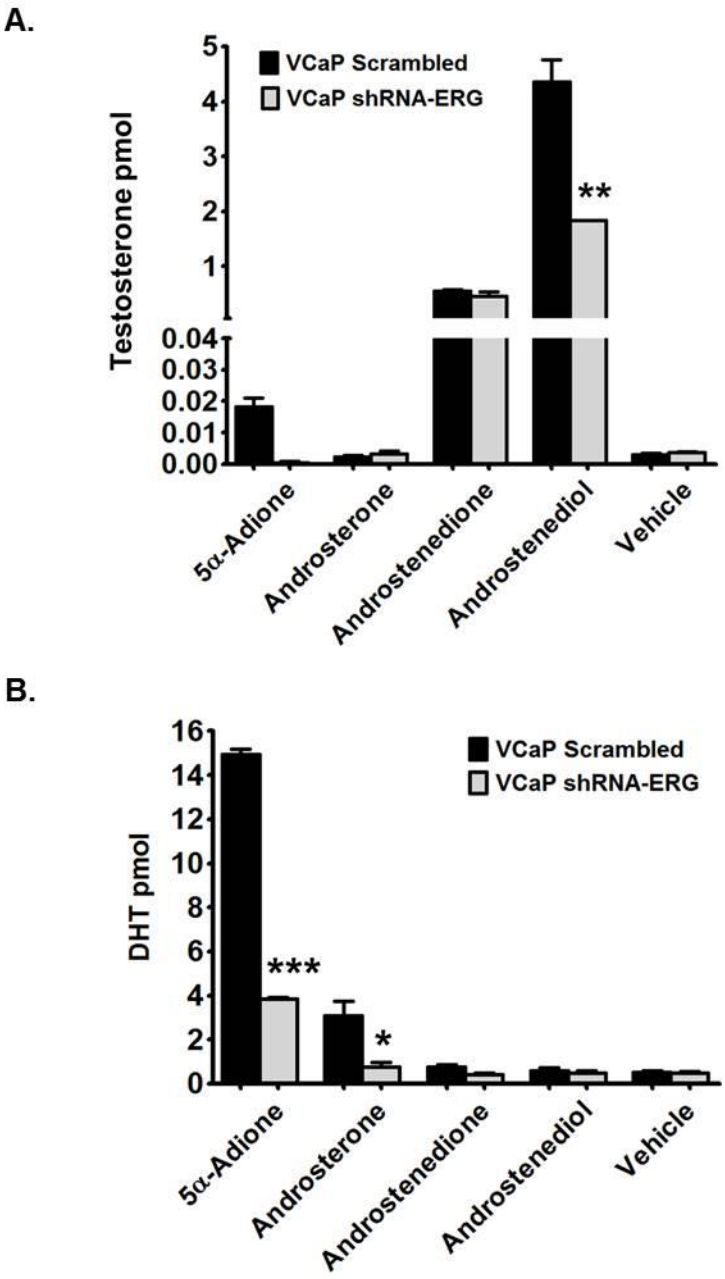

Figure 25. DHT Production from 5α-Adione is Impaired in ERG Knockdown Cells. A.) HPLC-MS/MS analysis of Testosterone levels in VCaP shScrambled and shERG cells treated with 100 nM androgen metabolites for 24 hours. B.) HPLC-MS/MS analysis of DHT levels in VCaP shScrambled and shERG cells treated with 100 nM androgen metabolites for 24 hours. Androgen metabolite treatments are listed on the x-axis. Vehicle controls represent 0.1% EtOH treated samples. Cells and media were collected for HPLC-MS/MS analysis and quantified as pmol/1,000,000 cells. Statistical analysis was a two-tailed, unpaired, student's t-test (N = 3) * $P<0.05$, ** $P<0.01$, *** $P<0.001$.

DISCUSSION

The HPLC-MS/MS data indicates that 5α-Adione is a key precursor metabolite for DHT synthesis in VCaP cells, and that ERG may regulate this reaction through upregulation of the AKR1C3 enzyme. Treatment with testosterone bypass pathway metabolites 5α-Adione and androsterone induced the largest amounts of DHT synthesis. It is interesting that the enzymes that are known to be active in the synthesis of androsterone → 5α-Adione → DHT are HSD17B6 and AKR1C3. These are the same enzymes that were shown from the RT-PCR and RT-qPCR data to be regulated by TMPRSS2-ERG in VCaP cells. This suggests that ERG may enhance DHT production through upregulation of these enzymes. HSD17B3 is also known to synthesize 5α-Adione to DHT; however the RT-PCR and RT-qPCR data indicated that HSD17B3 was expressed at very low levels and AKR1C3 was expressed at very high levels in VCaP cells. The CT value for AKR1C3 was 23, whereas the CT value for HSD17B3 was 35. In addition, the AKR1C3 PCR band showed up at cycle 30, whereas the HSD17B3 PCR band showed up at cycle 40. These data suggest that AKR1C3 is the more likely enzyme to catalyze the biochemical reduction of 5α-Adione to DHT in PCa cells, rather than the HSD17B3 enzyme.

It was surprising to see that the testosterone produced from 100 nM androstenedione and androstenediol treatment did not elicit a significant increase in DHT synthesis. It is well known that testosterone is converted into DHT by SRD5A enzyme in the classical DHT synthesis pathway (Penning 2010). The SRD5A enzyme was shown to be highly expressed from the RT-PCR and RT-qPCR data; therefore the reasoning as to why this reaction was not highly active in the VCaP cells is currently unknown. It may be that in PCa cells SRD5A has a higher affinity to convert androstenedione to 5α-Adione for bypass pathway production of DHT rather than androstenedione to testosterone for classical pathway production of DHT. Indeed, this concept

has been shown previously in a study that showed PCa cells treated with androstenedione had a higher rate of 5α-Adione synthesis compared to testosterone synthesis (Chang et al. 2011). These data suggest that the bypass pathway is the predominant pathway for DHT synthesis in PCa cells, rather than the classical pathway. It may also be that the testosterone being synthesized is binding directly to the AR before it is converted to DHT. It is possible that in PCa cells testosterone binds AR with a greater affinity than the SRD5A1 enzyme. This would leave SRD5A1 less occupied with testosterone and more available to bind androstenedione.

4.2 AKR1C3 synthesis of 5α-Androstanedione into DHT Activates the AR and Promotes Cell Cycle Progression

RESULTS

5α-Adione treatment induces AR nuclear translocation and PSA gene activation in VCaP cells, and PSA gene activation is reduced in ERG and AKR1C3 knockdown cells

The HPLC-MS/MS data indicated that 5α-Adione treatment induced DHT synthesis in VCaP cells. In order to determine whether this had a functional consequence on AR activation, AR nuclear translocation and PSA gene expression were investigated. When the AR is activated by its ligands DHT and testosterone, it translocates from the cytoplasm into the nucleus. Once inside the nucleus, the AR can homodimerize and bind to the DNA of its target genes and activate gene expression (Lonergan & Tindall 2011). A well-known target gene of the AR is KLK3, or prostate specific antigen (PSA) (Lonergan & Tindall 2011, Yu et al. 2010). Therefore, AR nuclear translocation and PSA gene expression activation can be used to determine if AR signaling has been activated.

Immunocytochemistry was used to analyze AR localization in the nucleus. VCaP cells were plated on cover slips and serum starved and androgen starved for 24 hours in 1% C.S.S.

phenol-red free media prior to treatment with either 100 nM 5α-Adione or 0.1% EtOH vehicle for 24 hours. Cells were fixed with formaldehyde, the AR was stained with fluorescent antibodies, and the nucleus was stained with DAPI fluorescent dye. Treatment with 100 nM 5α-Adione caused a marked increase in AR translocation into the nucleus compared to vehicle controls (Figure 26). In VCaP vehicle cells AR can be seen in the cytoplasm surrounding the nucleus, as indicated by the distinct red color (cytoplasmic AR) and green color (nucleus) (Figure 27A). In VCaP 5α-Adione cells the AR can be seen predominantly inside the nucleus, as indicated by the distinct yellowish orange color (AR/nucleus overlap) (Figure 27A). AR colocalization with the nucleus was quantified using Volocity colocalization software (PerkinElmer) and represented as a Pearson's correlation coefficient. In VCaP cells treated with 0.1% vehicle there was a weak to moderate correlation of AR with the nucleus ($r = 0.35$); however, in 5α-Adione treated cells there was a strong correlation of AR with the nucleus ($r = 0.72$) (Figure 27B).

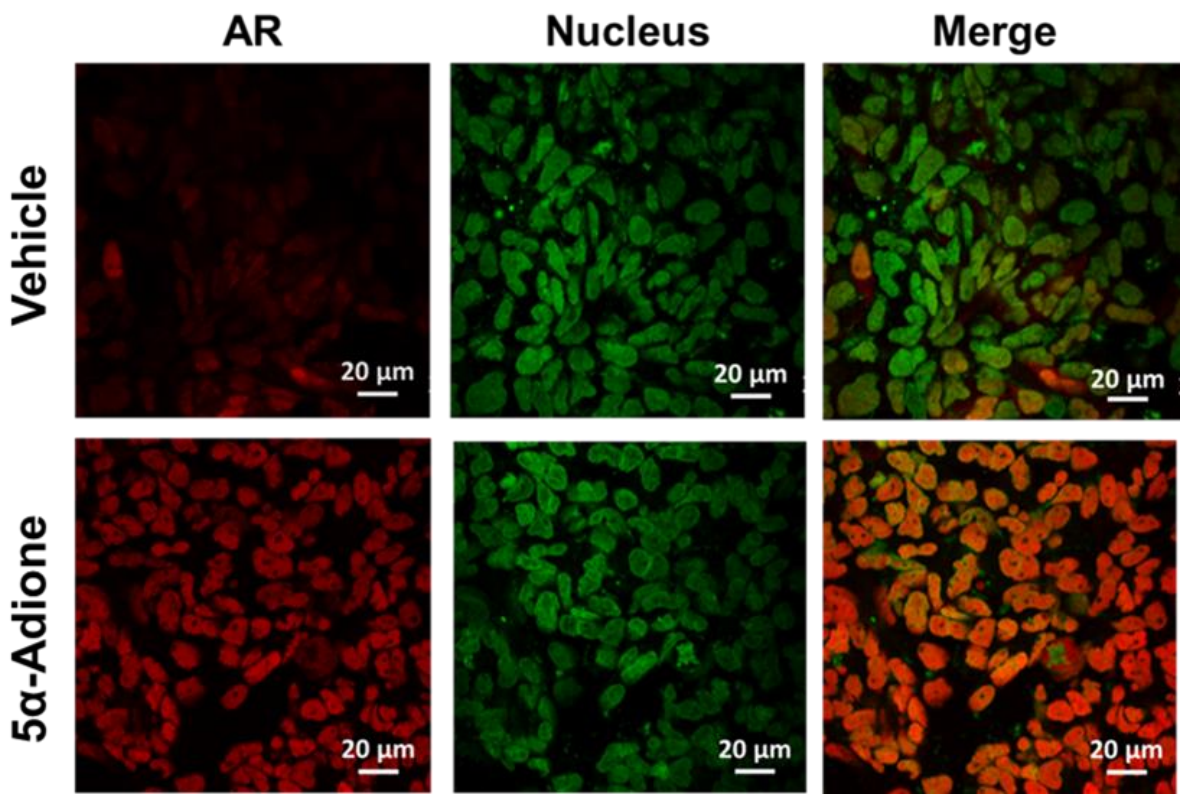

Figure 26. 5α-Adione Treatment Induces AR Activation in VCaP Cells. Immunocytochemistry was performed in VCaP cells treated with 100 nM 5α-Adione for 24 hours. Vehicle cells represent 0.1% EtOH treated control cells. Cells were plated on cover slips and stained with anti-AR antibody, Texas Red fluorophore conjugated antibody, and DAPI. Cover slips were mounted onto slides and subjected to confocal imaging at 40X magnification. Vehicle cells represent 0.1% EtOH treated control cells.

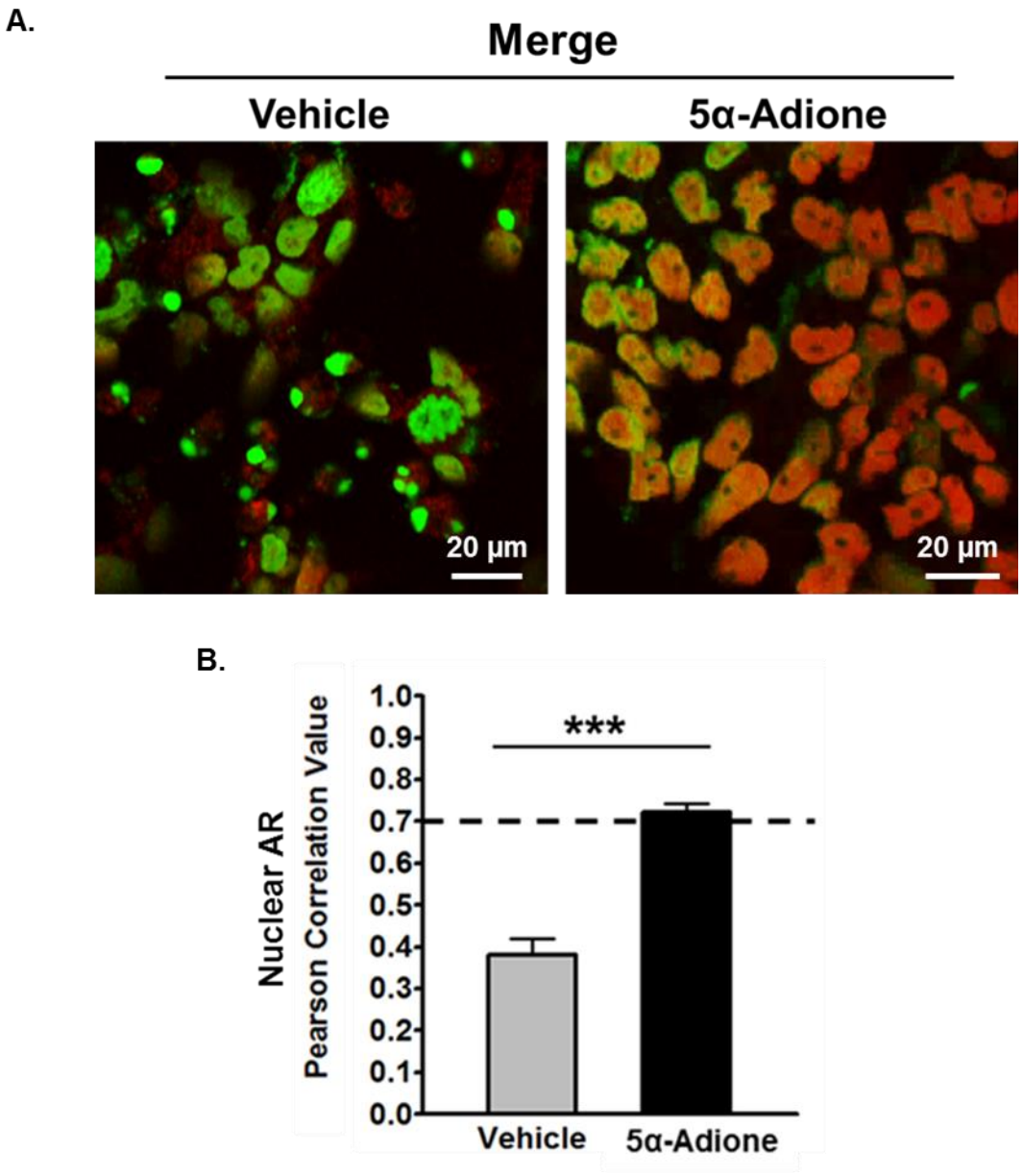

Figure 27. 5α-Adione Treatment Induces AR Nuclear Translocation in VCaP Cells. A.) Immunocytochemistry was performed in VCaP cells treated with 100 nM 5α-Adione for 24 hours. Cells were plated on cover slips and stained with anti-AR antibody, Alexa Flour 633 fluorophore conjugated antibody, and DAPI. Cover slips were mounted onto slides and subjected to confocal imaging at 40X magnification. B.) VCaP confocal images shown in part A. were quantified for nuclear AR using merged images (AR/DAPI) in the Volocity colocalization software program. Statistical analysis was a two-tailed, unpaired, student's t-test (N = 4) *** $P<0.001$. The dashed line indicates a strong Pearson's correlation value of $r > 0.7$.

AR translocation into the cell nucleus was previously verified, thus warranting investigation of AR target gene activation. RT-qPCR and RT-PCR was used to analyze PSA expression in VCaP shScrambled, shERG, and shAKR1C3 cells. Cells were serum starved and androgen starved for 24 hours in 1% C.S.S. phenol-red free media prior to treatment with either 100 nM 5α-Adione or 0.1% EtOH vehicle for 24 hours. VCaP shERG cells had significantly decreased PSA expression in 5α-Adione treated cells compared to VCaP shScrambled controls (Figure 28A and 28B). In addition, VCaP shAKR1C3 cells also had significantly decreased PSA expression in 5α-Adione treated cells compared to VCaP shScrambled controls (Figure 28C). ERG knockdown and reduced AKR1C3 expression were validated in VCaP shERG cells (Figure 28D). AKR1C3 knockdown was validated in VCaP shAKR1C3 cells (Figure 28E). The absence of AKR1C3 enzyme and reduced PSA gene activation during 5α-Adione treatment in both knockdown cell lines suggests that AKR1C3 may use 5α-Adione as a substrate to synthesize DHT and activate the AR in PCa cells.

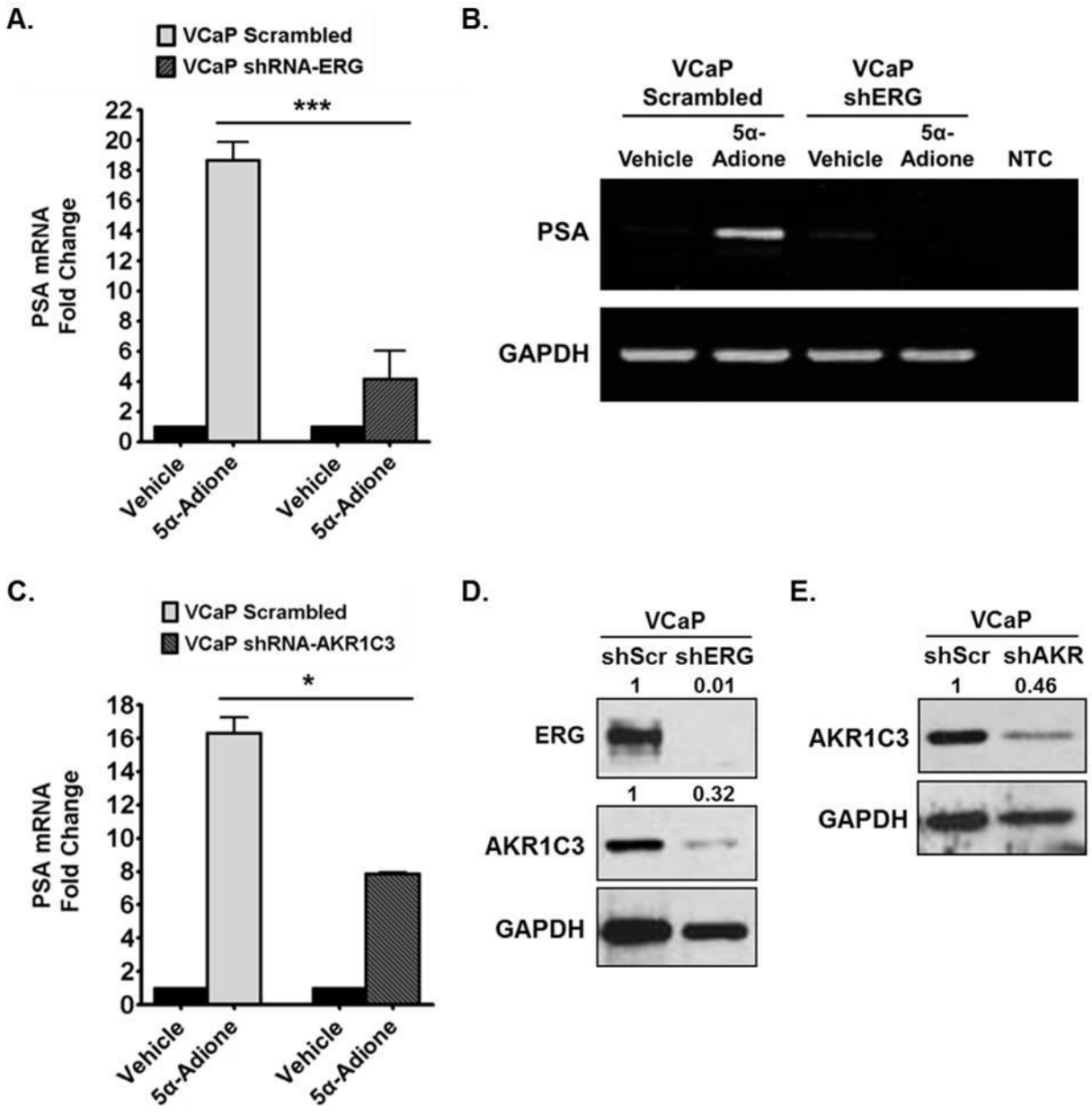

Figure 28. 5α-Adione Induced PSA Gene Activation is Decreased in ERG and AKR1C3 Knockdown Cells. A.) RT-qPCR and B.) RT-PCR analysis of PSA expression in VCaP shScrambled and shERG cells treated with 100 nM 5α-Adione for 24 hours. NTC = non-template control. C.) RT-qPCR analysis of PSA expression in VCaP shScrambled and shAKR1C3 cells treated with 100 nM 5α-Adione for 24 hours. Statistical analysis was a two-tailed, unpaired, student's t-test A.) (N = 5) and C.) (N = 2) * $P<0.05$, *** $P<0.001$. D.) Western blot analysis of ERG and AKR1C3 expression in VCaP shScrambled and shERG cells. E.) Western blot analysis of AKR1C3 expression in VCaP shScrambled and shAKR1C3 cells. GAPDH was used as a loading control. Numbers above blots represent fold changes determined by densitometry.

The AR has been shown to regulate cell cycle progression in androgen-independent PCa cells through upregulation of cell cycle genes UBE2C, CDK1, and CDC20 (Wang et al. 2009). Through upregulation of these M-phase cell cycle genes, AR can increase cell cycle progression and facilitate tumor growth in CRPC. Data from previous figures suggests that TMPRSS2-ERG and AKR1C3 enhance DHT production and increase AR activation in PCa cells; therefore cell cycle progression in ERG and AKR1C3 knockdown cells was investigated. Knockdown of ERG or AKR1C3 in VCaP cells significantly reduced cell proliferation rate compared to VCaP shScrambled controls (Figure 29A and 29B). The cell proliferation rate may be partially impacted by CDC20 expression during 5α-Adione treatment. CDC20 expression was increased by 2-fold in VCaP shScrambled cells treated with 100 nM 5α-Adione for 24 hours compared to vehicle controls (Figure 29C). PSA was used as a positive control for AR activation and was increased by 9-fold compared to vehicle controls, whereas CDK1 expression was not affected by 5α-Adione treatment (Figure 29C). Interestingly, there was no induction of CDC20 or PSA expression in VCaP shERG cells treated with 100 nM 5α-Adione for 24 hours compared to vehicle controls (Figure 29D). ERG40 was transiently overexpressed in LNCaP cells and cell cycle genes and AKR1C3 were analyzed. LNCaP ERG40 cells had significantly increased expression of AKR1C3, and a moderate increase in CDC20 and CDK1 expression compared to empty vector controls (Figure 29E). UBE2C was not significantly increased in LNCaP ERG40 cells compared to empty vector controls (Figure 29E). A model diagram summarizing the findings from the data thus far can be seen in Figure 30.

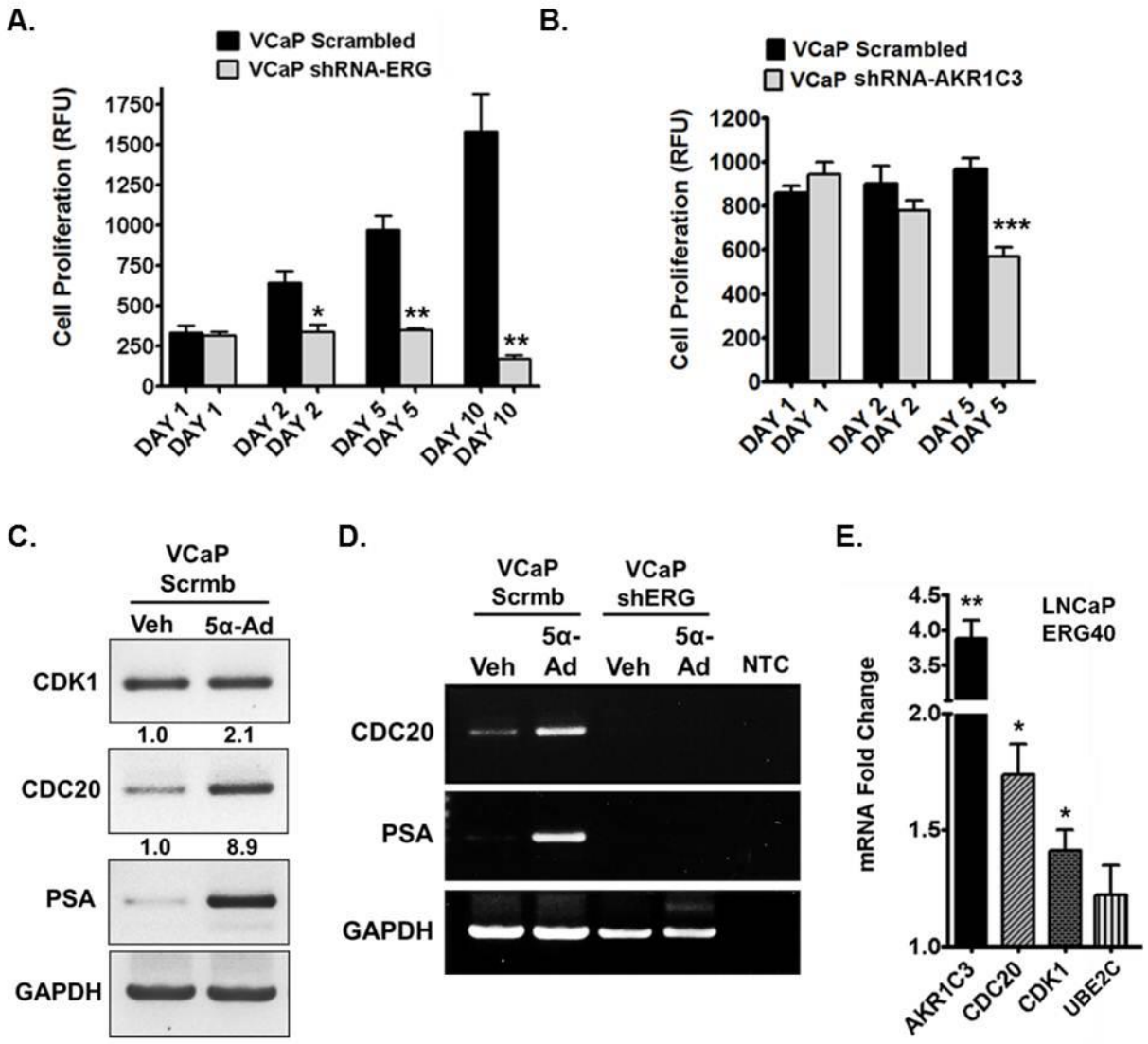

Figure 29. Cell Proliferation is Hindered in ERG and AKR1C3 Knockdown Cells. Cell proliferation assay in VCaP shScrambled and A.) shERG B.) shAKR1C3 cells grown in regular 10% FBS media for 5-10 days. RFU = relative fluorescent units. Statistical analysis was a two-tailed, unpaired, student's t-test A.) (N = 3) and B.) (N = 4) * P<0.05, ** P<0.01, *** P<0.001. C.) RT-PCR analysis of CDK1, CDC20, and PSA in VCaP shScrambled cells treated with 100 nM 5α-Adione for 24 hours. Numbers above DNA gel represent fold changes determined by densitometry. D.) RT-PCR analysis of CDC20 and PSA in VCaP shScrambled and shERG cells treated with 100 nM 5α-Adione for 24 hours. NTC = non-template control. GAPDH was used as a loading control. E.) RT-qPCR analysis of AKR1C3, CDC20, CDK1 and UBE2C expression in LNCaP ERG40 cells. Samples were normalized to GAPDH. Statistical analysis was a two-tailed, paired, student's t-test (N = 3) * P<0.05, ** P<0.01.

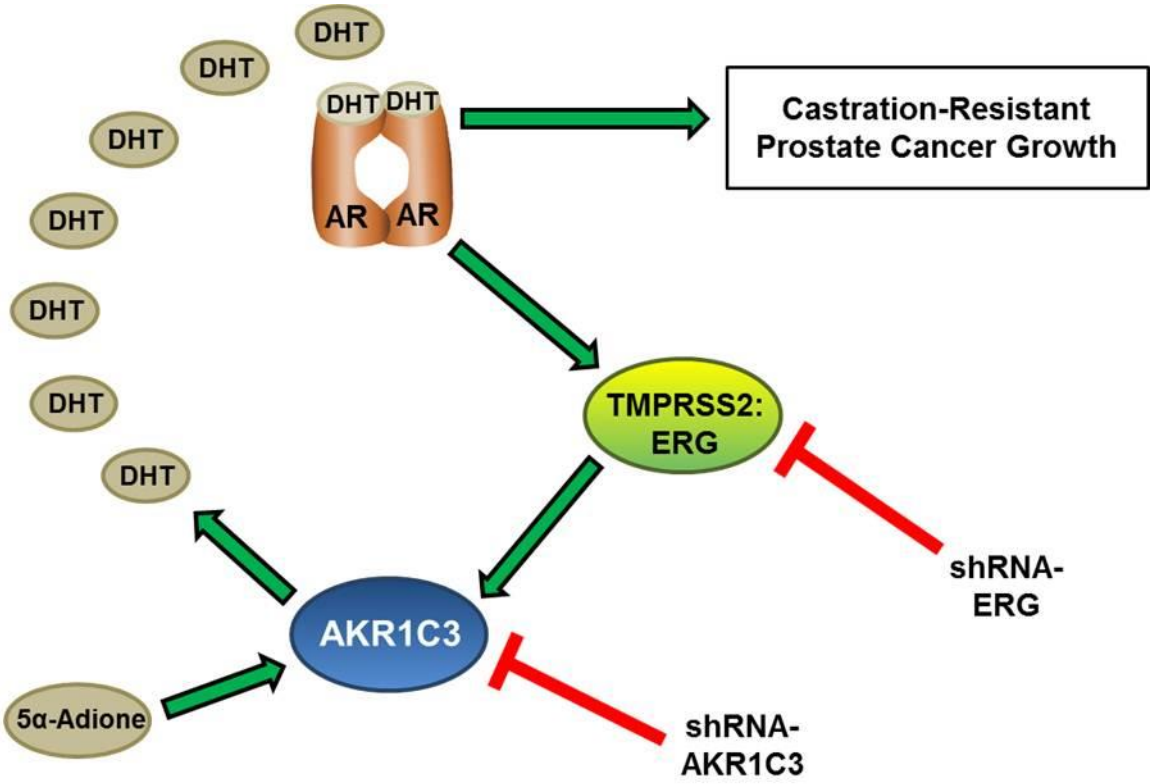

Figure 30. A Model Diagram Summarizing ERG Regulation of Androgen Biosynthetic Enzyme Expression and AR Activation in Prostate Cancer Cells. The TMPRSS2-ERG fusion gene is activated by the AR in PCa cells. This leads to overexpression of ERG and activation of AKR1C3 gene expression via direct binding of ERG to the AKR1C3 gene. AKR1C3 can use 5α-Adione as a substrate to synthesize DHT, which can then activate AR signaling. The AR can translocate into the cell nucleus, activate expression of target genes including cell cycle genes, and promote tumor growth in CRPC. Note the feed-forward activation loop of AR→ ERG→ AKR1C3→ DHT→ AR and so on. Under this model, PCa cells can continue to activate AR signaling even in the presence of androgen ablation therapies and low intratumoral androgen levels.

DISCUSSION

The immunocytochemistry data clearly indicated that treatment of VCaP cells with 100 nM 5α-Adione for 24 hours activated translocation of AR into the cell nucleus. This finding is consistent with the HPLC-MS/MS data where it was shown that treatment of VCaP cells with 100 nM 5α-Adione for 24 hours caused a significant increase in DHT production. Once inside the cell nucleus, AR activated expression of its target gene PSA. This PSA activation was very significant in the VCaP shScrambled cells where it was shown to be almost ~18-fold higher than the vehicle control. The PCR data was also consistent with the HPLC-MS/MS data where it was shown that knockdown of ERG caused a significant decrease in DHT production. This was reflected in the VCaP shERG cells that showed a significant decrease in PSA activation following 5α-Adione treatment. Consistent with previous data where it was shown that knockdown of ERG caused a significant reduction in AKR1C3 expression; AKR1C3 knockdown cells also had significantly reduced PSA activation following 5α-Adione treatment. These data suggest that AKR1C3 converts 5α-Adione to DHT, and that ERG regulates this step through upregulation of AKR1C3 expression in PCa cells. These data suggest a model where ERG regulates ABE gene expression, which enhances DHT production and AR activation. This can fuel AR regulated cell cycle progression, and provide a feed-forward activation loop for continuous ERG and AKR1C3 expression (Figure 30). Under this model, PCa cells can continue to activate AR signaling even in the presence of androgen ablation therapies and low intratumoral androgen levels.

It was clear from the cell proliferation assay data that knockdown of ERG or AKR1C3 caused impairment in PCa cell proliferation compared to shScrambled controls. However, the cell cycle genes responsible for impaired proliferation remain to be fully elucidated. The data

indicated CDC20 may have been responsible to a moderate degree because it was not induced by 5α-Adione treatment in VCaP shERG cells; however, it was only induced by 2-fold in VCaP shScrambled cells. In addition, CDK1 was not affected by AR activation suggesting it is not the cell cycle gene responsible for impaired proliferation rate in ERG and AKR1C3 knockdown cells. The LNCaP ERG40 cells showed only slight increases in CDC20 and CDK1. This may have been induced by the presence of higher AKR1C3 levels and therefore higher DHT production and AR activation. However, this data was not performed under 5α-Adione stimulation, so further experiments will need to be investigated in order to directly link these findings to the model in figure 30.

The effects of ERG on cell cycle progression and cell survival signals mediated through AR activation remain to be fully characterized. There are a large number of genes involved in cell cycle progression that remain to be interrogated under this model. The small analysis performed thus far focused on several M-phase genes. It may be beneficial to perform a cell cycle analysis in ERG and AKR1C3 knockdown cells in order to determine which phase of the cell cycle is being directly hindered. This will help yield a better understanding of which cell cycle genes may be affected by the ERG → AKR1C3 → AR signaling axis in PCa cells. Cell survival signals also need to be investigated in this model as it appears shERG and shAKR1C3 cells are not growing and eventually dying. It may be that AR regulates cell proliferation signals as well as cell survival signals in the VCaP cells.

Chapter 5

Clinical Implications for TMPRSS2-ERG and AKR1C3 in Prostate Cancer Patients

RESULTS

The cell line data in PCa cells and BPH-1 cells indicated that ERG regulated AKR1C3 expression. In order to access the clinical implications of this regulation process, ERG and AKR1C3 expression were analyzed in human prostate tumor tissue specimens using immunohistochemistry (IHC) analysis, microarray database analysis, and Kaplan-Meier survival outcome analysis. IHC analysis was performed using formalin-fixed, paraffin embedded serial sections from human prostate tumor tissue specimens that were stained with anti-ERG and anti-AKR1C3 antibodies. IHC data revealed that ERG and AKR1C3 were co-expressed in human prostate tumor tissue specimens (Figure 31A). The IHC data was scored based on the presence (+) or absence (-) of ERG and AKR1C3 expression, and co-expression of the two genes was shown to be statistically significant (Figure 31B). In addition, formalin-fixed, paraffin embedded serial sections from LuCaP PCa tumor xenografts were also subjected to IHC analysis. IHC data revealed that ERG and AKR1C3 were co-expressed in LuCaP tumor xenograft samples (Figure 32).

A.

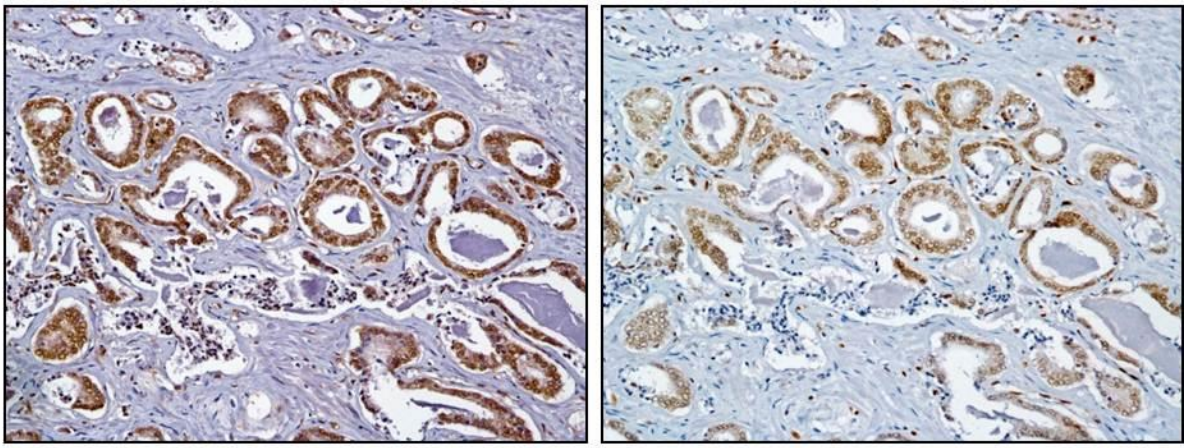

B.

*** P < 0.0001

N = 64	AKR1C3 +	AKR1C3 -
ERG +	24	9
ERG -	6	25

Figure 31. AKR1C3 and ERG are Co-Expressed in Human Prostate Tumor Tissue Specimens. A.) Immunohistochemistry staining analysis in human prostate tumor tissue specimens (N = 64) using anti-AKR1C3 (left) and anti-ERG (right) antibodies. B.) IHC staining analysis in 64 human prostate tumor tissue specimens was scored based on the presence (+) or absence (-) of ERG and AKR1C3 staining. Values are presented in a quantification table and statistical analysis was performed.

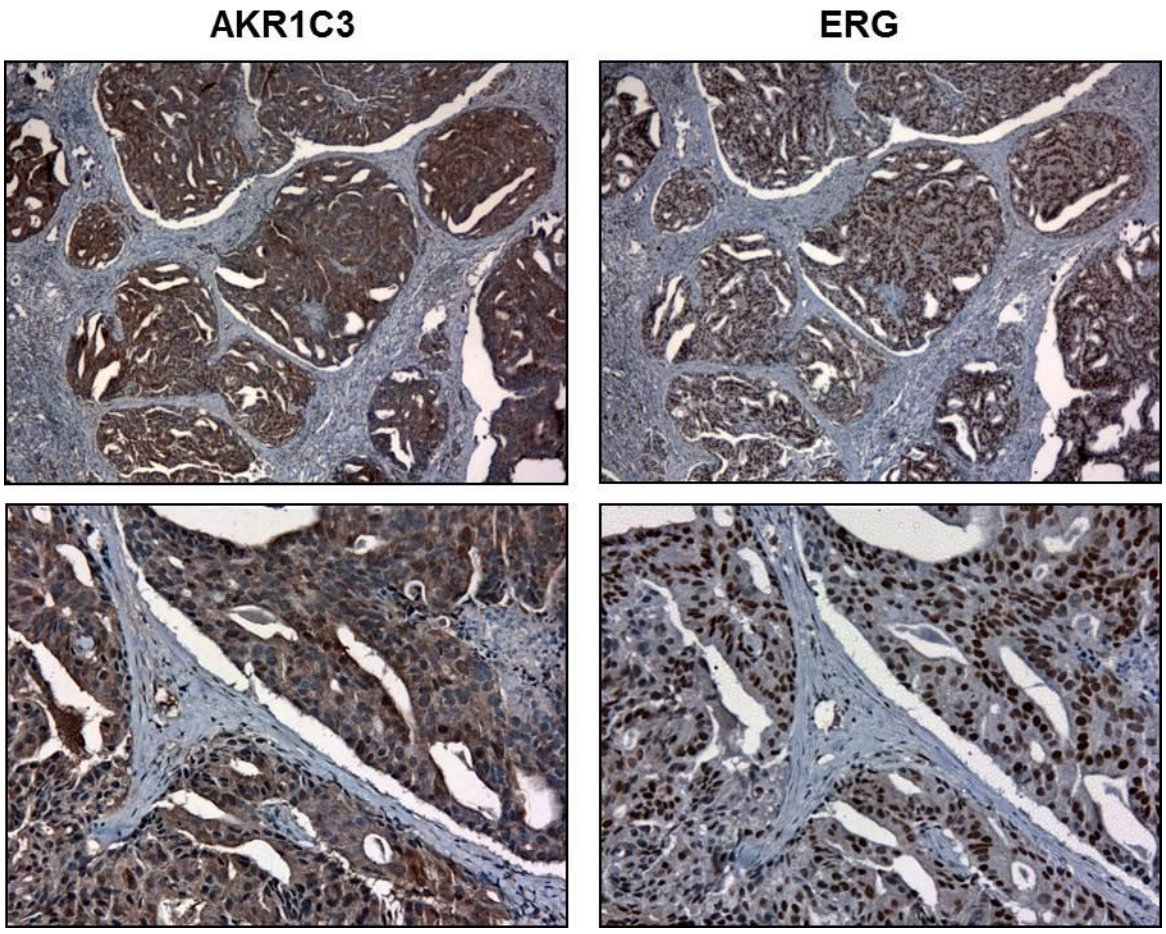

Figure 32. AKR1C3 and ERG are Co-Expressed in LuCaP Xenograft Tumor Tissue Specimens. Immunohistochemistry staining analysis in LuCaP xenograft tumor tissue specimens using anti-AKR1C3 (left) and anti-ERG (right) antibodies.

Publicly available microarray data were utilized to investigate whether ERG and AKR1C3 expression correlated in human metastatic prostate tumor tissue samples (N = 25). Microarray data for ERG and AKR1C3 expression was extracted from Gene Expression Omnibus (GEO) database GDS2545. A Pearson's correlation plot was performed for ERG and AKR1C3 expression and the two genes were shown to have a fairly strong and significant correlation in human metastatic prostate tumor tissue samples (r = 0.69) (Figure 33).

In order to investigate whether ERG and AKR1C3 expression in human prostate tumor tissue samples had an effect on patient survival outcome, Kaplan-Meier survival plots were performed. Patient survival data for AKR1C3 high and low expression tumors, as well as TMPRSS2-ERG fusion-positive and fusion-negative tumors was extracted from the Oncomine database study Setlur et al. prostate cancer (Setlur et al. 2008). These patients were diagnosed by transurethral resection performed for obstruction many years ago in the pre-PSA era. They were thought to have clinically localized cancer and had no further treatment. This is a unique data set that provides insight into the natural history of prostate cancer followed for decades until death. Microarray data for AKR1C3 expression was extracted from GEO database GSE8402. AKR1C3 expression in PCa tumors was divided into low expression tumors and high expression tumors (Figure 34A). The presence or absence of the TMPRSS2-ERG fusion gene was determined by FISH and PCR analysis, and this data was extracted from GEO database GSE8402. Patient survival data from the GSE8402 database was available on the Oncomine database. Kaplan-Meier survival plots revealed that patients with AKR1C3 high expression tumors had significantly lower survival probability compared to AKR1C3 low expression tumors (Figure 34B). In addition, patients with TMPRSS2-ERG fusion-positive tumors had significantly lower survival probability compared to fusion-negative tumors (Figure 34C). Patients with AKR1C3

low expression tumors or TMPRSS2-ERG fusion-negative tumors had a median survival of 15 years, whereas patients with AKR1C3 high expression tumors or TMPRSS2-ERG fusion-positive tumors had a median survival of 10 years. A limitation in using these data, however, is that the patients had untreated disease as opposed to castrate-resistant disease. A model diagram summarizing the hypothesis presented in this paper is shown in Figure 35.

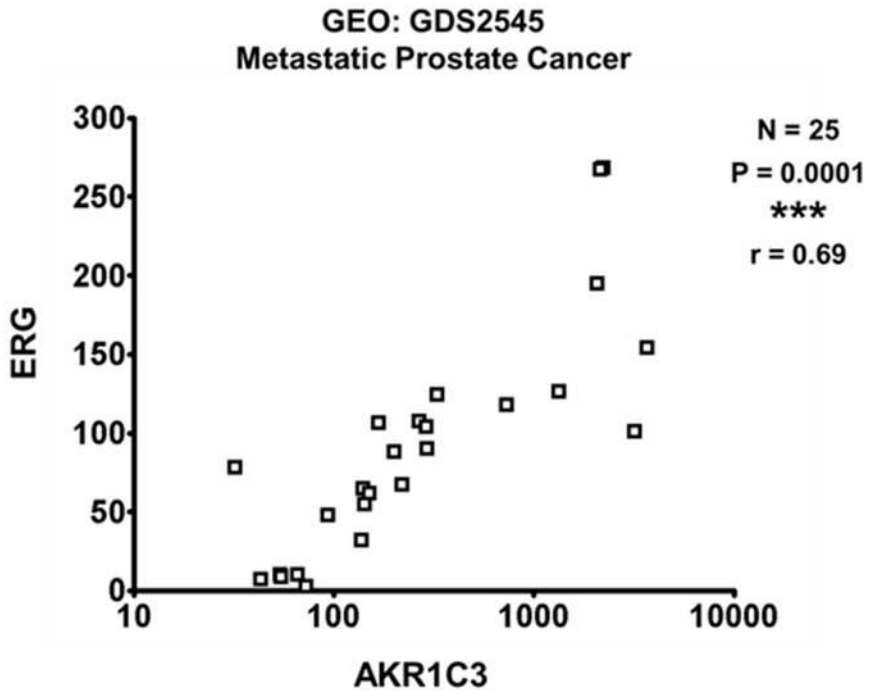

Figure 33. Correlation of AKR1C3 and ERG Expression in Human Metastatic Prostate Tumor Samples. A correlation plot was performed for AKR1C3 and ERG expression in 25 metastatic prostate tumor samples. Microarray expression data for AKR1C3 and ERG was extracted from the Gene Expression Omnibus database GDS2545. Statistical analysis was a Pearson's Correlation plot (N = 25) with an r value of r = 0.69, *** P<0.001.

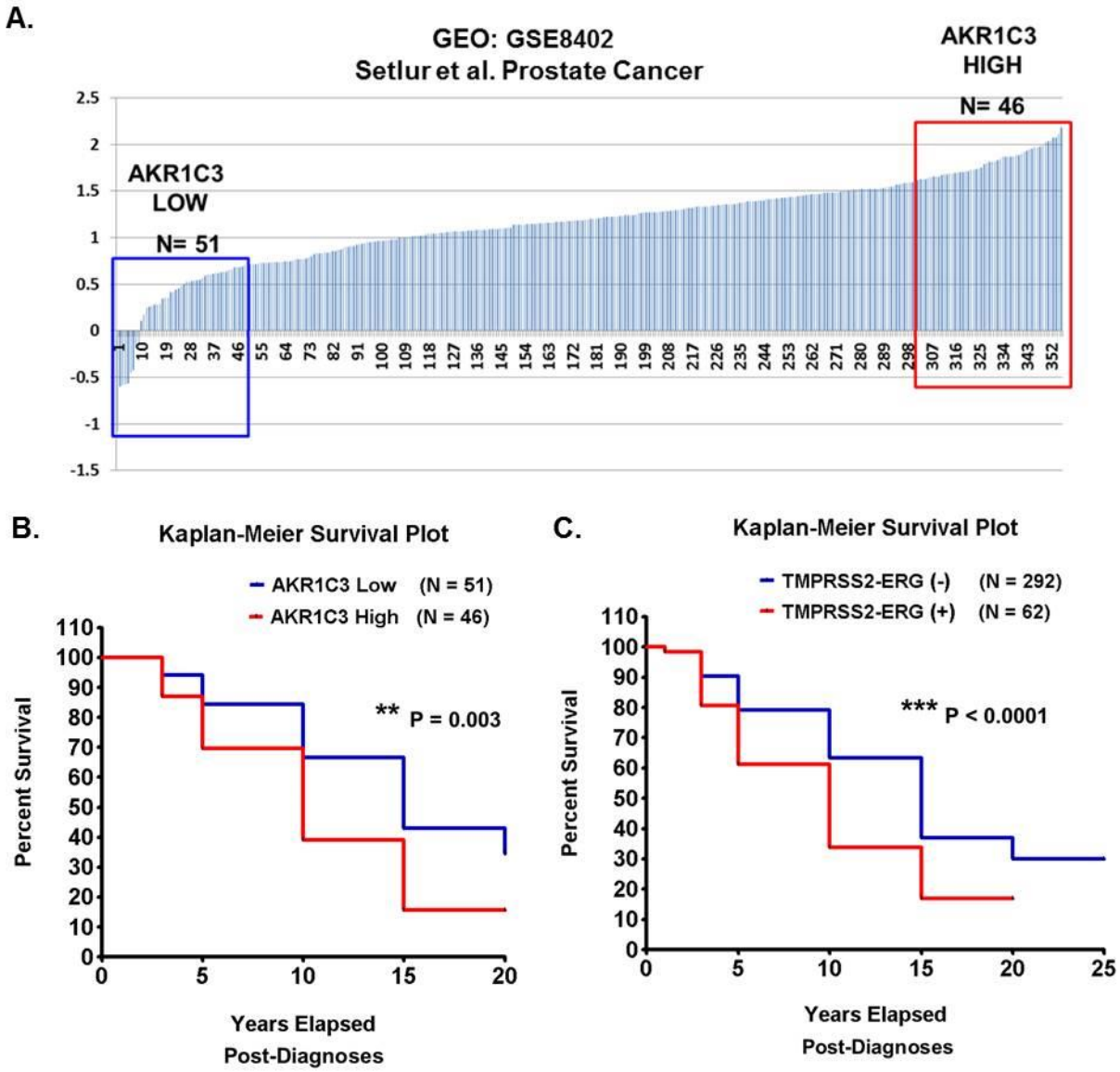

Figure 34. The Presence of AKR1C3 or TMPRSS2-ERG fusion gene in PCa Tumors Predicts for Worse Survival Outcome. A.) AKR1C3 microarray expression values extracted from Gene Expression Omnibus database GSE8402 (N = 363) used to determine high vs. low expression tumors. B.) Kaplan-Meier survival plot of AKR1C3 low expression tumors (N = 51) vs. AKR1C3 high expression tumors (N = 46). Patient survival data was extracted from the Oncomine database Setlur et al. prostate cancer (2008). C.) Kaplan-Meier survival plot of TMPRSS2-ERG fusion-negative tumors (N = 292) vs. TMPRSS2-ERG fusion-positive tumors (N = 62). Patient survival data was extracted from the Oncomine database Setlur et al. prostate cancer (2008). TMPRSS2-ERG fusion status was determined by FISH and PCR. For statistical analysis a Gehan-Breslow-Wilcoxon Test and a Mantel-Cox Test were performed ** P<0.01, *** P<0.001.

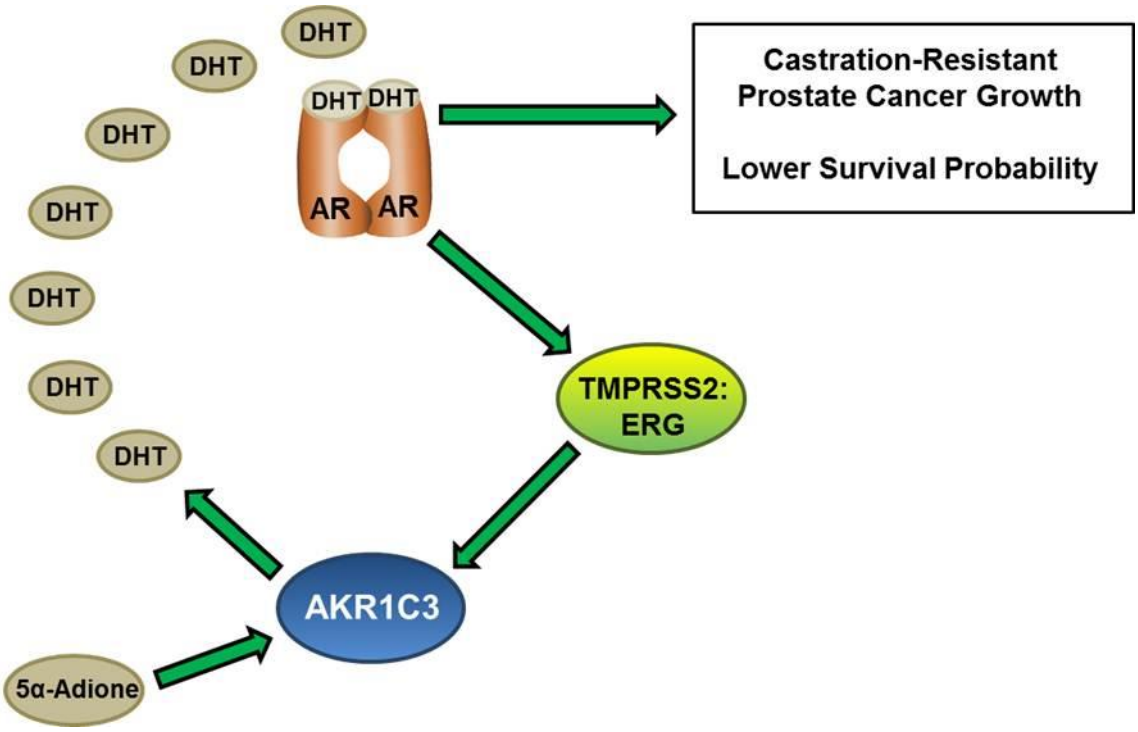

Figure 35. A Model Diagram Summarizing the Hypothesis of ERG Regulation of Androgen Biosynthetic Enzyme Expression in Prostate Cancer. The TMPRSS2-ERG fusion gene is activated by the AR in PCa cells. This leads to overexpression of ERG and activation of AKR1C3 gene expression via direct binding of ERG to the AKR1C3 gene. AKR1C3 can use 5α-Adione as a substrate to synthesize DHT, which can then activate AR signaling. The AR can translocate into the cell nucleus, activate expression of target genes including cell cycle genes, and promote tumor growth in CRPC. Increased tumor growth results in lower patient survival outcome. Under this model, PCa cells can continue to activate AR signaling even in the presence of androgen ablation therapies and low intratumoral androgen levels. This may result in the development and progression of CRPC.

DISCUSSION

The PCa patient tumor data was consistent with the PCa cell line data. The cell line data indicated that ERG positively regulated the expression of AKR1C3 enzyme in PCa. The PCa patient tumor data and LuCaP tumor xenograft data indicated that there was co-expression of ERG and AKR1C3 in human prostate tumor tissue specimens. This suggests that ERG regulates the expression of AKR1C3 in PCa tumor tissue specimens and LuCaP tumor xenografts. In addition, the Kaplan-Meier survival data showed that the presence of AKR1C3 or ERG in PCa tumor tissue specimens was correlated with lower survival probability. The IHC data and the Kaplan-Meier survival data support the model presented in Figure 35, where ERG regulates AKR1C3 expression and induces an AR regulated increase in tumor growth. It is interesting to note that ERG and AKR1C3 are associated with reduced survival even prior to the institution of androgen deprivation therapy. Future studies may help determine whether ERG and AKR1C3 are prognostic in CRPC patients. In any case, these data support a rationale for therapeutically targeting ERG and AKR1C3 in the clinic. The data presented in this paper suggest it may be beneficial to treat PCa patients with a combination of TMPRSS2-ERG inhibitor, AR antagonist, and ABE inhibitors. Specifically, TMPRSS2-ERG fusion-positive and AKR1C3-positive PCa patients may respond well to combination treatment with TMPRSS2-ERG inhibitor, AR antagonist (Enzalutamide), CYP17A1 inhibitor (Abiraterone), and AKR1C3 specific inhibitor.

APPENDIX A: PUBLICATIONS

Cavallin MA, **Powell K**, Biju KC, and Fadool DA. 2010. State-dependent sculpting of olfactory sensory neurons is attributed to sensory enrichment, odor deprivation, and aging. *Neuroscience Letters* 483, 90-5.

Mueller KL, **Powell K**, Madden JM, Eblen ST, and Boerner JL. 2012. EGFR tyrosine 845 phosphorylation dependent proliferation and transformation of breast cancer cells requires activation of p38MAPK. *Translational oncology* 5, 327-34.

St. John J*, **Powell K*,** Conley-LaComb M, and Chinni S. 2012. TMPRSS2-ERG fusion gene expression in prostate tumor cells and its clinical and biological significance in prostate cancer progression. *Journal of Cancer Science & Therapy* 4, 94-101. *Authors contributed equally.

Singareddy R, Semaan L, Conley-LaComb MK, St. John J, **Powell K**, Iyer M, Smith D, Heilbrun LK, Shi D, Sakr W, Cher ML, Chinni SR. 2013. Transcriptional regulation of CXCR4 in prostate tumor cells: Significance of TMPRSS2-ERG fusions. *Molecular cancer research: MCR* 11, 1349-61.

Herroon MK, Rajagurubandara E, Hardaway AL, **Powell K**, Turchick A, Feldmann D, Podgorski I. 2013. Bone marrow adipocytes promote tumor growth in bone via FABP4-dependent mechanisms. *Oncotarget* 4, 2108-23.

Powell K, Semaan L, Conley-LaComb MK, Asangani I, Wu YM, Williams J, Squire J, Maddipati KR, Cher M, Chinni SR. 2014. ERG/AKR1C3/AR constitutes a feed-forward loop for AR signaling in prostate cancer cells. (Under Review).

REFERENCES

Adeniji AO, Chen M, Penning TM. 2013. AKR1C3 as a target in castrate resistant prostate cancer. *The Journal of steroid biochemistry and molecular biology* 137, 136-49.

Albadine R, Latour M, Toubaji A, Haffner M, Isaacs WB, et al. 2009. TMPRSS2-ERG gene fusion status in minute (minimal) prostatic adenocarcinoma. *Modern pathology : an official journal of the United States and Canadian Academy of Pathology, Inc* 22, 1415-22.

Attard G, Clark J, Ambroisine L, Fisher G, Kovacs G, et al. 2008. Duplication of the fusion of TMPRSS2 to ERG sequences identifies fatal human prostate cancer. *Oncogene* 27, 253-63.

Attard G, Swennenhuis JF, Olmos D, Reid AH, Vickers E, et al. 2009. Characterization of ERG, AR and PTEN gene status in circulating tumor cells from patients with castration-resistant prostate cancer. *Cancer research* 69, 2912-8.

Baena E, Shao Z, Linn DE, Glass K, Hamblen MJ, et al. 2013. ETV1 directs androgen metabolism and confers aggressive prostate cancer in targeted mice and patients. *Genes & development* 27, 683-98.

Baldi E, Bonaccorsi L, Nesi G, Serni S, Forti G, Luzzatto L. 2010. TMPRSS2:ERG fusion gene and androgen-ablation therapy in prostate cancer. *Archives of pathology & laboratory medicine* 134, 964-5; author reply 65.

Balk SP, Knudsen KE. 2008. AR, the cell cycle, and prostate cancer. *Nuclear receptor signaling* 6, e001.

Barwick BG, Abramovitz M, Kodani M, Moreno CS, Nam R, et al. 2010. Prostate cancer genes associated with TMPRSS2-ERG gene fusion and prognostic of biochemical recurrence in multiple cohorts. *British journal of cancer* 102, 570-76.

Basuyaux JP, Ferreira E, Stehelin D, Buttice G. 1997. The Ets transcription factors interact with each other and with the c-Fos/c-Jun complex via distinct protein domains in a DNA-dependent and -independent manner. *The Journal of biological chemistry* 272, 26188-95.

Bauman DR, Steckelbroeck S, Williams MV, Peehl DM, Penning TM. 2006. Identification of the major oxidative 3alpha-hydroxysteroid dehydrogenase in human prostate that converts 5alpha-androstane-3alpha,17beta-diol to 5alpha-dihydrotestosterone: a potential therapeutic target for androgen-dependent disease. *Molecular endocrinology* 20, 444-58.

Bismar TA, Yoshimoto M, Duan Q, Liu S, Sircar K, Squire JA. 2012. Interactions and relationships of PTEN, ERG, SPINK1 and AR in castration-resistant prostate cancer. *Histopathology* 60, 645-52.

Bismar TA, Yoshimoto M, Vollmer RT, Duan Q, Firszt M, et al. 2011. PTEN genomic deletion is an early event associated with ERG gene rearrangements in prostate cancer. *BJU international* 107, 477-85.

Bonaccorsi L, Nesi G, Nuti F, Paglierani M, Krausz C, et al. 2009. Persistence of expression of the TMPRSS2:ERG fusion gene after pre-surgery androgen ablation may be associated with early prostate specific antigen relapse of prostate cancer: preliminary results. *J Endocrinol Invest* 32, 590-6.

Boormans JL, Hermans KG, Made AC, van Leenders GJ, Wildhagen MF, et al. 2010. Expression of the androgen-regulated fusion gene TMPRSS2-ERG does not predict

response to endocrine treatment in hormone-naive, node-positive prostate cancer. *European urology* 57, 830-5.

Brenner JC, Ateeq B, Li Y, Yocum AK, Cao Q, et al. 2011. Mechanistic rationale for inhibition of poly(ADP-ribose) polymerase in ETS gene fusion-positive prostate cancer. *Cancer cell* 19, 664-78.

Buttice G, Duterque-Coquillaud M, Basuyaux JP, Carrere S, Kurkinen M, Stehelin D. 1996. Erg, an Ets-family member, differentially regulates human collagenase1 (MMP1) and stromelysin1 (MMP3) gene expression by physically interacting with the Fos/Jun complex. *Oncogene* 13, 2297-306.

Cai C, Chen S, Ng P, Bubley GJ, Nelson PS, et al. 2011a. Intratumoral de novo steroid synthesis activates androgen receptor in castration-resistant prostate cancer and is upregulated by treatment with CYP17A1 inhibitors. *Cancer research* 71, 6503-13.

Cai C, He HH, Chen S, Coleman I, Wang H, et al. 2011b. Androgen receptor gene expression in prostate cancer is directly suppressed by the androgen receptor through recruitment of lysine-specific demethylase 1. *Cancer cell* 20, 457-71.

Cai C, Wang H, He HH, Chen S, He L, et al. 2013. ERG induces androgen receptor-mediated regulation of SOX9 in prostate cancer. *The Journal of clinical investigation* 123, 1109-22.

Cai C, Wang H, Xu Y, Chen S, Balk SP. 2009. Reactivation of Androgen Receptor-Regulated TMPRSS2:ERG Gene Expression in Castration-Resistant Prostate Cancer. *Cancer research* 69, 6027-32.

Cai JPK, Rajareddy Singareddy, Anthony Kropinski, Shijie Sheng, Michael L Cher and Sreenivasa R Chinni. 2010. Androgens Induce Functional CXCR4 via ERG Factor

Expression in TMPRSS2-ERG Fusion Positive Prostate Cancer Cells. *Translational oncology* 3.

Carrere S, Verger A, Flourens A, Stehelin D, Duterque-Coquillaud M. 1998. Erg proteins, transcription factors of the Ets family, form homo, heterodimers and ternary complexes via two distinct domains. *Oncogene* 16, 3261-8.

Carver BS, Tran J, Gopalan A, Chen Z, Shaikh S, et al. 2009. Aberrant ERG expression cooperates with loss of PTEN to promote cancer progression in the prostate. *Nature genetics* 41, 619-24.

Chang KH, Li R, Kuri B, Lotan Y, Roehrborn CG, et al. 2013. A gain-of-function mutation in DHT synthesis in castration-resistant prostate cancer. *Cell* 154, 1074-84.

Chang KH, Li R, Papari-Zareei M, Watumull L, Zhao YD, et al. 2011. Dihydrotestosterone synthesis bypasses testosterone to drive castration-resistant prostate cancer. *Proceedings of the National Academy of Sciences of the United States of America* 108, 13728-33.

Chen Y, Chi P, Rockowitz S, Iaquinta PJ, Shamu T, et al. 2013. ETS factors reprogram the androgen receptor cistrome and prime prostate tumorigenesis in response to PTEN loss. *Nature medicine* 19, 1023-9.

Clark J, Merson S, Jhavar S, Flohr P, Edwards S, et al. 2006. Diversity of TMPRSS2-ERG fusion transcripts in the human prostate. *Oncogene* 26, 2667-73.

Danila DC, Anand A, Sung CC, Heller G, Leversha MA, et al. 2011. TMPRSS2-ERG status in circulating tumor cells as a predictive biomarker of sensitivity in castration-resistant prostate cancer patients treated with abiraterone acetate. *European urology* 60, 897-904.

Darnel AD, Lafargue CJ, Vollmer RT, Corcos J, Bismar TA. 2009. TMPRSS2-ERG fusion is frequently observed in Gleason pattern 3 prostate cancer in a Canadian cohort. *Cancer biology & therapy* 8, 125-30.

de Bono JS, Logothetis CJ, Molina A, Fizazi K, North S, et al. 2011. Abiraterone and increased survival in metastatic prostate cancer. *The New England journal of medicine* 364, 1995-2005.

Demichelis F, Fall K, Perner S, Andren O, Schmidt F, et al. 2007. TMPRSS2:ERG gene fusion associated with lethal prostate cancer in a watchful waiting cohort. *Oncogene* 26, 4596-99.

Deryugina EI, Quigley JP. 2006. Matrix metalloproteinases and tumor metastasis. *Cancer metastasis reviews* 25, 9-34.

Dong Y, Zhang H, Gao AC, Marshall JR, Ip C. 2005. Androgen receptor signaling intensity is a key factor in determining the sensitivity of prostate cancer cells to selenium inhibition of growth and cancer-specific biomarkers. *Molecular cancer therapeutics* 4, 1047-55.

Dozmorov MG, Azzarello JT, Wren JD, Fung KM, Yang Q, et al. 2010. Elevated AKR1C3 expression promotes prostate cancer cell survival and prostate cell-mediated endothelial cell tube formation: implications for prostate cancer progression. *BMC cancer* 10, 672.

Efstathiou E, Titus M, Tsavachidou D, Tzelepi V, Wen S, et al. 2012. Effects of abiraterone acetate on androgen signaling in castrate-resistant prostate cancer in bone. *Journal of clinical oncology : official journal of the American Society of Clinical Oncology* 30, 637-43.

Efstathiou E, Titus M, Wen S, Hoang A, Karlou M, et al. 2014. Molecular Characterization of Enzalutamide-treated Bone Metastatic Castration-resistant Prostate Cancer. *European urology*.

Esgueva R, Perner S, J LaFargue C, Scheble V, Stephan C, et al. 2010. Prevalence of TMPRSS2-ERG and SLC45A3-ERG gene fusions in a large prostatectomy cohort. *Modern pathology : an official journal of the United States and Canadian Academy of Pathology, Inc*.

Fine SW, Gopalan A, Leversha MA, Al-Ahmadie HA, Tickoo SK, et al. 2010. TMPRSS2-ERG gene fusion is associated with low Gleason scores and not with high-grade morphological features. *Modern pathology : an official journal of the United States and Canadian Academy of Pathology, Inc* 23, 1325-33.

FitzGerald L, Agalliu I, Johnson K, Miller M, Kwon E, et al. 2008. Association of TMPRSS2-ERG gene fusion with clinical characteristics and outcomes: results from a population-based study of prostate cancer. *BMC cancer* 8, 230.

Flajollet S, Tian TV, Flourens A, Tomavo N, Villers A, et al. 2011. Abnormal expression of the ERG transcription factor in prostate cancer cells activates osteopontin. *Molecular cancer research : MCR* 9, 914-24.

Flanagan JU, Yosaatmadja Y, Teague RM, Chai MZ, Turnbull AP, Squire CJ. 2012. Crystal structures of three classes of non-steroidal anti-inflammatory drugs in complex with aldo-keto reductase 1C3. *PloS one* 7, e43965.

Foti DM, Reichardt JK. 2004. YY1 binding within the human HSD3B2 gene intron 1 is required for maximal basal promoter activity: identification of YY1 as the 3beta1-A factor. *Journal of molecular endocrinology* 33, 99-119.

Fung KM, Samara EN, Wong C, Metwalli A, Krlin R, et al. 2006. Increased expression of type 2 3alpha-hydroxysteroid dehydrogenase/type 5 17beta-hydroxysteroid dehydrogenase (AKR1C3) and its relationship with androgen receptor in prostate carcinoma. *Endocrine-related cancer* 13, 169-80.

Furusato B, Gao CL, Ravindranath L, Chen Y, Cullen J, et al. 2008. Mapping of TMPRSS2-ERG fusions in the context of multi-focal prostate cancer. *Modern pathology : an official journal of the United States and Canadian Academy of Pathology, Inc* 21, 67-75.

Furusato B, Tan SH, Young D, Dobi A, Sun C, et al. 2010. ERG oncoprotein expression in prostate cancer: clonal progression of ERG-positive tumor cells and potential for ERG-based stratification. *Prostate cancer and prostatic diseases* 13, 228-37.

Gazvoda M, Beranic N, Turk S, Burja B, Kocevar M, et al. 2013. 2,3-Diarylpropenoic acids as selective non-steroidal inhibitors of type-5 17beta-hydroxysteroid dehydrogenase (AKR1C3). *European journal of medicinal chemistry* 62, 89-97.

Gopalan A, Leversha MA, Satagopan JM, Zhou Q, Al-Ahmadie HA, et al. 2009. TMPRSS2-ERG Gene Fusion Is Not Associated with Outcome in Patients Treated by Prostatectomy. *Cancer research* 69, 1400-06.

Haffner MC, Aryee MJ, Toubaji A, Esopi DM, Albadine R, et al. 2010. Androgen-induced TOP2B-mediated double-strand breaks and prostate cancer gene rearrangements. *Nature genetics* 42, 668-75.

Hagglof C, Hammarsten P, Stromvall K, Egevad L, Josefsson A, et al. 2014. TMPRSS2-ERG expression predicts prostate cancer survival and associates with stromal biomarkers. *PloS one* 9, e86824.

Hamid AR, Pfeiffer MJ, Verhaegh GW, Schaafsma E, Brandt A, et al. 2012. Aldo-keto reductase family 1 member C3 (AKR1C3) is a biomarker and therapeutic target for castration-resistant prostate cancer. *Mol Med* 18, 1449-55.

Han B, Mehra R, Lonigro RJ, Wang L, Suleman K, et al. 2009. Fluorescence in situ hybridization study shows association of PTEN deletion with ERG rearrangement during prostate cancer progression. *Modern pathology : an official journal of the United States and Canadian Academy of Pathology, Inc* 22, 1083-93.

Hanahan D, Weinberg RA. 2011. Hallmarks of cancer: the next generation. *Cell* 144, 646-74.

Heinrich DM, Flanagan JU, Jamieson SM, Silva S, Rigoreau LJ, et al. 2013. Synthesis and structure-activity relationships for 1-(4-(piperidin-1-ylsulfonyl)phenyl)pyrrolidin-2-ones as novel non-carboxylate inhibitors of the aldo-keto reductase enzyme AKR1C3. *European journal of medicinal chemistry* 62, 738-44.

Hofer MD, Kuefer R, Maier C, Herkommer K, Perner S, et al. 2009. Genome-Wide Linkage Analysis of TMPRSS2-ERG Fusion in Familial Prostate Cancer. *Cancer research* 69, 640-46.

Hofland J, van Weerden WM, Dits NF, Steenbergen J, van Leenders GJ, et al. 2010. Evidence of limited contributions for intratumoral steroidogenesis in prostate cancer. *Cancer research* 70, 1256-64.

Ishizaki F, Nishiyama T, Kawasaki T, Miyashiro Y, Hara N, et al. 2013. Androgen deprivation promotes intratumoral synthesis of dihydrotestosterone from androgen metabolites in prostate cancer. *Scientific reports* 3, 1528.

Jamieson SM, Brooke DG, Heinrich D, Atwell GJ, Silva S, et al. 2012. 3-(3,4-Dihydroisoquinolin-2(1H)-ylsulfonyl)benzoic Acids: highly potent and selective

inhibitors of the type 5 17-beta-hydroxysteroid dehydrogenase AKR1C3. *Journal of medicinal chemistry* 55, 7746-58.

King JC, Xu J, Wongvipat J, Hieronymus H, Carver BS, et al. 2009. Cooperativity of TMPRSS2-ERG with PI3-kinase pathway activation in prostate oncogenesis. *Nature genetics* 41, 524-26.

Kirby M, Hirst C, Crawford ED. 2011. Characterising the castration-resistant prostate cancer population: a systematic review. *International journal of clinical practice* 65, 1180-92.

Kissick HT, Sanda MG, Dunn LK, Arredouani MS. 2013. Development of a peptide-based vaccine targeting TMPRSS2:ERG fusion-positive prostate cancer. *Cancer immunology, immunotherapy : CII* 62, 1831-40.

Klezovitch O, Risk M, Coleman I, Lucas JM, Null M, et al. 2008. A causal role for ERG in neoplastic transformation of prostate epithelium. *Proceedings of the National Academy of Sciences* 105, 2105-10.

Kolell KJ, Crawford DL. 2002. Evolution of Sp transcription factors. *Molecular biology and evolution* 19, 216-22.

Korenchuk S, Lehr JE, L MC, Lee YG, Whitney S, et al. 2001. VCaP, a cell-based model system of human prostate cancer. *In Vivo* 15, 163-8.

Leinonen KA, Saramaki OR, Furusato B, Kimura T, Takahashi H, et al. 2013. Loss of PTEN is associated with aggressive behavior in ERG-positive prostate cancer. *Cancer epidemiology, biomarkers & prevention : a publication of the American Association for Cancer Research, cosponsored by the American Society of Preventive Oncology* 22, 2333-44.

Leshem O, Madar S, Kogan-Sakin I, Kamer I, Goldstein I, et al. 2011. TMPRSS2/ERG promotes epithelial to mesenchymal transition through the ZEB1/ZEB2 axis in a prostate cancer model. *PloS one* 6, e21650.

Liedtke AJ, Adeniji AO, Chen M, Byrns MC, Jin Y, et al. 2013. Development of potent and selective indomethacin analogues for the inhibition of AKR1C3 (Type 5 17beta-hydroxysteroid dehydrogenase/prostaglandin F synthase) in castrate-resistant prostate cancer. *Journal of medicinal chemistry* 56, 2429-46.

Lin C, Yang L, Tanasa B, Hutt K, Ju BG, et al. 2009. Nuclear receptor-induced chromosomal proximity and DNA breaks underlie specific translocations in cancer. *Cell* 139, 1069-83.

Liu F, Pore N, Kim M, Voong KR, Dowling M, et al. 2006. Regulation of histone deacetylase 4 expression by the SP family of transcription factors. *Molecular biology of the cell* 17, 585-97.

Lonergan PE, Tindall DJ. 2011. Androgen receptor signaling in prostate cancer development and progression. *Journal of carcinogenesis* 10, 20.

Lovering AL, Ride JP, Bunce CM, Desmond JC, Cummings SM, White SA. 2004. Crystal structures of prostaglandin D(2) 11-ketoreductase (AKR1C3) in complex with the nonsteroidal anti-inflammatory drugs flufenamic acid and indomethacin. *Cancer research* 64, 1802-10.

Lubik AA, Gunter JH, Hendy SC, Locke JA, Adomat HH, et al. 2011. Insulin increases de novo steroidogenesis in prostate cancer cells. *Cancer research* 71, 5754-64.

Mani RS, Iyer MK, Cao Q, Brenner JC, Wang L, et al. 2011. TMPRSS2-ERG-Mediated Feed-Forward Regulation of Wild-Type ERG in Human Prostate Cancers. *Cancer research* 71, 5387-92.

Mani RS, Tomlins SA, Callahan K, Ghosh A, Nyati MK, et al. 2009. Induced chromosomal proximity and gene fusions in prostate cancer. *Science* 326, 1230.

Mani SA, Guo W, Liao MJ, Eaton EN, Ayyanan A, et al. 2008. The epithelial-mesenchymal transition generates cells with properties of stem cells. *Cell* 133, 704-15.

Mehra R, Tomlins SA, Shen R, Nadeem O, Wang L, et al. 2007. Comprehensive assessment of TMPRSS2 and ETS family gene aberrations in clinically localized prostate cancer. *Modern pathology : an official journal of the United States and Canadian Academy of Pathology, Inc* 20, 538-44.

Mehra R, Tomlins SA, Yu J, Cao X, Wang L, et al. 2008. Characterization of TMPRSS2-ETS Gene Aberrations in Androgen-Independent Metastatic Prostate Cancer. *Cancer research* 68, 3584-90.

Mitsiades N, Sung CC, Schultz N, Danila DC, He B, et al. 2012. Distinct patterns of dysregulated expression of enzymes involved in androgen synthesis and metabolism in metastatic prostate cancer tumors. *Cancer research* 72, 6142-52.

Mohamed AA, Tan SH, Sun C, Shaheduzzaman S, Hu Y, et al. 2011. ERG oncogene modulates prostaglandin signaling in prostate cancer cells. *Cancer biology & therapy* 11, 410-7.

Mohler JL, Titus MA, Wilson EM. 2011. Potential prostate cancer drug target: bioactivation of androstanediol by conversion to dihydrotestosterone. *Clinical cancer research : an official journal of the American Association for Cancer Research* 17, 5844-9.

Mosquera J-M, Mehra R, Regan MM, Perner S, Genega EM, et al. 2009. Prevalence of TMPRSS2-ERG Fusion Prostate Cancer among Men Undergoing Prostate Biopsy in the United States. *Clinical Cancer Research* 15, 4706-11.

Mosquera J-M, Perner S, Genega EM, Sanda M, Hofer MD, et al. 2008. Characterization of TMPRSS2-ERG Fusion High-Grade Prostatic Intraepithelial Neoplasia and Potential Clinical Implications. *Clinical Cancer Research* 14, 3380-85.

Mostaghel EA, Marck BT, Plymate SR, Vessella RL, Balk S, et al. 2011. Resistance to CYP17A1 inhibition with abiraterone in castration-resistant prostate cancer: induction of steroidogenesis and androgen receptor splice variants. *Clinical cancer research : an official journal of the American Association for Cancer Research* 17, 5913-25.

Mwamukonda K, Chen Y, Ravindranath L, Furusato B, Hu Y, et al. 2009. Quantitative expression of TMPRSS2 transcript in prostate tumor cells reflects TMPRSS2-ERG fusion status. *Prostate cancer and prostatic diseases* 13, 47-51.

Nagle RB, Algotar AM, Cortez CC, Smith K, Jones C, et al. 2013. ERG overexpression and PTEN status predict capsular penetration in prostate carcinoma. *The Prostate* 73, 1233-40.

Nakabeppu Y, Ryder K, Nathans D. 1988. DNA binding activities of three murine Jun proteins: stimulation by Fos. *Cell* 55, 907-15.

Nakamura Y, Hornsby PJ, Casson P, Morimoto R, Satoh F, et al. 2009. Type 5 17beta-hydroxysteroid dehydrogenase (AKR1C3) contributes to testosterone production in the adrenal reticularis. *The Journal of clinical endocrinology and metabolism* 94, 2192-8.

Nam RK, Sugar L, Wang Z, Yang W, Kitching R, et al. 2007a. Expression of TMPRSS2:ERG gene fusion in prostate cancer cells is an important prognostic factor for cancer progression. *Cancer biology & therapy* 6, 40-5.

Nam RK, Sugar L, Yang W, Srivastava S, Klotz LH, et al. 2007b. Expression of the TMPRSS2:ERG fusion gene predicts cancer recurrence after surgery for localised prostate cancer. *British journal of cancer* 97, 1690-95.

Nhili R, Peixoto P, Depauw S, Flajollet S, Dezitter X, et al. 2013. Targeting the DNA-binding activity of the human ERG transcription factor using new heterocyclic dithiophene diamidines. *Nucleic acids research* 41, 125-38.

Park K, Dalton JT, Narayanan R, Barbieri CE, Hancock ML, et al. 2014. TMPRSS2:ERG gene fusion predicts subsequent detection of prostate cancer in patients with high-grade prostatic intraepithelial neoplasia. *Journal of clinical oncology : official journal of the American Society of Clinical Oncology* 32, 206-11.

Penning TM. 2010. New frontiers in androgen biosynthesis and metabolism. *Current opinion in endocrinology, diabetes, and obesity* 17, 233-9.

Penning TM, Burczynski ME, Jez JM, Hung CF, Lin HK, et al. 2000. Human 3alpha-hydroxysteroid dehydrogenase isoforms (AKR1C1-AKR1C4) of the aldo-keto reductase superfamily: functional plasticity and tissue distribution reveals roles in the inactivation and formation of male and female sex hormones. *The Biochemical journal* 351, 67-77.

Penning TM, Drury JE. 2007. Human aldo-keto reductases: Function, gene regulation, and single nucleotide polymorphisms. *Archives of biochemistry and biophysics* 464, 241-50.

Penning TM, Jin Y, Steckelbroeck S, Lanisnik Rizner T, Lewis M. 2004. Structure-function of human 3 alpha-hydroxysteroid dehydrogenases: genes and proteins. *Molecular and cellular endocrinology* 215, 63-72.

Perner S, Demichelis F, Beroukhim R, Schmidt FH, Mosquera JM, et al. 2006. TMPRSS2:ERG fusion-associated deletions provide insight into the heterogeneity of prostate cancer. *Cancer research* 66, 8337-41.

Perner S, Svensson MA, Hossain RR, Day JR, Groskopf J, et al. 2010. ERG rearrangement metastasis patterns in locally advanced prostate cancer. *Urology* 75, 762-7.

Pfeiffer MJ, Smit FP, Sedelaar JP, Schalken JA. 2011. Steroidogenic enzymes and stem cell markers are upregulated during androgen deprivation in prostate cancer. *Mol Med* 17, 657-64.

Pflueger D, Rickman DS, Sboner A, Perner S, LaFargue CJ, et al. 2009. N-myc downstream regulated gene 1 (NDRG1) is fused to ERG in prostate cancer. *Neoplasia* 11, 804-11.

Rahim S, Beauchamp EM, Kong Y, Brown ML, Toretsky JA, Uren A. 2011. YK-4-279 inhibits ERG and ETV1 mediated prostate cancer cell invasion. *PloS one* 6, e19343.

Rasiah KK, Gardiner-Garden M, Padilla EJ, Moller G, Kench JG, et al. 2009. HSD17B4 overexpression, an independent biomarker of poor patient outcome in prostate cancer. *Molecular and cellular endocrinology* 301, 89-96.

Reya T, O'Riordan M, Okamura R, Devaney E, Willert K, et al. 2000. Wnt signaling regulates B lymphocyte proliferation through a LEF-1 dependent mechanism. *Immunity* 13, 15-24.

Rheault P, Charbonneau A, Luu-The V. 1999. Structure and activity of the murine type 5 17beta-hydroxysteroid dehydrogenase gene(1). *Biochimica et biophysica acta* 1447, 17-24.

Rickman DS, Chen YB, Banerjee S, Pan Y, Yu J, et al. 2010. ERG cooperates with androgen receptor in regulating trefoil factor 3 in prostate cancer disease progression. *Neoplasia* 12, 1031-40.

Rostad K, Hellwinkel OJ, Haukaas SA, Halvorsen OJ, Oyan AM, et al. 2009. TMPRSS2:ERG fusion transcripts in urine from prostate cancer patients correlate with a less favorable prognosis. *APMIS : acta pathologica, microbiologica, et immunologica Scandinavica* 117, 575-82.

Rouzier C, Haudebourg J, Carpentier X, Valério L, Amiel J, et al. 2008. Detection of the TMPRSS2-ETS fusion gene in prostate carcinomas: retrospective analysis of 55 formalin-fixed and paraffin-embedded samples with clinical data. *Cancer Genetics and Cytogenetics* 183, 21-27.

Ryan CJ, Smith MR, de Bono JS, Molina A, Logothetis CJ, et al. 2013. Abiraterone in metastatic prostate cancer without previous chemotherapy. *The New England journal of medicine* 368, 138-48.

Saramäki OR, Harjula AE, Martikainen PM, Vessella RL, Tammela TLJ, Visakorpi T. 2008. TMPRSS2:ERG Fusion Identifies a Subgroup of Prostate Cancers with a Favorable Prognosis. *Clinical Cancer Research* 14, 3395-400.

Schmidt EV. 1999. The role of c-myc in cellular growth control. *Oncogene* 18, 2988-96.

Schrecengost R, Knudsen KE. 2013. Molecular pathogenesis and progression of prostate cancer. *Seminars in oncology* 40, 244-58.

Setlur SR, Mertz KD, Hoshida Y, Demichelis F, Lupien M, et al. 2008. Estrogen-Dependent Signaling in a Molecularly Distinct Subclass of Aggressive Prostate Cancer. *J. Natl. Cancer Inst.* 100, 815-25.

Shao L, Tekedereli I, Wang J, Yuca E, Tsang S, et al. 2012. Highly specific targeting of the TMPRSS2/ERG fusion gene using liposomal nanovectors. *Clinical cancer research : an official journal of the American Association for Cancer Research* 18, 6648-57.

Singareddy R, Semaan L, Conley-Lacomb MK, St John J, Powell K, et al. 2013. Transcriptional regulation of CXCR4 in prostate cancer: significance of TMPRSS2-ERG fusions. *Molecular cancer research : MCR* 11, 1349-61.

Sitlani A, Crothers DM. 1996. Fos and Jun do not bend the AP-1 recognition site. *Proceedings of the National Academy of Sciences of the United States of America* 93, 3248-52.

Spencer ES, Johnston RB, Gordon RR, Lucas JM, Ussakli CH, et al. 2013. Prognostic value of ERG oncoprotein in prostate cancer recurrence and cause-specific mortality. *The Prostate* 73, 905-12.

Sreekumar A, Poisson LM, Rajendiran TM, Khan AP, Cao Q, et al. 2009. Metabolomic profiles delineate potential role for sarcosine in prostate cancer progression. *Nature* 457, 910-14.

Stanbrough M, Bubley GJ, Ross K, Golub TR, Rubin MA, et al. 2006. Increased expression of genes converting adrenal androgens to testosterone in androgen-independent prostate cancer. *Cancer research* 66, 2815-25.

Sun C, Dobi A, Mohamed A, Li H, Thangapazham RL, et al. 2008. TMPRSS2-ERG fusion, a common genomic alteration in prostate cancer activates C-MYC and abrogates prostate epithelial differentiation. *Oncogene* 27, 5348-53.

Szasz AM, Majoros A, Rosen P, Srivastava S, Dobi A, et al. 2013. Prognostic potential of ERG (ETS-related gene) expression in prostatic adenocarcinoma. *International urology and nephrology* 45, 727-33.

Teng LH, Wang C, Dolph M, Donnelly B, Bismar TA. 2013. ERG Protein Expression Is of Limited Prognostic Value in Men with Localized Prostate Cancer. *ISRN urology* 2013, 786545.

Tomlins SA, Laxman B, Varambally S, Cao X, Yu J, et al. 2008. Role of the TMPRSS2-ERG gene fusion in prostate cancer. *Neoplasia* 10, 177-88.

Tomlins SA, Rhodes DR, Perner S, Dhanasekaran SM, Mehra R, et al. 2005. Recurrent Fusion of TMPRSS2 and ETS Transcription Factor Genes in Prostate Cancer. *Science* 310, 644-48.

Tu JJ, Rohan S, Kao J, Kitabayashi N, Mathew S, Chen Y-T. 2007. Gene fusions between TMPRSS2 and ETS family genes in prostate cancer: frequency and transcript variant analysis by RT-PCR and FISH on paraffin-embedded tissues. *Modern pathology : an official journal of the United States and Canadian Academy of Pathology, Inc* 20, 921-28.

Verdu M, Trias I, Roman R, Rodon N, Garcia-Pelaez B, et al. 2013. ERG expression and prostatic adenocarcinoma. *Virchows Archiv : an international journal of pathology* 462, 639-44.

Wang J, Cai Y, Ren C, Ittmann M. 2006. Expression of Variant TMPRSS2/ERG Fusion Messenger RNAs Is Associated with Aggressive Prostate Cancer. *Cancer research* 66, 8347-51.

Wang J, Cai Y, Yu W, Ren C, Spencer DM, Ittmann M. 2008. Pleiotropic Biological Activities of Alternatively Spliced TMPRSS2/ERG Fusion Gene Transcripts. *Cancer research* 68, 8516-24.

Wang Q, Li W, Zhang Y, Yuan X, Xu K, et al. 2009. Androgen receptor regulates a distinct transcription program in androgen-independent prostate cancer. *Cell* 138, 245-56.

Wang S, Kollipara RK, Srivastava N, Li R, Ravindranathan P, et al. 2014. Ablation of the oncogenic transcription factor ERG by deubiquitinase inhibition in prostate cancer. *Proceedings of the National Academy of Sciences of the United States of America* 111, 4251-6.

Watanabe K, Kakefuda A, Yasuda M, Enjo K, Kikuchi A, et al. 2013. Discovery of 2-methyl-1-{1-[(5-methyl-1H-indol-2-yl)carbonyl]piperidin-4-yl}propan-2-ol: a novel, potent and selective type 5 17beta-hydroxysteroid dehydrogenase inhibitor. *Bioorganic & medicinal chemistry* 21, 5261-70.

Winnes M, Lissbrant E, Damber JE, Stenman G. 2007. Molecular genetic analyses of the TMPRSS2-ERG and TMPRSS2-ETV1 gene fusions in 50 cases of prostate cancer. *Oncol Rep* 17, 1033-6.

Wu L, Zhao JC, Kim J, Jin HJ, Wang CY, Yu J. 2013. ERG is a critical regulator of Wnt/LEF1 signaling in prostate cancer. *Cancer research* 73, 6068-79.

Yao V, Parwani A, Maier C, Heston WD, Bacich DJ. 2008. Moderate expression of prostate-specific membrane antigen, a tissue differentiation antigen and folate hydrolase, facilitates prostate carcinogenesis. *Cancer research* 68, 9070-7.

Yepuru M, Wu Z, Kulkarni A, Yin F, Barrett CM, et al. 2013. Steroidogenic enzyme AKR1C3 is a novel androgen receptor-selective coactivator that promotes prostate cancer growth. *Clinical cancer research : an official journal of the American Association for Cancer Research* 19, 5613-25.

Yin L, Rao P, Elson P, Wang J, Ittmann M, Heston WD. 2011. Role of TMPRSS2-ERG gene fusion in negative regulation of PSMA expression. *PloS one* 6, e21319.

Yin YD, Fu M, Brooke DG, Heinrich DM, Denny WA, Jamieson SM. 2014. The Activity of SN33638, an Inhibitor of AKR1C3, on Testosterone and 17beta-Estradiol Production and Function in Castration-Resistant Prostate Cancer and ER-Positive Breast Cancer. *Frontiers in oncology* 4, 159.

Yoshimoto M, Joshua AM, Cunha IW, Coudry RA, Fonseca FP, et al. 2008. Absence of TMPRSS2:ERG fusions and PTEN losses in prostate cancer is associated with a favorable outcome. *Modern pathology : an official journal of the United States and Canadian Academy of Pathology, Inc* 21, 1451-60.

Yu J, Mani RS, Cao Q, Brenner CJ, Cao X, et al. 2010. An integrated network of androgen receptor, polycomb, and TMPRSS2-ERG gene fusions in prostate cancer progression. *Cancer cell* 17, 443-54.

Yuan X, Cai C, Chen S, Chen S, Yu Z, Balk SP. 2014. Androgen receptor functions in castration-resistant prostate cancer and mechanisms of resistance to new agents targeting the androgen axis. *Oncogene* 33, 2815-25.

Zong Y, Xin L, Goldstein AS, Lawson DA, Teitell MA, Witte ON. 2009. ETS family transcription factors collaborate with alternative signaling pathways to induce carcinoma from adult murine prostate cells. *Proceedings of the National Academy of Sciences* 106, 12465-70.

ABSTRACT

TMPRSS2-ERG REGULATION OF ANDROGEN BIOSYNTHETIC ENZYME EXPRESSION, DHT SYNTHESIS, AND ANDROGEN RECEPTOR ACTIVATION IN PROSTATE CANCER

by

KATELYN A. POWELL

December 2014

Advisor: Sreenivasa R. Chinni, PhD

Major: Cancer Biology

Degree: Doctor of Philosophy

Intratumoral androgen synthesis in prostate cancer (PCa) contributes to the development of castration-resistant prostate cancer (CRPC). Several enzymes responsible for androgen biosynthesis have been shown to be overexpressed in CRPC, thus, contributing to CRPC in a castrated environment. Although intratumoral androgen synthesis is thought to contribute to the development and progression of CRPC, currently little is known regarding the regulation of androgen biosynthetic enzyme gene expression in PCa. The TMPRSS2-ERG transcription factor has been shown to be present in primary PCa tumors as well as CRPC tumors. The hypothesis was investigated that TMPRSS2-ERG fusions regulate androgen biosynthetic enzyme (ABE) gene expression and the production of androgens, which contributes to the development of CRPC. Data revealed that ERG regulated the expression of ABE, AKR1C3, in PCa cells via direct binding to the AKR1C3 gene region. Knockdown of ERG resulted in reduced AKR1C3 expression, which caused a reduction in both DHT synthesis and PSA expression in VCaP PCa cells treated with 5α-Androstanedione, a DHT precursor metabolite. Immunohistochemical

staining revealed that ERG was co-expressed with AKR1C3 in PCa tissue samples. These data suggest that AKR1C3 catalyzes the biochemical reduction of 5α-Androstanedione to DHT in PCa cells, and that ERG regulates this step through upregulation of AKR1C3 expression. Elucidation of ERG regulation of ABEs in CRPC may help to stratify TMPRSS2-ERG fusion-positive PCa patients in the clinic for anti-hormone driven therapies; and AKR1C3 may serve as a valuable therapeutic target in the treatment of CRPC.

AUTOBIOGRAPHICAL STATEMENT

KATELYN A. POWELL

Katelyn Powell was born and raised in Saginaw, Michigan. Katelyn graduated from Heritage High School, where she participated in softball and basketball, in 2001. She received her Bachelor of Science degree in Studio Art in 2006 and a Bachelor of Science degree in Biological Science in 2009 from Florida State University, Tallahassee, FL. At FSU, Katelyn participated in two years of undergraduate research studying neuroscience in the laboratory of Dr. Debra Fadool. After graduation from FSU, Katelyn spent six months working as a laboratory animal technician at University of South Florida, Moffitt Cancer Center, Tampa, FL. In 2010, she began her PhD degree in Cancer Biology at the Wayne State University, School of Medicine, Cancer Biology Graduate Program, Detroit, Michigan. She participated in two rotations her first year at WSU, studying breast cancer in the laboratory of Dr. Julie Boerner, and studying prostate cancer in the laboratory of Dr. Izabela Podgorski. Katelyn began her PhD dissertation project in 2011 working in the laboratory of Dr. Sreenivasa Chinni. Her dissertation project was focused on studying the effects of the TMPRSS2-ERG fusion gene on androgen biosynthetic enzyme expression and DHT synthesis in prostate cancer. While working in Dr. Chinni's lab, Katelyn was able to competitively obtain funding from a National Institute of Health, National Research Service Award T32 Institutional Training Grant Fellowship. In addition, she participated in seven abstract presentations of her research, including an international meeting at the 105th Annual Meeting of the American Association of Cancer Research, in San Diego, CA.